The consequences of dwarf galaxies colliding with the Milky Way

Ryan Skeoch

Lund Observatory
Lund University

2014-EXA78

Degree project of 60 higher education credits (for a degree of Master)
May 2014

Supervisor: Melvyn B. Davies

Lund Observatory
Box 43
SE-221 00 Lund
Sweden

Abstract

I simulate the collision of satellite galaxies with the Milky Way and observe the effects that this has on the orbits of the globular cluster populations within both the Milky Way and the satellite galaxies. This is done in order to investigate whether some of the Milky Way's globular clusters could have been donated from satellite galaxies which have been tidally stripped, since it is believed that the Sagittarius dwarf spheroidal galaxy is being tidally disrupted and that some of its globular clusters have been tidally stripped from it (such as Pal 12 and NGC 4147). It is also believed that there have been other Sagittarius-like satellite galaxies in the past which have donated globular clusters to the Milky Way.

From a simulation of the 63 Casetti-Dinescu globular clusters orbiting in the Milky Way, I find that most of the encounters between the globular clusters occur at separations between 0.1 kpc and 10 kpc. I also find that there are approximately 24 (0.64%) collisions that may occur between the globular clusters in the next 10 Gyr. However some of these 24 collisions involve the same globular cluster (for example NGC 2808 which has 7 collisions). I vary the initial position values of the globular cluster pair which has the closest encounter, and I find that the collision is very dependant upon the initial conditions of the globular clusters.

I then include the classical satellite galaxies in a simulation with the 63 globular clusters, and I find that most of the encounters between the satellite galaxies and the globular clusters occur at separations between 1 kpc and 10 kpc. However there is one encounter with a separation of 227 pc, this is between the SMC and NGC 7006, which has a probability of 1 for occurring in the next 10 Gyr. I also find that there are 10 (1.44%) collisions between the satellite galaxies and the globular clusters that may occur in the next 10 Gyr. The only satellite galaxies that are involved however are the Sagittarius dwarf galaxy, the LMC and the SMC.

I generate 500 random Sagittarius-like satellite galaxies based upon the initial conditions of the Sagittarius dwarf galaxy, and I generate 500 random globular clusters. I simulate 10 randomly selected Sagittarius-like satellite galaxies, each containing 10 randomly selected globular clusters which are initially on circular orbits around their host galaxy, and the globular clusters have spacings from their host galaxy in steps of 0.45 kpc. The simulated dwarf galaxies use a decreasing mass function, and I find that after 1 Gyr they have lost all of their globular clusters to the Milky Way. I continue this simulation for a further 10 Gyr, and upon investigation of some of the globular clusters' properties (eccentricity, j_z, orbital energy, and pericentre-apocentre distances), and compare them to the globular clusters from the Casetti-Dinescu database. I find that there are 5 (8%) Casetti-Dinescu globular clusters which have similar properties to the accreted globular clusters from the Sagittarius-like satellite galaxies. These are NGC 1851, NGC 3201, NGC 4590, NGC 7006, and Pal 13. In appendix 3 I run a more realistic simulation and find that there are 6 ($\sim$10%) Casetti-Dinescu globular clusters which have similar properties to the accreted globular clusters from the Sagittarius-like satellite galaxies. These are NGC 1851, NGC 4147, NGC 4590, NGC 5024, NGC 6205, NGC 6284.

I also calculate that if we have two Sagittarius-like satellite galaxies orbiting within the Milky Way every 5 Gyr and they each donate 9 globular clusters, then this means that 36 - 45 (23 - 29%) of the Milky Way's globular cluster population may have come from tidal stripping events (i.e. 4 - 5 Sagittarius-like satellite galaxies). This is in good agreement with Forbes et al., (2010), van den Bergh (2000), and Mackey & Gilmore (2004), who suggested that there were 27 - 47, 35, and 41 globular clusters which were accreted from satellite galaxies respectively. I believe that the 9 globular clusters previously mention are members of the 36 - 45 globular clusters that have been accreted in the Milky Way's history.

Populärvetenskaplig sammanfattning

Vi vet att galaxer kolliderar eftersom vi kan observera dem i många olika etapper av deras kollisioner, och vi kan också simulera denna process. Det har spekulerats om huruvida några av Vintergatans klotformiga stjärnhopar har blivit uppfångade från mindre galaxer som kommer nära Vintergatans centrum. När de kommer nära känner de en starkare gravitationskraft från Vintergatan än sin värdgalax. Denna process pågår för närvarande på de klotformiga stjärnhoparna som rör sig i omloppsbana kring Sagittarius dvärggalaxen. Det har spekulerats om det fanns sådana galaxer i Vintergatans historia.

Därfor simulerar jag kollisioner där 10 Sagittarius-liknande satellitgalaxer är inblandade, vars initialtillstånd är slumpvis utvalda, men baserat på Sagittarius dvärggalaxen. De 10 satellitgalaxerna innehåller var och en 10 klotformiga stjärnhopar, och det jag har sett är att efter 1 Går har alla klotformiga stjärnhopar från Sagittarius-liknande satellitgalaxer blivit uppfångade av Vintergatan från sin värdgalax. Jag fortsätter simulationen för ytterligare 10 Går, och jämför egenskaperna hos 100 (från de Sagittarius-liknande satellitgalaxerna) klotformiga stjärnhoparna med de motsvarande egenskaperna hos 63 av Vintergatans klotformiga stjärnhopar, vars egenskaper jag får från en 10 Går simulering.

Jag finner att fem av de här 63 klotformiga stjärnhoparna har egenskaper lika de klotformiga stjärnhoparna som uppfångats från Sagittarius-liknande satellitgalaxer. Jag har också hittat att om där var 2 Sagittarius-liknande satellitgalaxer som överlevde i 5 Går, så skulle där upsprungligen ha varit 4 - 5 Sagittarius-liknande satellitgalaxer i Vintergatan. Om varje av dessa satellitgalaxer innehållit 9 klotformiga stjärnhopar, som alla donerats till Vintergatan, så det är möjligt att 36 - 46 klotformiga stjärnhopar (23 - 29 $\%$) i Vintergatan har blivit uppfångade på detta sätt.

Acknowledgements

First I would like to thank my supervisor, Melvyn B. Davies for his assistance throughout this project, and being able to provide help when it was needed, as well as for reading through the different draft versions of the thesis before this one.

Another person I would like to thank is Anders Johansen, for reading through the draft thesis and providing me with great comments and suggestions on how to improve it.

I would also like to thank Giorgi Kokaia, Jonas Andersson, and Ylva Götberg, who I am extremely grateful for helping to translate my popular science summary into Swedish, and without whose help it would not be what it is today.

Lastly I would like to thank all of my friends and fellow students for always being there to help bounce ideas off and being a welcome distraction.

Contents

1 Galaxy components

In the simplified model of a galaxy that is used here, the galaxy is composed of three components, the bulge, the disk and the dark matter halo. There are also globular clusters and satellite galaxies which orbit within the galaxy. The Milky Way's bulge, disk, and dark matter halo have masses of 1.12×10^{10} $M_\odot$, 8.07×10^{10} $M_\odot$, (Paczyński, 1990) and 1.88×10^{12} $M_\odot$ respectively.[1] This then gave a total mass of the Milky Way as $M_{tot} = 1.97 \times 10^{12}$ $M_\odot$, this value was similar to that used in Piffl et al., 2014 ($M_{200} = 1.6 \times 10^{12} M_\odot$)[2], and Boylan-Kolchin et al., 2013 ($M_{vir} = 1.6 \times 10^{12} M_\odot$)[3]. Some other papers such as Sohn et al., (2013) and Irrgang et al., (2013) used a higher mass of $M_{vir} \sim 3.1 - 3.4 \times 10^{12}$ $M_\odot$. However the majority of papers viewed these masses as too large for the Milky Way, and therefore preferred to use a mass of $M_{vir} \sim 1 - 2 \times 10^{12}$ $M_\odot$.

An artist's impression of what the Milky Way may look like based upon other similar spiral galaxies is shown in Figure 1 (Bennett et al., 2009). The galactic bulge is shown by the bright white central oval, the disk and its spiral arms can be seen by the blue / purple areas as well as the spiral pattern, and the galaxy's halo is depicted by the outer section of the figure, shown as the black background. There are some globular clusters illustrated here via the large white circles in the halo.

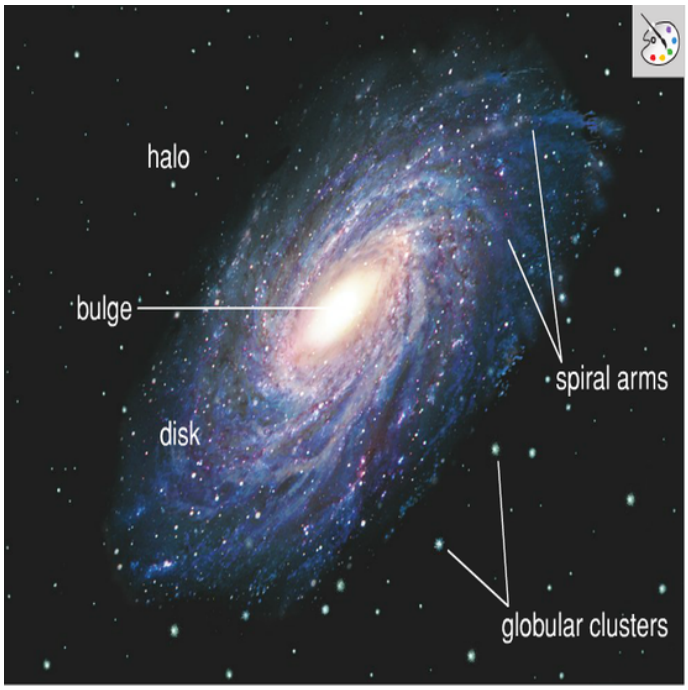

Figure 1: An artist's illustration of what the Milky Way may look like, based upon similar spiral galaxies. The bulge, disk and halo have all been labelled, along with some of the Milky Way's globular clusters, and the Milky Way's spiral arms. (Bennett et al., 2009).

[1] $M_\odot$ is the mass of the sun, approximately 1.989×10^{30}kg.

[2] M_{200} is the mass interior to r_{200}, where r_{200} is sometimes known as the virial radius (r_{vir}). r_{200} is defined as the radius at which the density equals 200 times the critical density, and inside of this radius the system is assumed to be in virial equilibrium (Binney & Tremaine, 2008).

[3] M_{vir} is the virial mass, which is the mass interior to the virial radius.

Satellite galaxies are dark matter[4] dominated, this means that most of the mass of a satellite galaxy is contributed by dark matter[5], which can enable a satellite galaxy to appear to survive being tidally disrupted longer than if it was entirely composed of baryonic matter (Jiang & Binney, 2000). This is one explanation for why the Sagittarius dwarf galaxy has not been completely destroyed yet, despite being tidally disrupted for at least 3 Gyr, i.e. the age of the youngest Sagittarius stream (Law & Majewski, 2010a). Dwarf galaxies (a sub-class of satellite galaxies) are classified due to their B-band magnitude[6] being $M_B \geq$ -18 [i.e the LMC (Large Magellanic Cloud) is the brightest satellite galaxy that we know of], and they are the most abundant type of galaxy in the universe (Mo et al., 2010). Dwarf spheroidal galaxies are a sub-class of dwarf galaxies with absolute magnitudes, M_V, of approximately -5 to -13.5 (Binney & Tremaine, 2008) and they have no gas nor any young stars (Mo et al., 2010). In the Milky Way the classical satellite galaxies [the first 11 satellite galaxies discovered in the Milky Way, from 1938 to 1994, although the LMC and the SMC (Small Magellanic Cloud) were discovered pre-history (McConnachie, 2012)] have M_V from -8.8 to -18.1. This therefore means that the LMC and the SMC are not dwarf spheroidal galaxies, but they are instead dwarf ellipticals. The Sagittarius dwarf spheroidal galaxy[7] is also known as the Sagittarius dwarf elliptical galaxy due to it lying on the edge of the definition.

Some satellite galaxies are believed to contain globular clusters orbiting within them, according to the literature the Sagittarius dwarf galaxy contains 4 globular clusters, however it is believed that it used to contain more, in total approximately 9 globular clusters (Forbes & Bridges, 2010; Law & Majewski, 2010b). The LMC, SMC, and Fornax satellite galaxies contain around 45, 8, and 5 globular clusters respectively (Aaronson & Mould, 1982; Beaulieu et al., 1999; Chrysovergis et al., 1989; Elson et al., 1987; Lloyd Evans, 1980; Johnson et al., 1999; Kontizas et al., 1987; Lyubenova et al., 2012; Mackey & Gilmore, 2003; Mould et al., 1982; Mould et al., 1984; Noyola & Gebhardt, 2007; van den Bergh, 2000a). Globular clusters are believed to contain little or no dark matter, and would therefore be easier to tidally disrupt (van den Bergh, 2000a). The globular clusters used here have masses of $10^3 - 10^6$ $M_\odot$ (Gnedin & Ostriker, 1997), whereas the satellite galaxies used here have masses between $10^7 - 10^{10}$ $M_\odot$ (Sohn et al., 2013). It is therefore clear that there is a distinction here between what a globular cluster is and what a satellite galaxy is, however the masses of the Milky Way's satellite galaxies (i.e. those which are not included in the classical 11 satellite galaxies), such as Segue II have masses as low as 10^5 $M_\odot$ (Kirby et al., 2013).

Shown in Table 1 are the range of masses that have been used to model the Milky Way (Barber et al., 2014). The number of stars (Binney & Tremaine, 2008) clearly show that there is a difference in composition of galaxies, satellite galaxies, and globular clusters. However note that the number of stars for the satellite galaxies used in Table 1 are for the classical satellite galaxies only. The average tidal radius for the globular clusters was calculated by taking an average of the globular clusters' tidal radii (Harris, 1996 [2003 edition])[8], which were calculated using the entire 157 known globular clusters that were in the Harris database. Here I defined the tidal radius (r_t) as the radius at which the density drops to zero (i.e. the size of the object, also if any of it's constituents traverse outside of this radius they become unbound), and the half-mass radius (r_h) as the radius of a sphere which contains half of the total mass (Binney & Tremaine, 2008). However in my simulations I only used the 63 globular clusters that were given in the Casetti-Dinescu database[9] (Dinescu et al., 1999; Dinescu et al;, 2003; Casetti-Dinescu

[4]Dark matter is a kind of matter which only interacts via gravity, and hence it appears to be invisible.

[5]We know this from the rotation curves (see section 2.3) and the large mass-to-light ratios of the satellite galaxies (Klessen & Zhao, 2002).

[6]The blue-band (i.e. B-band) magnitude (M_B) is the magnitude obtained from a luminosity that was centred on $\lambda_{\rm central}$ = 450 nm, likewise the visual-band magnitude (M_V) has $\lambda_{\rm central}$ = 550 nm (Binney & Tremaine, 2008). The fainter the object then the larger its magnitude is.

[7]Note that this should not be confused with the Sagittarius dwarf irregular galaxy.

[8]http://physwww.mcmaster.ca/∼harris/mwgc_2003.dat

[9]http://www.astro.yale.edu/dana/gc.html

et al., 2007; Casetti-Dinescu et al., 2010; Casetti-Dinescu et al., 2013), since these all had positions and proper motions. The average tidal radius for the satellite galaxies was taken from averaging over the Milky Way's classical satellite galaxies tidal radii (Mateo, 1998 [hereafter M98]; Subramanian & Subramaniam, 2012; van der Marel, 2006), and the average tidal radius for the Milky Way is the one that I used in my simulations, which is almost half the distance between the Milky Way and the Andromeda galaxy (our nearest neighbouring galaxy).

	Milky Way	Satellite galaxies	Globular clusters
Mass ($M_\odot$)	$10^{11} - 10^{12}$	$10^{7} - 10^{10}$	$10^{3} - 10^{6}$
Average tidal radius (kpc)	235	3.86	0.034
Number of stars	10^{12}	$10^{8} - 10^{10}$	$10^{4} - 10^{6}$

Table 1: Typical properties of the Milky Way, its classical satellite galaxies and globular clusters. The average tidal radii were calculated by taking the mean of the tidal radii for the classical satellite galaxies (M98; Subramanian & Subramaniam, 2012; van der Marel, 2006), and the globular clusters (Harris, 1996 [2003 edition]). The masses for the satellite galaxies and the globular clusters were taken from Barber et al., (2014), Sohn et al., (2013), Wadepuhl & Springel, 2001, and Gnedin & Ostriker (1997) respectively, and the number of stars was taken from Binney & Tremaine (2008).

2 Galactic model

2.1 Galactic potential

I used a galactocentric coordinate system, with the sun located at [x,y,z] = [8,0,0] kpc, where x is positive outwards from the galactic centre, y is positive towards the galactic rotation, z is positive towards the north galactic pole, and u, v, and w are their corresponding velocities. To model the Milky Way's bulge and disk I used a Miyamoto-Nagai axisymmetric potential (Miyamoto & Nagai, 1975), as shown in equation (1). I used this model since it is believed to be a good model, which is free from singularities, and it tends to the potential of a point mass at large R and z values.

$$\psi(R,z) = -\frac{\mathrm{GM}}{\sqrt{R^2 + \left(\mathrm{a} + \sqrt{z^2 + \mathrm{b}^2}\right)^2}} \tag{1}$$

In the above equation, M is the mass of the component being modelled ($\mathrm{M_b}$ for the bulge and $\mathrm{M_d}$ for the disk), a and b are constants which were used for determining the size and flattening of the system. R is the galactocentric cylindrical distance and was calculated by $R^2 = x^2 + y^2$, and G is the gravitational constant[10], which I took to be G = 4.499 $\times 10^{-12}$ kpc (kpc/Myr)^2 $\mathrm{M_\odot}$.

For the dark matter halo I used a spherically symmetric potential (Paczyński, 1990) as shown in equation (2), where r is the galactic separation and was calculated by $r^2 = R^2 + z^2$, and $\mathrm{M_c}$ is the halo core mass.

$$\psi_\mathrm{h}(r) = \frac{\mathrm{GM_c}}{\mathrm{r_c}} \left[\frac{1}{2} \ln\left(1 + \frac{r^2}{\mathrm{r_c}^2}\right) + \frac{\mathrm{r_c}}{r} \arctan\left(\frac{r}{\mathrm{r_c}}\right) \right] \tag{2}$$

The constants that I used in equations (1) and (2) are shown in Table 2, these were taken from Paczyński, (1990). These parameters were chosen by Paczyński in order to reproduce values of the local volume density (of the disk) near the sun, ρ_0 = 0.18 $\mathrm{M_\odot pc^{-3}}$, and the column density (from z = - 700 pc to z = +700 pc), Σ[700 pc] = 75 $\mathrm{M_\odot pc^{-2}}$.

$\mathrm{a_b}$ = 0 kpc	$\mathrm{b_b}$ = 0.277 kpc	$\mathrm{M_b}$ = 1.12 x $10^{10}\mathrm{M_\odot}$
$\mathrm{a_d}$ = 3.7 kpc	$\mathrm{b_d}$ = 0.200 kpc	$\mathrm{M_d}$ = 8.07 x $10^{10}\mathrm{M_\odot}$
	$\mathrm{r_c}$ = 6.000 kpc	$\mathrm{M_c}$ = 5.00 x $10^{10}\mathrm{M_\odot}$

Table 2: Parameters for the above potentials (Paczyński, 1990).

The total potential of the simulated Milky Way was given by the superposition of these three potentials (bulge, disk and halo), such that:

$$\psi(r) = \psi_\mathrm{b}(R,z) + \psi_\mathrm{d}(R,z) + \psi_\mathrm{h}(r) \tag{3}$$

[10] In S.I. units G = 6.67 $\times 10^{-11}$ $\mathrm{m^3 kg^{-1} s^{-3}}$.

2.2 Calculation of the acceleration

The total force[11] for an arbitrary set of point masses at different locations is given by the summation of the forces from each individual point mass (Lindegren, 2010).

$$a(r) = \sum_i \frac{\mathrm{G}m_i}{|r_i - r|^3}(r_i - r) \tag{4}$$

We know that for a similar mass distribution the potential is given by:

$$\psi(r) = -\sum_i \frac{\mathrm{G}m_i}{|r_i - r|} \tag{5}$$

Using the expression below, relating equations (4) and (5), allowed me to obtain the accelerations from the potential given in equation (3).

$$\begin{aligned} a &= -\nabla\psi(r) \\ &= -\nabla(\psi_{\mathrm{bulge}}(R,z) + \psi_{\mathrm{disk}}(R,z) + \psi_{\mathrm{halo}}(r)) \\ &= -\nabla\psi_{\mathrm{b}}(R,z) - \nabla\psi_{\mathrm{d}}(R,z) - \nabla\psi_{\mathrm{h}}(r) \end{aligned} \tag{6}$$

$$\begin{aligned} a_x = {} & \frac{\mathrm{GM_b}x}{\left(R^2 + z^2 + \mathrm{b_b^2}\right)^{\frac{3}{2}}} + \frac{\mathrm{GM_d}x}{\left(R^2 + \left(\mathrm{a_d} + \sqrt{z^2 + \mathrm{b_d^2}}\right)^2\right)^{\frac{3}{2}}} \\ & - \mathrm{GM_c}x\left(\frac{1}{\mathrm{r_c^3} + r^2\mathrm{r_c}} - \frac{\tan^{-1}\left(\frac{r}{\mathrm{r_c}}\right)}{r^3} + \frac{1}{\frac{r^4}{\mathrm{r_c}} + r^2\mathrm{r_c}}\right) \end{aligned} \tag{7}$$

$$\begin{aligned} a_y = {} & \frac{\mathrm{GM_b}y}{\left(R^2 + z^2 + \mathrm{b_b^2}\right)^{\frac{3}{2}}} + \frac{\mathrm{GM_d}y}{\left(R^2 + \left(\mathrm{a_d} + \sqrt{z^2 + \mathrm{b_d^2}}\right)^2\right)^{\frac{3}{2}}} \\ & - \mathrm{GM_c}y\left(\frac{1}{\mathrm{r_c^3} + r^2\mathrm{r_c}} - \frac{\tan^{-1}\left(\frac{r}{\mathrm{r_c}}\right)}{r^3} + \frac{1}{\frac{r^4}{\mathrm{r_c}} + r^2\mathrm{r_c}}\right) \end{aligned} \tag{8}$$

$$\begin{aligned} a_z = {} & \frac{\mathrm{GM_b}z\sqrt{z^2 + \mathrm{b_b^2}}}{\left(R^2 + z^2 + \mathrm{b_b^2}\right)^{\frac{3}{2}}\sqrt{z^2 + \mathrm{b_b^2}}} + \frac{\mathrm{GM_d}z\left(\mathrm{a_d} + \sqrt{z^2 + \mathrm{b_d^2}}\right)}{\left(R^2 + \left(\mathrm{a_d} + \sqrt{z^2 + \mathrm{b_d^2}}\right)^2\right)^{\frac{3}{2}}\sqrt{z^2 + \mathrm{b_d^2}}} \\ & - \mathrm{GM_c}z\left(\frac{1}{\mathrm{r_c^3} + r^2\mathrm{r_c}} - \frac{\tan^{-1}\left(\frac{r}{\mathrm{r_c}}\right)}{r^3} + \frac{1}{\frac{r^4}{\mathrm{r_c}} + r^2\mathrm{r_c}}\right) \end{aligned} \tag{9}$$

[11] Here the term force refers to the force per unit mass, i.e. the acceleration.

2.3 Why do we require a Dark Matter halo ?

Simulations suggest that there must be more mass in galaxies than what we can see. We know this from comparing the rotation curves (i.e. plots of the circular velocities as a function of radius), these showed observationally that the circular velocity should be nearly constant at large radii, however it was predicted that the circular velocity decreases at large radii. The circular velocity is the velocity where the centrifugal force is equal in strength to the gravitational force, one can then equate these two forces and rearrange the equation for the velocity.

$$\begin{aligned} \frac{V^2}{R} &= -\nabla\psi(r) \\ V_{\text{circular}} &= \sqrt{-\nabla\psi(r)\,R} \end{aligned} \tag{10}$$

This therefore implied that there must be more mass within large radii than was seen, in order for the circular velocity not to decrease. This relation can be seen from the equation for the circular velocity, shown in equation (10), where the mass is found from the potential. This matter that we cannot see has since been called dark matter due to it not giving off electromagnetic radiation (light / radio waves etc.). Shown in Figure 2 are the rotation curves for the theoretical circular velocity, i.e. without a dark matter halo (shown in black), and the observed circular velocity (shown in blue), which can be measured via HI velocity curves (radio observations of the 21cm neutral hydrogen line). This therefore showed that there was more mass contained in each galaxy than what was previously believed and hence they needed the dark matter halo potential in order to account for the 'missing' mass at large radii.

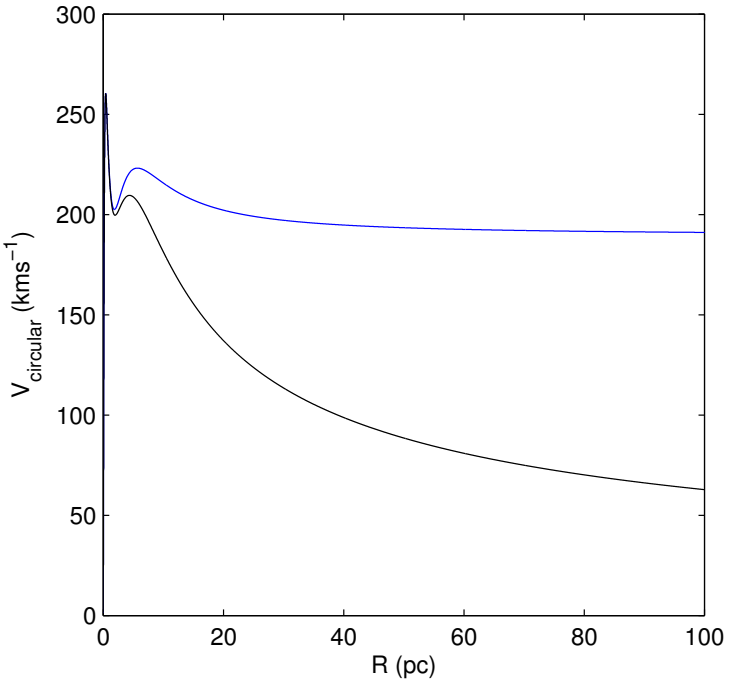

Figure 2: The black curve represents the circular velocity calculated without a dark matter halo potential (the theoretical circular velocity), and the blue curve shows the observed circular velocity (measured from the HI velocity curves).

2.4 Runge-Kutta integrator

I simulated the orbits of the Casetti-Dinescu globular clusters and the Milky Way's classical satellite galaxies in the potential of the Milky Way forwards in time using a self written Runge-Kutta $4^{\rm th}$ order integrator (RK4). I used the RK4 integrator since it is a simple single step procedure which has been commonly used for the numerical solutions of ordinary differential equations [ODEs] (Dormand & Prince, 1978). The RK4 integrator was first published in the early 20th century (Kutta, 1901), and it evaluates the acceleration four times per timestep in order to arrive at an accurate estimate of the numerical solution. The RK4 scheme is detailed below (Bodenheimer et al., 2006).

$$\mathbf{f}_{\rm a} = \mathbf{g}(t^n, \mathbf{sv}^n) \tag{11}$$

$$\mathbf{sv}_{\rm b} = \mathbf{sv}^n + \frac{\rm h}{2}\mathbf{f}_{\rm a} \tag{12}$$

$$\mathbf{f}_{\rm b} = \mathbf{g}(t^n + \frac{\rm h}{2}, \mathbf{sv}_{\rm b}) \tag{13}$$

$$\mathbf{sv}_{\rm c} = \mathbf{sv}^n + \frac{\rm h}{2}\mathbf{f}_{\rm b} \tag{14}$$

$$\mathbf{f}_{\rm c} = \mathbf{g}(t^n + \frac{\rm h}{2}, \mathbf{sv}_{\rm c}) \tag{15}$$

$$\mathbf{sv}_{\rm d} = \mathbf{sv}^n + {\rm h}\mathbf{f}_{\rm c} \tag{16}$$

$$\mathbf{f}_{\rm d} = \mathbf{g}(t^n + {\rm h}, \mathbf{sv}_{\rm d}) \tag{17}$$

$$\mathbf{sv}^{n+1} = \mathbf{sv}^n + \frac{1}{6}{\rm h}\mathbf{f}_{\rm a} + \frac{1}{3}{\rm h}\mathbf{f}_{\rm b} + \frac{1}{3}{\rm h}\mathbf{f}_{\rm c} + \frac{1}{6}{\rm h}\mathbf{f}_{\rm d} \tag{18}$$

Here I used **sv** = [x, y, z, u, v, w], which was the phase-space matrix, and **g**, which was the acceleration ODE (see section 2.2 for more details), and h was the timestep (h = 0.3 for all simulations). Equation (11) calculates $\mathbf{f}_{\rm a}$, which is the first iteration of the RK4, the values of $\mathbf{f}_{\rm a}$ correspond to the acceleration values for a particle with initial conditions given by **sv** at time, t. The results from equation (11) are then used to compute a new six dimensional phase-space matrix ($\mathbf{sv}_{\rm b}$), by progressing the object (globular cluster / satellite galaxy) forward half a time step. This process is then repeated another two times, however whilst calculating the $\mathbf{sv}_{\rm d}$ values in equation (16), the object is progressed a full timestep forward. In equation (18) the four iterations [i.e. the results from equations (11), (13), (15), and (17)] are combined with the initial phase-space matrix to produce a weighted average, with respective weights of $\frac{1}{6}$, $\frac{1}{3}$, $\frac{1}{3}$ and $\frac{1}{6}$.

3 Interaction of galaxies

3.1 Observational evidence

We know that galaxies collide since we are able to observe them in many different stages of colliding. It is believed that 5 - 10 $\%$ of all galaxies within the local universe (i.e. within 100 Mpc [Schneider, 2006]) are interacting and merging (Karl et al, 2010). In 1977 Toomre compiled a list of 11 observed colliding galaxies ordered by which he perceived to be in the earliest stages. The pair that he stated as being in the earliest stage of merging were the Antennae galaxies (NGC 4038/NGC 4039), these are two spiral galaxies which are the closest and most investigated major merger (i.e. a merger between two galaxies of similar masses). They have been studied in most wavelength regions, and their distance is approximately 22 Mpc. They have been theorised as having their 1^{st} close passage $\sim$ 600 Myr ago, and the final collision will occur in $\sim$ 50 Myr (Karl et al, 2010).

Figure 3 was produced by Lars Christensen (ESA) and was published in Whitmore et al., (2010). The bright yellow regions shown in Figure 3 are intense areas of star formation, which are caused during galaxy mergers as the gas is compressed due to the tidal torques. The pinkish-red regions are due to strong Hα emission, and the orange-brown regions are due to strong reddening from the dust (Whitmore et al., 2010). These two galaxies will eventually form a single elliptical galaxy, as this is the end stage of all major mergers.

Figure 3: A HST image of the Antennae galaxies colliding, produced by Lars Christensen (ESA). The bright yellow regions are the starburst regions, which are regions of intense star formation. The pink-red regions are due to strong Hα emission, and the orange-brown regions are due to strong reddening from the dust (Whitmore et al., 2010).

3.2 Theoretical evidence

Another way that we know galaxies collide is that we are able to simulate galaxies colliding (Helmi & White, 2001; Johnston et al., 1995; Law et al., 2005; Martínez-Delgado, 2004), for example the Sagittarius dwarf galaxy is currently being tidally stripped by the Milky Way due to its proximity to the galactic centre, approximately 17 kpc. This tidal stripping (also called tidal disruption) causes stars and globular clusters to be stripped from the dwarf galaxy, it also creates a stream of gas and dust (for example the Sagittarius stream) both behind and in front of the orbit of the dwarf galaxy. Tidal stripping also affects the orbit (velocity and eccentricity) and structure (mass and radius) of the dwarf galaxy. Due to this any results from using the Sagittarius dwarf galaxy without taking into account the effects of tidal disruption will be unreliable, unless we just want a general idea of what may occur. The globular clusters that may have been stripped from the Sagittarius dwarf galaxy are Pal 12 (ID 58), NGC 4147 (ID 9), Whiting 1, AM 4 and NGC 5634 (Forbes & Bridges, 2010). They are associated with the Sagittarius dwarf galaxy due to the similarities in their phase space (i.e. their positions and velocities). There are many other streams which have been produced by satellite galaxies ($\sim$ 6 such streams [Pawlowski et al., 2012]), such as the Magellanic stream (produced by the LMC and the SMC), there have also been streams produced by completely tidally disrupted satellite galaxies. There may still be some remnants of these tidally destroyed satellite galaxies, such as ω Cen (NGC 5139 / ID 14), which is believed to be the remnant of a nucleus of a tidally destroyed satellite galaxy (Freeman, 1993). There are also a couple of globular clusters that are believed to be associated with ω Cen, they are NGC 362 (ID 3) and 6779 (ID 50), (Dinescu et al., 1999). The progenitor of ω Cen is believed to have had an absolute magnitude of $M_V \sim -14.5$, (Bekki & Freeman, 2003). This means that it would have been a dwarf elliptical galaxy, more massive than the Sagittarius dwarf galaxy but less massive than the SMC. However the exact mass is much debated, with Ideta & Makino (2004) finding a mass of $1.3\times10^8 M_\odot$, and Chiba & Mizutani (2004) finding a mass $5.74\times10^8 M_\odot$ for ω Cen's progenitor. Therefore due to this mass it is reasonable to assume that ω Cen may have contained a number of globular clusters similar to those of the Sagittarius dwarf galaxy and the SMC (i.e. around 9 globular clusters). M 54 (the Sagittarius dwarf galaxy's core, NGC 6715) may have the same fate as ω Cen once the Sagittarius dwarf galaxy is tidally destroyed. Shown in Figure 4 is an artist's (Amanda Smith, Institute of Astronomy, University of Cambridge) impression of what the Sagittarius stream may look like around the Milky Way. In this image we can see the Sagittarius dwarf galaxy as the pinkish-red circle (left-hand side), the sun as the yellow circle (right-hand side) and the galactic bulge as the central white dome. There is also the galactic disk shown by the blue oval, and the Sagittarius streams are shown by the four arms coming off the Sagittarius dwarf galaxy in both the forward and rearward direction of its orbit.

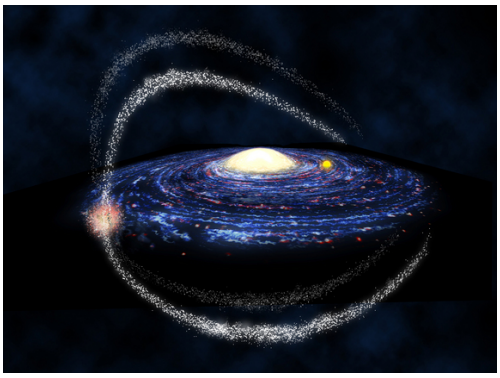

Figure 4: An artist's (Amanda Smith, Institute of Astronomy, University of Cambridge) impression of the Sagittarius dwarf galaxy being tidally stripped by the Milky Way. Also shown here are the tidal streams of the Sagittarius dwarf galaxy as well as the Sun (the yellow circle) near the bulge (which is shown as the white semi-circle in the centre).

4 Globular cluster - Globular cluster encounters

4.1 Globular cluster dataset

As can be seen in Figure 5 most (89%) of the globular clusters from the Casetti-Dinescu dataset (shown as the black open circles) are within R = 10kpc, whereas the Harris[12] sample (shown by the blue dots) extends out to $\sim$ 90 kpc with around 95% within 40kpc. However both samples have the majority of their clusters within z = $\pm$ 20 kpc, this therefore implies that there is no bias in the z-direction, however there may be bias in the R direction (if the Harris sample is taken to be unbiased) since it is easier to obtain values for objects which are closer to us. The distances from Harris were found by using the V-magnitude of the horizontal branch, where the horizontal branch was measured directly from a colour-magnitude diagram or from the mean magnitude of the RR Lyrae stars[13]. Casetti-Dinescu states that the error in the distance to any of the globular clusters in her database is 10%. Also shown in Figure 5 are the R-z locations of the Milky Way's globular clusters that are associated with ω cen [shown by the green stars, NGC 362 (ID 3), NGC 5139 (ω cen, ID 14), and NGC 6779 (M 56, ID 50)], and the Sagittarius dwarf galaxy [shown by the red stars, Whiting 1, NGC 4147 (ID 9), AM 4, NGC 5634, NGC 6715 (M 54, the Sagittarius dwarf galaxy's core), Pal 12 (ID 58)]. The ones that are associated with ω cen are all very tightly packed in this figure, whereas the ones associated with the Sagittarius dwarf galaxy are more dispersed, this could just be due to the methods that were used in connecting the globular clusters to their possible donor satellite galaxies. We can also see that there are 6 major outliers on this plot with larger R-z values than the other globular clusters, these are (from high positive z value to high negative z value) Pal 4, Pal 3, Pal 14, NGC 2419, Eridanus 1, AM 1. Due to their large R values it is possible that these have been recently accreted to the Milky Way.

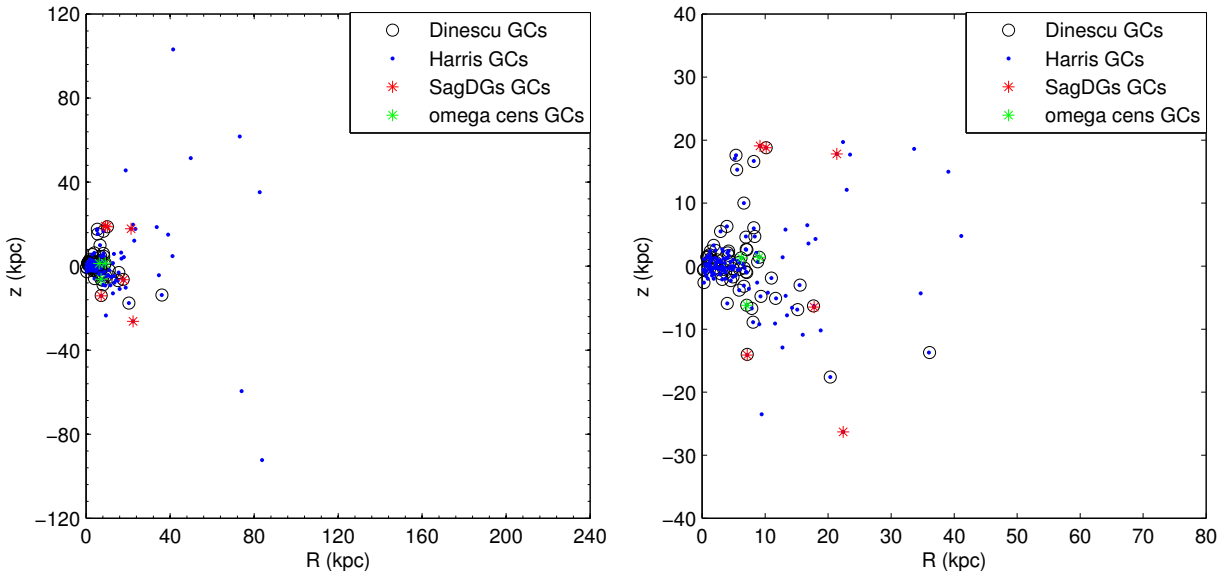

Figure 5: *Left*: R-z plot of the globular clusters' initial locations from the Casetti-Dinescu (black open circles) and the Harris (blue points) databases. I also highlighted the locations of the globular clusters associated with ω cen (green stars), and the Sagittarius dwarf galaxy (red stars). *Right*: A 'zoomed' version of the left hand plot, in order to have a better perspective on the distribution of the globular clusters within z = $\pm$ 40 kpc.

[12] http://physwww.physics.mcmaster.ca/ harris/mwgc.dat
[13] http://physwww.mcmaster.ca/ harris/mwgc.ref

I have included in Tables 6 and 7 (shown in Appendix 1) the initial conditions of the Casetti-Dinescu globular clusters, along with the ID numbers that I used to represent them in the simulations. In the name column are the NGC numbers [with the exceptions of HP 1 (1Or), Pal 5 (5KC), Pal 12 (12Di), and Pal 13 (13Si)], along with the reference initials associated with the Casetti-Dinescu database. In Tables 8 and 9 (shown in Appendix 1) are the globular clusters' masses (Gnedin & Ostriker, 1997), metallicities, half-mass radii, tidal radii, eccentricities (Harris, 1996 [2010 edition]) and the z-component of the angular momentum (j_z). Also in Tables 8 and 9 are the globular clusters' distances from the sun, these were used when I varied the initial positions of the globular cluster pair that had the closest encounter.

I assumed that the Milky Way's potential was constant with time, because the masses of the satellite galaxies and globular clusters were much less than the mass of the Milky Way. In Section 4 and 5 I modelled the satellite galaxies and globular clusters as point masses, but in Section 5.5 I modelled the satellite galaxies using a Plummer (1911) potential. I used a timestep of 0.3 Myr (approximately 0.1% of the orbital period in the Milky Way), but I also experimented with timesteps of 0.15 Myr and 0.6 Myr in order to see if and how this affected my results. I found that this had no bearing on my results, and therefore opted to use a timestep of 0.3 Myr for all of the simulations, and a timescale of 10 Gyr into the future for most of my simulations. I chose 10 Gyr due to this being roughly the age of our galaxy and it is approximately the length of time that a globular cluster survives for. In section 4.3 I only considered the gravitational effects of the Milky Way on the globular clusters and not the globular clusters effects on the other globular clusters. This was due to the mass of the globular clusters being much less than the mass of the Milky Way and hence the force exerted by the globular clusters on each other would be much less than the force exerted by the Milky Way on the globular clusters. However in section 4.4 I investigated how much of a difference the self interaction of the globular clusters would have on their orbits.

I found that the globular clusters which were most disk-like (low relative velocity with respect to the disk) were located within 30 Kpc of the galactic centre, this means that the majority of the close encounters should occur within this distance of the galactic centre due to them having many encounters with the non-disk like globular clusters. The disk-like globular clusters would spend most of their time in the disk, where the density is higher and hence there is a larger chance of collisions occurring. Whereas the non-disk like globular clusters would spend most of their time outside of the disk and ergo not have as much chance of having a collision.

4.2 Example orbits

I integrated the orbits of the 63 Casetti-Dinescu globular clusters in the potential of the Milky Way for 10 Gyr and I investigated the shape of their orbits. I found that there are various shaped orbits for some of the globular clusters, however there were mainly two different types. Shown in Figure 6 are two different globular cluster R-z orbital plots, the contrast in the shape of the orbits was due to the differences in their eccentricities. The left-hand plot (ID 1, NGC 104) had an eccentricity of 0.15 and the right-hand plot (ID 57, NGC 7099) had an eccentricity of 0.36. Here the eccentricity was derived from the equations for the periapsis and apoapsis distance equations. This is due to the globular clusters not orbiting around a point mass but instead orbiting inside a potential, therefore they sometimes have a different amount of mass inside of their orbit. The equation for the eccentricity was given by:

$$\text{“}e\text{”} = \frac{r_{\max} - r_{\min}}{r_{\max} + r_{\min}}$$

In Figure 7 are the x-y orbital plots for two different globular clusters, ID 1 and ID 54 (NGC 7006). The difference is due to ID 1 having a smaller galactocentric separation than ID 54, as can clearly be seen from the range of x-y values on their axes. Due to the proximity of ID 1 to the galactic centre, ID 1 can complete many more orbits than ID 54 can in 10 Gyr, and hence the plot of ID 1's orbit appears more like a tyre shape than ID 54's orbit. However given enough time ID 54's orbit would have a similar appearance to that of ID 1's orbit, but ID 54's 'tyre-shape' orbit would be thicker and there would be less of a 'hole' in the centre.

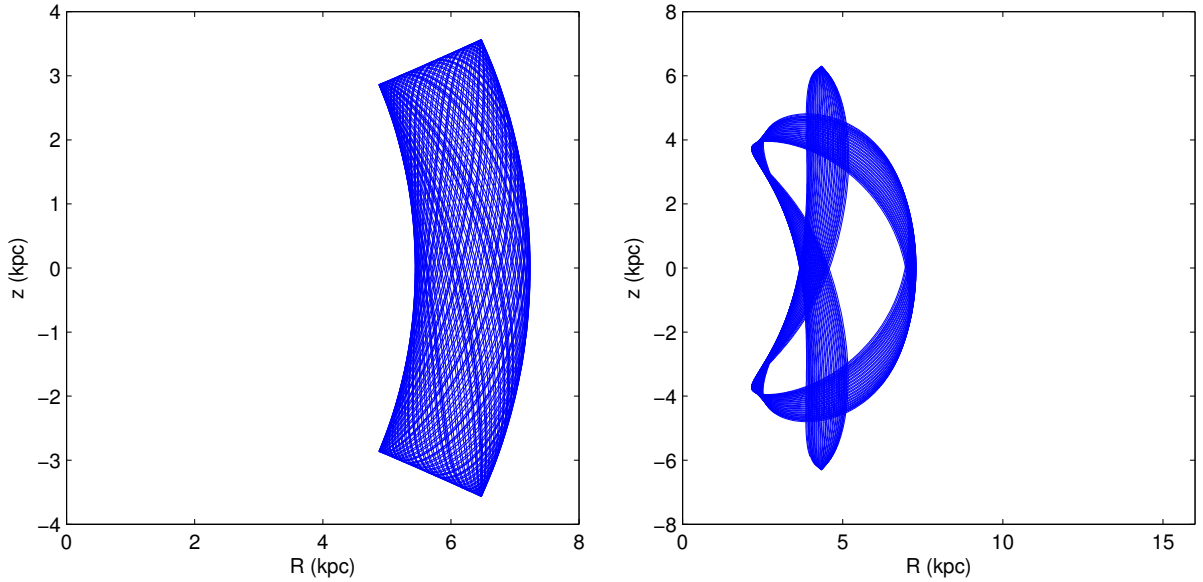

Figure 6: A comparison of two different R-Z orbital plots of globular clusters, ID 1 (left) and ID 57 (right). They have contrasting shapes due to the differences in their eccentricities. These were both simulated for 10 Gyr into the future.

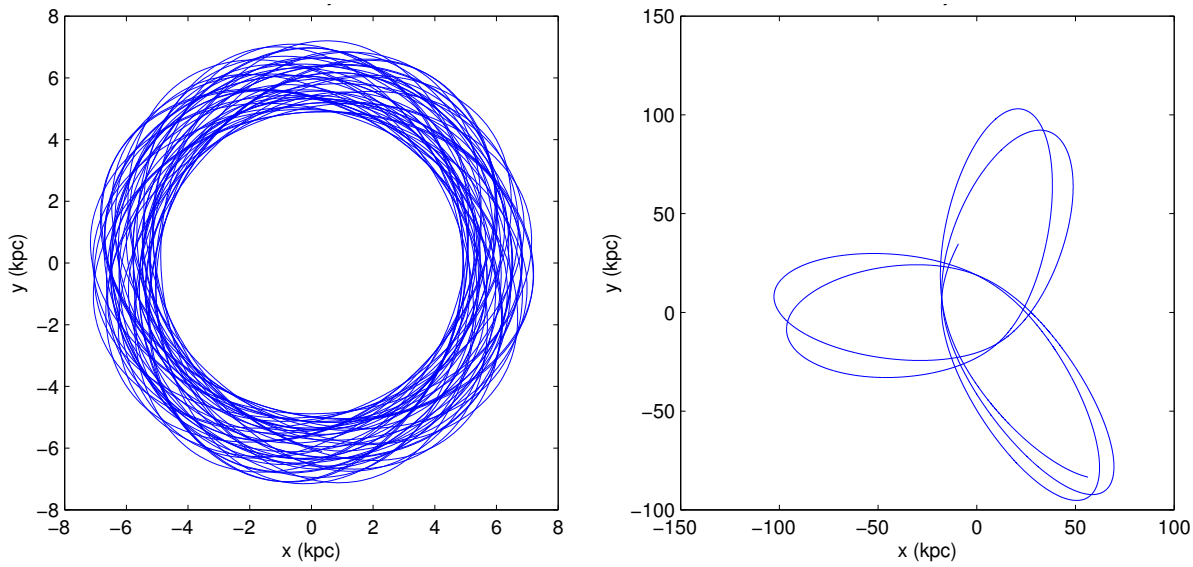

Figure 7: A comparison of the x-y orbital plots for the globular clusters ID 1 (left) and ID 54 (right). The difference is due to the differences in their distance from the galactic centre, with ID 1 being closer to the galactic centre than ID 54. These were both simulated for 10 Gyr into the future.

4.3 Globular cluster encounters - excluding self interactions

I simulated the 63 Casetti-Dinescu globular clusters as point masses orbiting within the Milky Way and investigated how close the globular clusters came to each other within the 10 Gyr of the simulation. In this section I did not include the gravitational effects of the globular clusters on the other globular clusters due to their masses being much less than the mass of the Milky Way, and hence the force that they would feel from each other would be much less than the force felt from the Milky Way. Shown in Figure 8 is the minimum separation distance ($r_{\rm sep,min}$) for each of the globular clusters encountering the other globular clusters. As can be seen this is symmetrical about the diagonal gap (which is due to the globular clusters not being able to encounter themselves but only the other 62 globular clusters), since the x-y axes are the same. Using both the x and y axes we can determine which pair were involved in the encounters which are of interest. I used different colours to represent the different minimum separations between the globular clusters in order to make the plot easier to read. The colour scheme was $r_{\rm sep,min} <$ 50pc = magenta, 50pc $\leq r_{\rm sep,min} <$ 100pc = green, 100pc $\leq r_{\rm sep,min} <$ 1kpc = red, 1kpc $\leq r_{\rm sep,min} <$ 10kpc = blue, $r_{\rm sep,min} \geq$ 10kpc = black. The size of the squares were given by $\log(\frac{100}{r_{\rm sep,min}})$. This was chosen so that the large squares would represent the closest encounters, and the distant encounters would be shown as small dots. This would then make the small $r_{\rm sep,min}$ easier to be seen in the plot, since most of the encounters occurred at large separations and ergo they appear as small dots. However this plot is still a bit hard to read but upon close inspection one can see that there are some of the squares which are slightly larger than others and many which look like dots. Those which look like dots are the encounters which had separations larger than 10 kpc (black), and those with the larger squares are the encounters with separations less than 40 pc (magenta). As can be seen there are many more dots (blue/black) than squares (magenta) and hence there were many more encounters which occurred at large separations than those at small separations. The closest encounter was $\sim$ 10 pc, which was between ID 38 (NGC 6342) and ID 61 (NGC 6528), this encounter occurred at t = 7.57 Gyr (where t = 0 is the present time), and they had a relative velocity of $\sim$ 266 kms^{-1}. The majority of the globular cluster encounters occurred between 100s of pc and 10s of kpc, and hence have very small squares in this figure. This therefore means that most of the globular clusters will not collide[14], however a few of the globular clusters may collide in the future.

[14]Here a collision means: an encounter between two objects, where one of these objects comes within the tidal radius of the other.

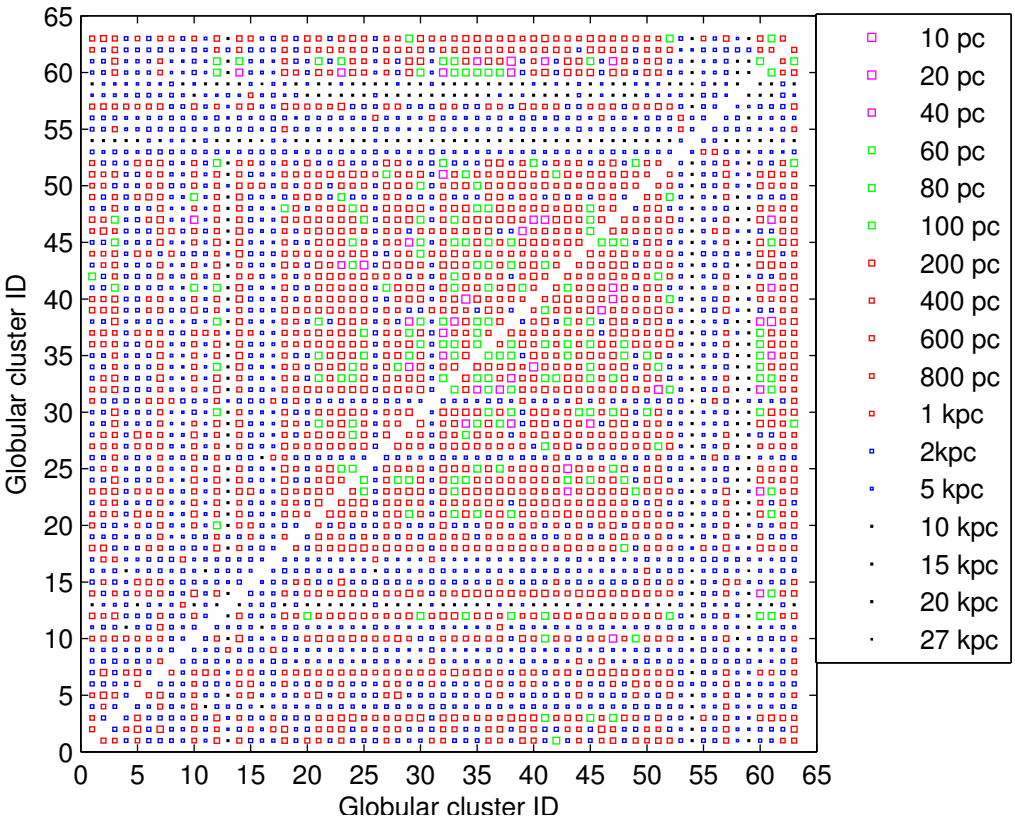

Figure 8: The minimum separation ($r_{sep,min}$) of each encounter between the globular clusters for 10 Gyr into the future. Here I did not include the mutual gravitational attraction of the globular clusters, since their masses ($\sim 10^5 M_\odot$) were much smaller than those of the Milky Way ($\sim 10^{12} M_\odot$), and hence the Milky Way would be the main perturber due to it supplying a much larger force. The colour scheme was $r_{sep,min} < 50$pc = magenta, $50\text{pc} \leq r_{sep,min} < 100$pc = green, $100\text{pc} \leq r_{sep,min} < 1$kpc = red, $1\text{kpc} \leq r_{sep,min} < 10$kpc = blue, $r_{sep,min} \geq 10$kpc = black. There were many more encounters with large separations (dots [blue/black], $r_{sep,min} > 1$kpc), than those with small separations (larger squares [green/magenta], $r_{sep,min} < 100$ pc).

The left-hand plot in Figure 9 shows the $\log(r_{sep,min})$ for each globular cluster - globular cluster encounter going 10 Gyr into the future. There were few globular clusters that got within $\sim$100 pc of each other, with only one pair getting within $\sim$10 pc of each other, which was ID 38 and ID 61. This can be seen from the two lowermost circles, i.e. one being from the encounter of ID 38 - ID 61 and the other from ID 61 - ID 38. There were also very few close encounters for some of the globular clusters, such as ID 54 and ID 59 (Pal 13) which only had distant encounters $\gtrsim$ 2 kpc. This means that there may be a collision between ID 38 and ID 61 in the future, however ID 54 and ID 59 will most likely not collide with any globular cluster (in the Casetti-Dinescu database) in the next 10 Gyr. The right-hand plot shows which globular clusters had an encounter within their current tidal radius. The red line is indicative of their current tidal radii, hence if any of the circles are below this line then it means that they have had an encounter within the tidal radius of that globular cluster, i.e. there was a collision. I found that there were 24 different collisions occurring, with IDs 14, 12 and 32 having 7, 5 and 4 collisions respectively. However ID 38 and ID 61 do not have a globular cluster colliding with them, despite there being an encounter of $\sim$ 10 pc between ID 38 and ID 61.

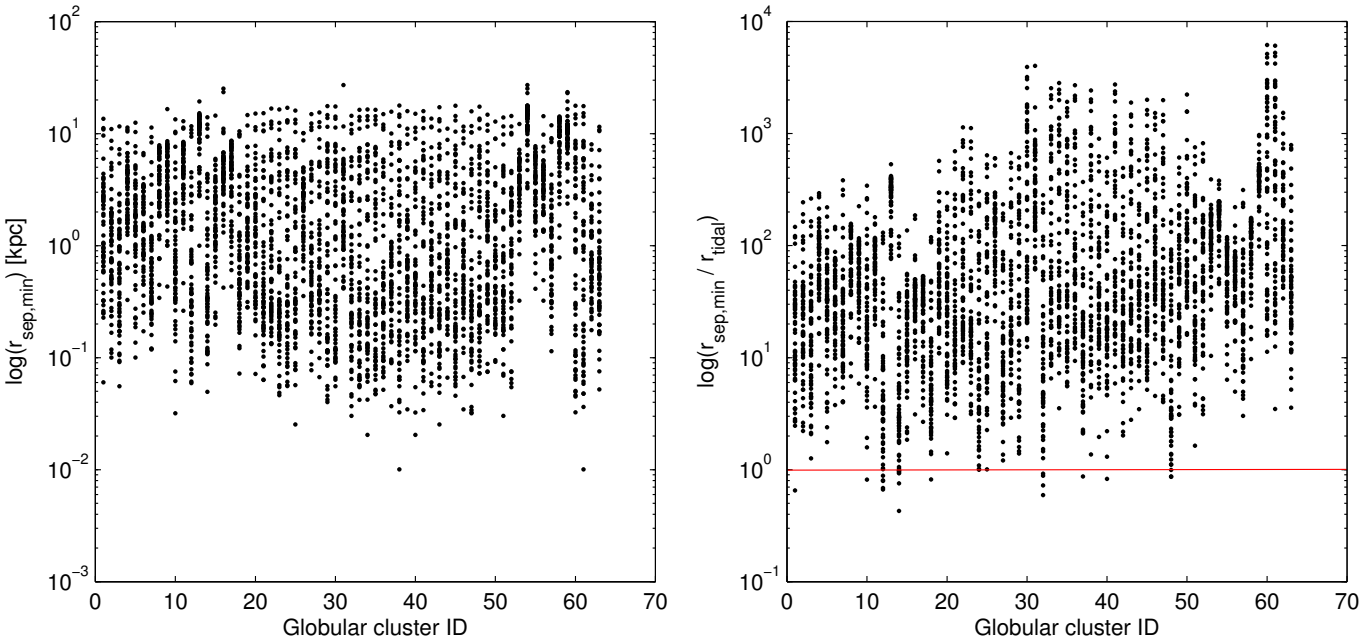

Figure 9: *Left*: The $\log(r_{sep,min})$ for each globular cluster - globular cluster encounter. There were very few globular clusters that got within 10's of pc of each other, the only pair were ID 38 and ID 61, this can be seen by the two lowermost circles. *Right*: Plot showing the separation distance divided by the current tidal radius. Therefore if a globular cluster (black circle) is below this red line then there was a collision involving that globular cluster. However the majority of encounters were far outside of the tidal radii of the globular clusters, with only 24 encounters occurring (7 of which involved ID 14). These simulation were run for 10 Gyr into the future.

I created a histogram of the number of encounters as a function of $r_{\mathrm{sep,min}}$ (shown by the left plot in Figure 10) and $\frac{r_{\mathrm{sep,min}}}{r_{\mathrm{t}}}$ (shown by the right plot in Figure 10) for all of the simulated encounters of the 63 Casetti-Dinescu globular clusters. The left hand plot shows the number of encounters within 1 kpc, I chose this range since any encounters outside of this range would have very little affect on the globular clusters' orbits / structures. There are approximately 48% of the encounters within this distance, with a peak in the number of encounters occurring between 100 and 200 pc. For the right hand plot I initially investigated the number of encounters within 200 tidal radii, this showed me that there was a peak in the number of encounters within 20 tidal radii. I therefore created the histogram shown below, which shows that there was a peak in the number of encounters between 2 and 4 tidal radii, however there were very few encounters within 2 tidal radii. This thus implies that most of the encounters between the globular clusters will not result in collisions. The percentage of the globular cluster encounters which resulted in a collision was $\sim 1.28\%$ (i.e. 24 different collisions occurred in 10 Gyr). There was one collision between ID 32 (NGC 6287) and ID 37 (NGC 6341), where the separation distance was smaller than the tidal radii of both globular clusters.

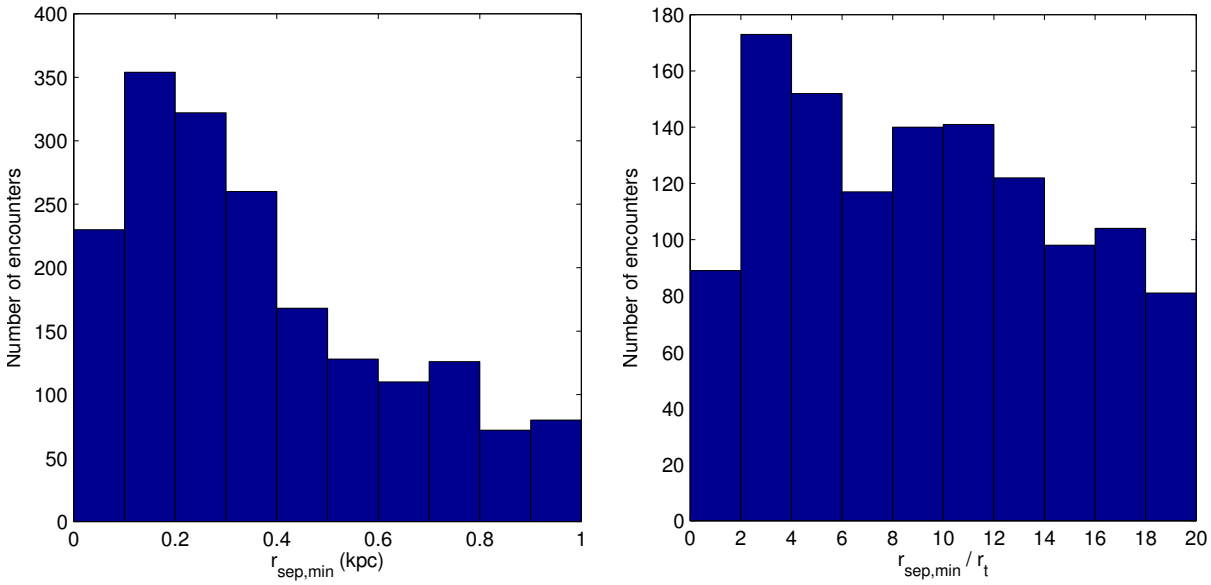

Figure 10: *Left*: Histogram of the number of encounters (within 1 kpc) as a function of $\mathrm{r_{sep,min}}$ for the globular clusters encountering each other. I chose this range since any encounter outside of this range would not have much of an effect on the globular clusters' orbits / structures. *Right*: This plot is similar to the left-hand histogram, however here the x-axis is that of the ratio of the minimum separation distance to the tidal radius ($\mathrm{r_t}$). We can see that there are slightly more encounters occurring within 2 - 4 times the globular clusters tidal radii than in any other section of the plot, and there were very few within 2 tidal radii. Therefore most encounters between the globular clusters will not result in a collision.

4.3.1 Varying the initial positions

In Figure 11 is shown the $r_{sep,min}$ for ID 38 and ID 61 interacting with different initial positions. The various initial positions were generated by adding / subtracting multiples of 0.1σ from their initial x, y, and z values. σ is the error (taken to be 10%, i.e. the same error as used by Harris and Casetti-Dinescu) in the initial r value, and δr is the difference between the initial r value (non-altered) and the new initial r value (the r value with the error either added or subtracted). Dinescu et al., (1999) state that they use an error of 10% in the globular clusters' positions, since they chose 'their distance errors to have a normal distribution with a representative standard deviation'. This was due to there being a systematic error in the position values found using Hipparcos, which varied with cluster metallicity, and foreground extinction also contributes to the distance errors.

With their non-altered initial positions they obtained a $r_{sep,min}$ of 10.1 pc, however when I varied their initial positions within $\pm$ 1σ (using steps of 0.1σ), they rarely got that close to each other, as can be seen in Figure 11. Nevertheless they had an encounter within 3 pc for certain initial position values. The scaling for the circles used in Figure 11 was set by 5 $\log(\frac{1}{r_{sep,min}})$, this meant that the larger the circle shown here, then the closer the globular clusters got to one another. From this plot we can state that globular cluster collisions depend upon (and are very sensitive to) the initial conditions. Therefore there may be globular cluster collisions occurring in the future, however we are currently unable to predict which ones will occur due to the uncertainties in the globular clusters' initial positions.

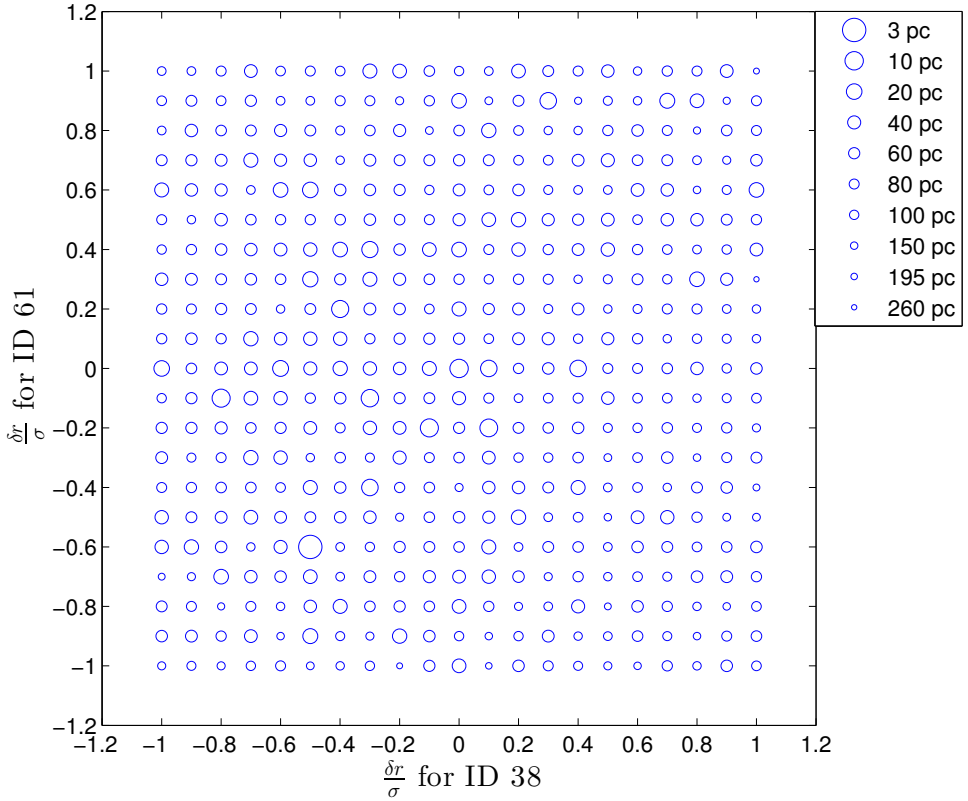

Figure 11: The $r_{sep,min}$ for varying the initial positions of the interaction between ID 38 and ID 61. The simulations were run for 10 Gyr into the future. Many of the interactions resulted in encounters that occurred at larger separations than those found for the unaltered initial positions (i.e. $r_{sep,min} > 10$ pc), however there were a few encounters that occurred at closer separations, with the closest being 3 pc.

I calculated the 2D Gaussian function (created by a product of 2 Gaussian functions), which calculates the probability of an event occurring, and is given by equation (19). I used the 2D Gaussian in order to investigate how likely it is to obtain a certain $r_{sep,min}$ from the various initial positions for the interaction between ID 38 and ID 61. Thus how likely it is that they will collide within the next 10 Gyr. In equation (19), $i = (\delta r_{38}/\sigma_{38})^2$, $j = (\delta r_{61}/\sigma_{61})^2$, and α = 0.49918, which was used to normalise the function (where δr and σ are the same as explained previously). I found the value of α by setting the sum of Ga to be equal to 1, and then I rearranged the equation to find α, since I knew the values of i and j from the previous plot.

$$\mathrm{Ga}(k,l) = \frac{1}{2\pi\alpha}\exp(-\frac{1}{2}[i_k + j_l]) \tag{19}$$

For the $\frac{\delta r}{\sigma}$ values I used those that are plotted in Figure 11, and hence the axes of Figure 12 (left-hand plot) are the same as those used in Figure 11. The left-hand image of Figure 12 shows a plot of the 2D Gaussian function, this shows (via the colour bar, where dark red is the most likely) that the most likely minimum separations were given by the unvaried initial position $\pm 0.2\sigma$. The colour bar gives an indication of how probabilistic it is for an encounter to occur given the initial conditions on the x-y axes. The right-hand image shows how likely the minimum separations are that were obtained by varying the initial positions. As can be seen there is a cumulative probability of 0.8 for an encounter to occur with a separation distance of less than 100 pc. This therefore means that it is very likely that they will encounter each other with a separation within this distance. The cumulative probability was calculated by finding the number of encounters within a given distance and summing up their probabilities [i.e. their G values, as given by equation (19)]. The red curve which has been fitted to the cumulative probability plot is an 8^{th} degree polynomial, which I used to calculate the probability of a collision occurring within the sum of the current tidal radii of ID 38 and ID 61 (i.e. r = 10.24 pc), the result was a probability of 0.005 (found by integrating the equation of the red curve between r = 0 and r = 0.01024 kpc). This therefore means that it is unlikely that ID 38 and ID 61 will collide in the next 10 Gyr, and since they had the closest encounter then this also means that it is rare for globular clusters to collide with each other.

I also investigated what the mean minimum separation was by using equation (20), and from this I obtained a value of 71.5 pc. This value agrees well with the range of values obtained from the right hand image of Figure 12.

$$\bar{r}_{\mathrm{sep,min}} = \frac{\sum r_{\mathrm{sep,min}} \times \mathrm{Ga}}{\sum \mathrm{Ga}} \tag{20}$$

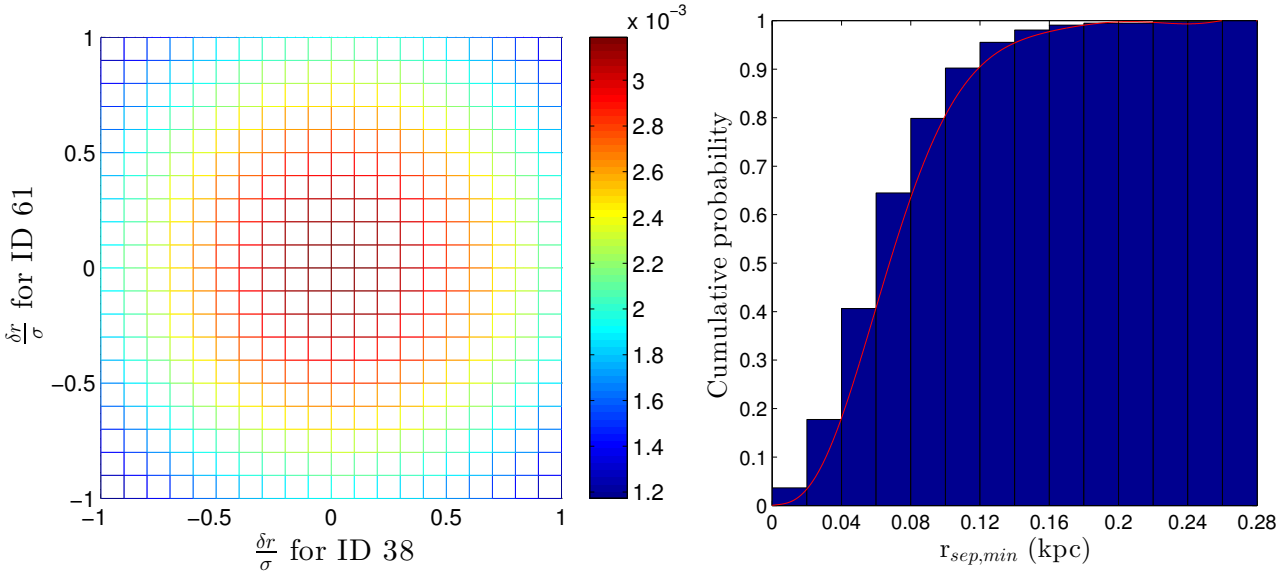

Figure 12: *Left*: The 2D Gaussian of the $r_{sep,min}$ for varying the initial positions of the ID 38 - ID 61 interactions. The colour bar shows how likely it is to acquire a certain $r_{sep,min}$ given the initial conditions on the x-y axes. *Right*: The cumulative probability for the minimum separations that were obtained by varying the initial positions. The probability of an encounter occurring within the sum of the current tidal radii of ID 38 and ID 61 was found to be 0.005. Hence it is unlikely that a collision between these two globular clusters will occur in the next 10 Gyr.

Next I wanted to investigate the effect on the separation distances between ID 38 and ID 61 from varying their initial positions. In order to do this I took a ratio of the separation distances between the encounter of ID 38 and ID 61 + 1σ (where I only changed the initial position of ID 61 by + 1σ) to the separation distance between the encounter of ID 38 and ID 61 (i.e. the unaltered globular cluster separations). The logarithm of this ratio is shown as the black curve in Figure 13, whereas the red curve is for the ratio of when I only changed the initial position of ID 38 by + 1σ and left ID 61 unaltered (i.e. ratio of ID 38 + 1σ and ID 61 to ID 38 and ID 61). The initial unvaried positions mentioned above were taken from Tables 6 and 7. As you can see in Figure 13 there is a very large difference in the ratio around t = 7564 Myr, this was due to there being the occurrence of a very close encounter between ID 38 and ID 61 ($r_{sep} \sim 230$ pc). The consequence of changing the initial positions by $+1\sigma$ for either ID 38 or ID 61 was that the close encounter never occurred.

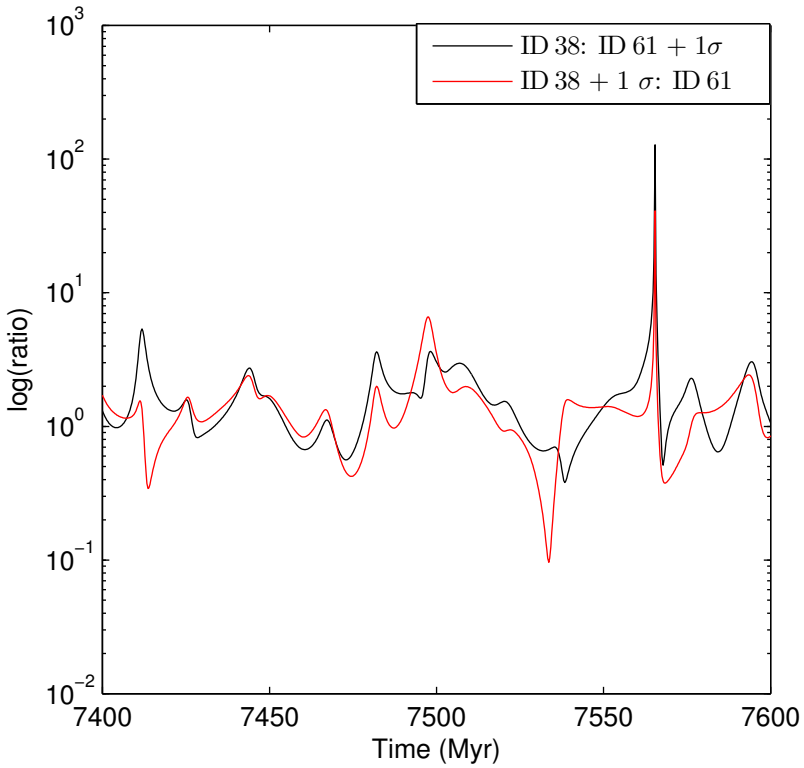

Figure 13: The logarithm of the ratio of the separation distance, where the ratio is between an encounter where one of the globular clusters had 1σ added to its initial position and another encounter where neither globular cluster had 1σ added to their initial position. The red curve is the logarithm of the ratio of the separation of ID 38 +1σ and ID 61 to the separation of ID 38 and ID 61. The black curve is the logarithm of the ratio of the separation of ID 38 and ID 61 +1σ to the separation of ID 38 and ID 61. The peak at t $\approx$ 7564 Myr was caused by there being a very close encounter occurring between IDs 38 and 61, but not occurring in the encounters where one of the globular clusters had 1σ added to their initial positions. The simulation was run for 10 Gyr.

How the orbit of ID 61 changed when I varied its initial position by $+1\sigma$ is shown in Figure 14 below. The blue curve is for ID 61's orbit using the non-altered initial position, the black curve shows ID 61's orbit after I have added 1σ to its initial position, and the red and green stars represent their respective starting positions. This change in its initial position resulted in its orbit being widened. This means that due to the uncertainties in the globular clusters' positions then their orbits are uncertain and hence predicting collisions is therefore dependant upon the initial positions and the respective errors of the globular clusters. The simulation was run for 2 Gyr into the future in order to allow the globular cluster to complete enough of its orbit for analysis.

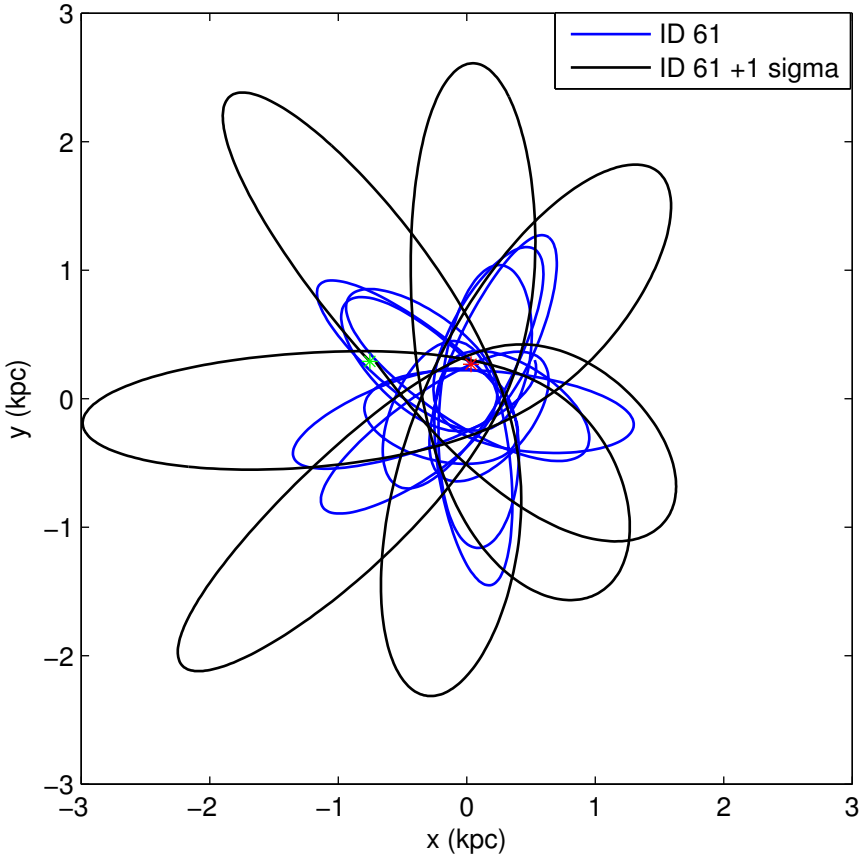

Figure 14: The x-y orbital plot using ID 61's non-altered initial position (shown in blue), with the starting position shown via the red star. How the orbit changed by the addition of 1σ to the initial position is shown in black, with the starting position shown via the green star. Here it can be seen that the overall effect is that the orbit widens, this simulation was run for 2 Gyr into the future.

4.4 Globular cluster encounters - including self interactions

I simulated the 63 Casetti-Dinescu globular clusters orbiting as point masses within the Milky Way's potential and I included the gravitational effects of the globular clusters on each other. I run the simulations for 10 Gyr and investigated how close the globular clusters got to each other and how big of a difference including the self interactions of the globular clusters was. The purpose of Section 4.4 was in order to see if the results from Section 4.3 were reliable and if I could minimise the computational time that would be required for Sections 5 and 6. In Figure 15 is shown how close the globular clusters came to each other within the simulated 10 Gyr. The size of the squares were chosen to be given by $\log\left(\frac{100}{r_{\rm sep,min}}\right)$ in order to allow the closest interactions to be more easily visible, since the majority of the interactions occurred at large separations. I have also used different colours for the different separation distances between the globular clusters, with the colour scheme being the same as previously described. Upon close inspection it can be seen that there are few large squares [magenta] (i.e. interactions with $r_{\rm sep,min} < 40$ pc), however there are many small squares / dots [blue/black] (i.e. interactions with $r_{\rm sep,min} > 5$ kpc). From comparing this plot to the plot in Figure 8, it can be seen that the close encounters, i.e. the encounters within 24 pc did not occur here as they did previously. For example in the case where I did not include the self interaction of the globular clusters the smallest minimum separation was found to be ~ 10 pc, however when I did include the self interaction the smallest minimum separation was found to be ~ 24 pc (between ID 14 [NGC 5139] and ID 35 [NGC 6316]). This therefore implies that despite the mass of the globular clusters being much less than the mass of the Milky Way, the self interaction of the globular clusters is important for the closest encounters.

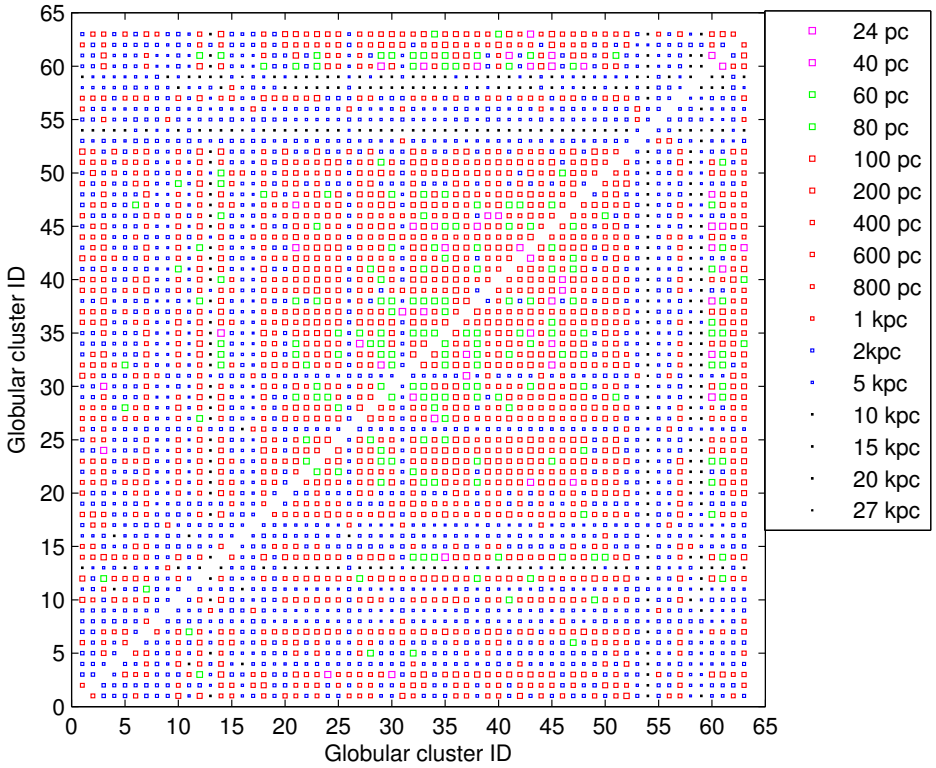

Figure 15: The minimum separation distance ($r_{\rm sep,min}$) between the globular clusters, the simulation was run for 10 Gyr into the future. Here I have included the self interaction of the globular clusters. The size of the squares were given by $\log\left(\frac{100}{r_{\rm sep,min}}\right)$, such that the largest squares are representative of the closest encounters. Here there were no encounters with separations less than 24 pc, unlike in the case where I did not include the self interactions.

Shown below on the left-hand side of Figure 16 is the logarithm of the minimum separation for the globular clusters encountering each other, for the case where I included the self interactions (i.e. the globular clusters are affected by the gravitational forces from every other globular cluster). This simulation was run for 10 Gyr and can be compared to the left-hand plot in Figure 9, which shows a similar plot, but for the case where the self interaction was excluded. From this comparison we can see that when the self interaction was included then there were no interactions within $\sim$ 25 pc, with the closest encounter being between ID 14 and ID 35, which had a $r_{sep,min} \sim 25$ pc. Another effect of including the self interaction was that some of the globular clusters had closer encounters with other globular clusters, however some of the globular clusters had encounters at larger distances than in the case where self interaction was neglected. The overall effect was that the more distant the encounter then the less of an effect it felt from the self interactions. Those with large $r_{sep,min}$ in the case where self interaction was neglected did not have their $r_{sep,min}$ altered by much, unlike those with small $r_{sep,min}$, which may have their values changed drastically. One example is the interaction between ID 38 and ID 61. This effect was expected since the gravitational force between two objects increases as their separation decreases. Hence the two plots look very similar to each other except for the closest encounters, and it is reasonable to neglect the self interaction effects for most of the encounters due to their large separations.

This can also be seen by comparing the two plots on the right hand side of Figures 9 and 16, which show the separation distance in units of the globular clusters' tidal radii. If there are any black dots beneath the red line then this indicates that there was a collision occurring for that globular cluster, i.e. there was an encounter with another globular cluster inside of its current tidal radius. The same trend is shown here as was seen by comparing the two left-hand figures, i.e. that only the closest encounters were affected by the self interaction with the majority of the encounters being unaffected. One thing to notice is that some of the collisions penetrated deeper into the globular clusters' tidal radii here, and would therefore have affected the structure of the globular cluster more than in the case where the self interactions were neglected.

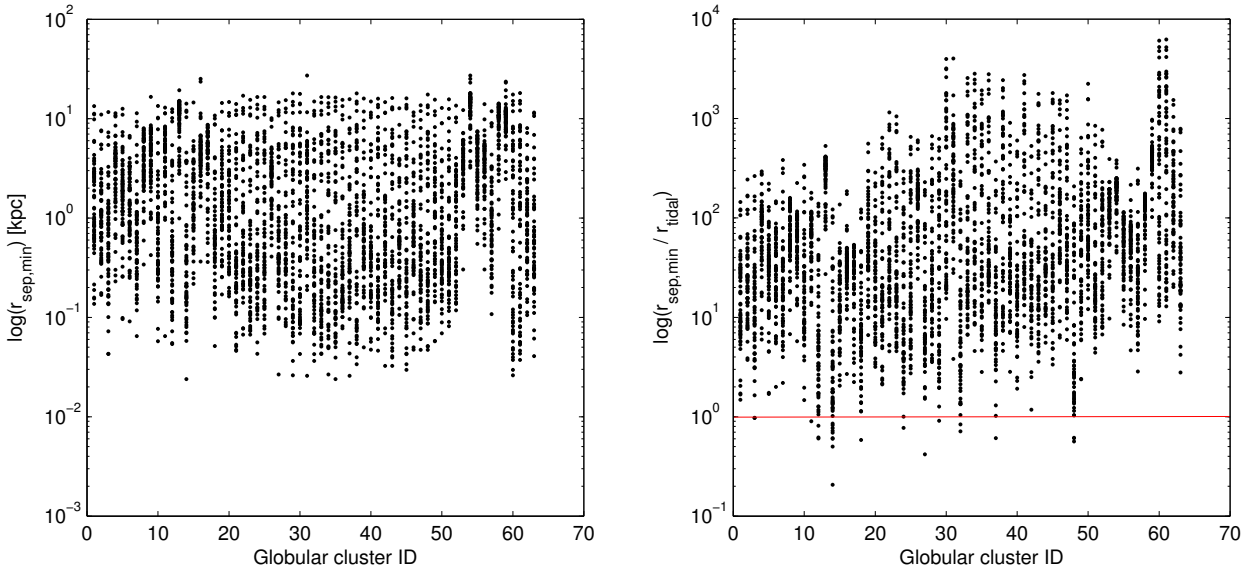

Figure 16: *Left*: Plot of the logarithm of the minimum separation vs the globular clusters' ID numbers, for the globular cluster - globular cluster encounters in the case where I included the effects of self interaction. *Right*: A similar plot to the left hand plot, however the y-axis is in terms of the tidal radius, with the red line indicating that a collision occurs if there is a black dot below it. Both simulations were run for 10 Gyr.

As done in section 4.3, I created a histogram of the number of encounters within 1 kpc, however here I included the effects of the self interaction between the globular clusters. The effect that this had was that there was $\sim 1\%$ more encounters within 1 kpc, and by comparing the left-hand plot shown in Figure 17 to the left-hand plot in Figure 10 it can be seen that there were ~ 20 more encounters within 100 pc. It can also be seen that there were ~ 10 less encounters between 700 - 800 pc, and ~ 20 more encounters between 800 - 900 pc, however the majority of the two plots look very similar to each other.

The right-hand plot in Figure 17 differs a lot from its counterpart in Figure 10, unlike the two left-hand plots. There were more encounters within 0 - 2, 4 - 10, 14 - 16 and 18 - 20 tidal radii, but there were less encounters within 2 - 4, 10 - 12 and 16 - 18 tidal radii (for the case including the self interactions). Despite this there was a similar percentage of collisions occurring i.e. $\sim 1.28\%$ (25 different collisions occurred, with ID 3 and ID 24 both having a collision within each others tidal radius). Like the left-hand plot here, there was also $\sim 1\%$ more encounters within the range of the plot than there was for the corresponding plot shown in Figure 10.

The result of including the self interactions was that, as was expected, there was not much of an effect on the globular clusters and that it is OK to assume that there are no self interactions occurring, as I had the same number of collisions occurring in both cases. However the globular clusters involved in the collisions differed, along with the penetration depth into the tidal radii and the separation distances. Therefore if we are only interested in the probability of a collision occurring and not in which clusters are colliding or the details of the collision, then we can neglect the effects of the self interactions and not lose any important statistics.

The bottom line was that there will be 24 / 25 collisions between the globular clusters in the next 10 Gyr in the cases of where I excluded / included the self-interactions. Hence for the next set of simulations I did not include the self-interaction as it was suitable to assume that the globular clusters did not affect each others orbits much.

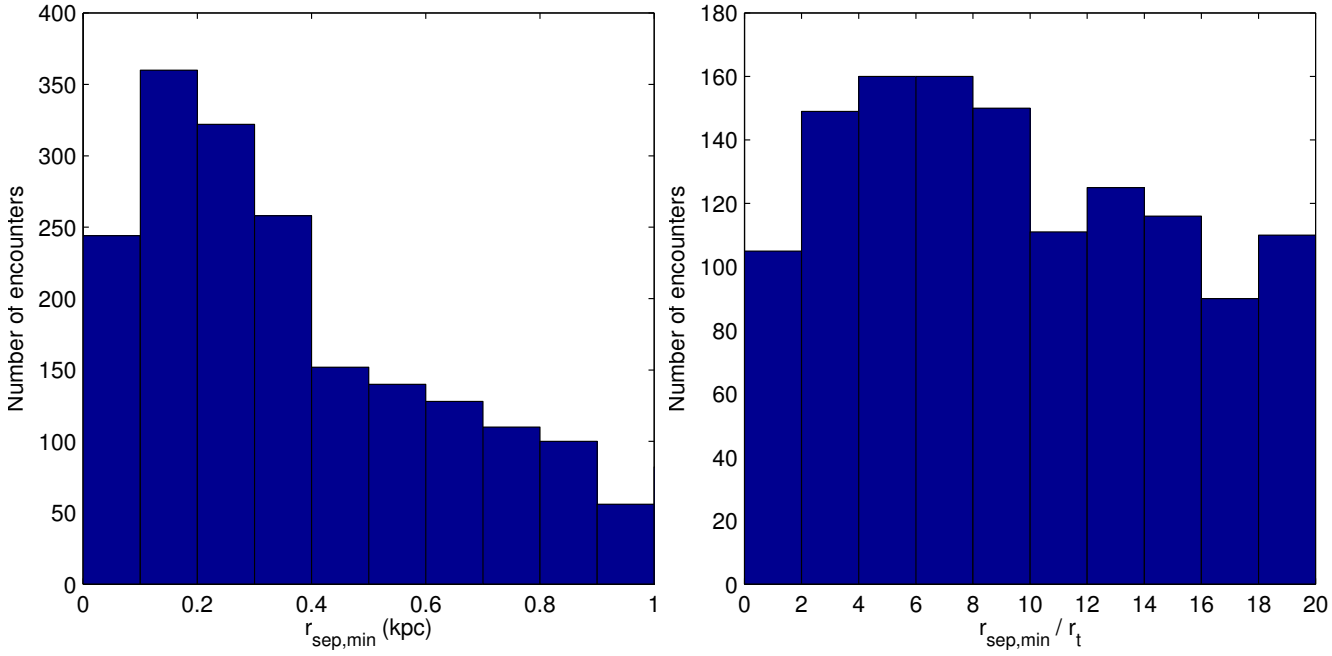

Figure 17: *Left*: Histogram of the number of encounters within 1 kpc as a function of the minimum separation for the globular cluster - globular cluster encounters where I included the effects of the self interactions. *Right*: Similar plot to the left hand plot, however the x-axis is in terms of the tidal radii of the globular clusters.

5 Satellite galaxy - Globular cluster encounters

5.1 Initial conditions

I integrated the orbits of the 11 classical satellite galaxies, along with the 63 Casetti-Dinescu globular clusters inside the potential of the Milky Way for 10 Gyr. The initial conditions for the satellite galaxies were taken from Pawlowski et al., (2013) and Barber et al., (2013). I used the 11 classical satellite galaxies as they would perturb the globular clusters by a greater amount than the other satellite galaxies in the Milky Way would, due to their large masses. I also used this set of satellite galaxies since some of them contained globular clusters within them, such as the Sagittarius dwarf galaxy, the LMC, the SMC, and the Fornax dwarf galaxy, which contain 4, 45, 8 and 5 globular clusters respectively. The 11 classical satellite galaxies are the only satellite galaxies in the Milky Way which have proper motions (i.e. velocities), the other 14 satellite galaxies do not, since they are a lot fainter and hence harder to detect and determine their proper motions.

Throughout Section 5, I considered the gravitational effects of the Milky Way and the satellite galaxies on the globular clusters as well as the gravitational effects of the Milky Way on the satellite galaxies. However I did not consider the gravitational effects on the satellite galaxies or the Milky Way from the globular clusters, nor the gravitational effects of the satellite galaxies on the Milky Way. The reason for this is that when I included the gravitational force of the globular clusters on each other this did not largely affect each others orbits, and hence they will affect the orbits of the satellite galaxies even less. I also simulated the satellite galaxies as point masses for the majority of this section, however in Section 5.5. I simulated the satellite galaxies by using Plummer (1911) potential.

The initial conditions for the satellite galaxies are shown below in Table 3, along with the ID numbers that I used in the simulations.

ID	Name	x (kpc)	y (kpc)	z (kpc)	u (kms^{-1})	v (kms^{-1})	w (kms^{-1})
64	Sagittarius	17.1	2.5	-6.4	233 ± 3	243 ± 9	222 ± 8
65	LMC	-0.6	-41.8	-27.5	-41 ± 11	-5 ± 4	234 ± 5
66	SMC	16.5	-38.5	-44.7	2 ± 17	59 ± 15	149 ± 13
67	Draco	-4.3	62.2	43.2	-59 ± 22	307 ± 13	-261 ± 19
68	Ursa Minor	-22.2	52.0	53.5	7 ± 28	309 ± 19	-186 ± 20
69	Sculptor	-5.2	-9.8	-85.3	-33 ± 44	408 ± 44	-99 ± 5
70	Sextans	-36.7	-56.9	57.8	-168 ± 160	332 ± 134	116 ± 129
71	Carina	-25.0	-95.9	-39.8	-74 ± 43	228 ± 18	40 ± 40
72	Fornax	-41.3	-51.0	-134.1	-38 ± 26	62 ± 26	114 ± 12
73	Leo II	-77.3	-58.3	215.2	101 ± 128	457 ± 158	117 ± 51
74	Leo I	-123.6	-119.3	191.7	-167 ± 31	185 ± 31	96 ± 23

Table 3: The initial conditions of the Milky Way's classical satellite galaxies. Here x is positive outwards from the galactic centre, y is positive towards the galactic rotation, z is positive towards the north galactic pole, and u, v and w are their corresponding velocities.

In Tables 4 and 5 are some of the properties of the classical satellite galaxies. In Table 4 there are listed for each satellite galaxy their: distance (D) from the galactic centre (Barber et al., 2013; M98), absolute velocity ($V_{tot} = \sqrt{u^2 + v^2 + w^2}$), tidal radius [$r_t$, (M98; Subramanian & Subramaniam, 2012; van der Marel, 2006)], half-mass radius[15] [r_h, (Wolf et al., 2010)], and eccentricity (e). In Table 5 there are listed for each satellite galaxy their: mass (M), metallicity ([Fe/H]), absolute luminosity in the visual band [M_V, (Barber et al., 2014; M98)], the number of globular clusters orbiting within them[16] [N_{GC}, (M98)], and the z-component of the angular momentum (j_z). The j_z values[17] in Table 5 were calculated by using $j_z = \underline{r} \times \underline{V}$ = (xv) - (yu).

ID	Name	D (kpc)	V_{tot} (kms^{-1})	r_t (kpc)	r_h (kpc)	e
64	Sagittarius	18 ± 2	403.26	>4.64	0.83	0.63
65	LMC	50 ± 2	238.88	15.00	-	0.61
66	SMC	61 ± 4	160.27	9.50	1.50	0.15
67	Draco	82 ± 6	407.25	0.62	3.10	0.46
68	Ursa Minor	78 ± 3	360.73	1.12	0.64	0.26
69	Sculptor	86 ± 6	421.13	1.91	2.22	0.29
70	Sextans	86 ± 4	232.86	3.99	0.48	0.31
71	Carina	107 ± 6	243.02	0.88	0.88	0.59
72	Fornax	149 ± 12	135.22	3.04	0.94	0.14
73	Leo II	236 ± 14	482.43	0.81	1.02	0.75
74	Leo I	258 ± 15	267.08	0.93	1.20	0.60

Table 4: Properties of the Milky Way's classical satellite galaxies, where D is their galactocentric distance (Barber et al., 2013; M98), V_{tot} is their absolute galactocentric velocity, r_t is their tidal radii (M98; Subramanian & Subramaniam, 2012; van der Marel, 2006), r_h is their half mass radii (Wolf et al., 2010), and e is their eccentricity.

ID	Name	M (10^8 $M_\odot$)	[Fe/H]	M_V	N_{GC}	j_z (kpc^2 Myr^{-1})
64	Sagittarius	1.50	-1.00	-13.5	4	0.51
65	LMC	500	-0.30	-18.1	45	-1.61
66	SMC	4.00	-0.73	-16.8	8	-2.64
67	Draco	3.90	-2.00	-8.8	-	3.37
68	Ursa Minor	0.77	-2.20	-8.8	-	-2.39
69	Sculptor	1.35	-1.80	-11.1	-	-1.33
70	Sextans	0.29	-1.70	-9.5	-	-13.98
71	Carina	0.57	-2.00	-9.1	-	-7.46
72	Fornax	1.45	-1.30	-13.4	5	4.69
73	Leo II	0.64	-1.90	-9.8	-	-12.71
74	Leo I	1.30	-1.50	-12.0	-	-15.95

Table 5: Properties of the Milky Way's classical satellite galaxies, where M is their mass (Sohn et al., 2013; M98; Wadepuhl & Springel, 2011), [Fe/H] is their metallicity, M_V is their v-band absolute luminosity (Barber et al., 2014; M98), N_{GC} is the number of globular clusters orbiting within them (M98), and j_z is the z-component of their angular momentum.

[15]The - mark is used here for the LMC's r_h since I was unable to find a value in the literature search.

[16]From the literature search there were no confirmed globular clusters in the satellite galaxies with the - mark.

[17]In this set-up j_z and energy should always be conserved.

5.2 Example orbits

The left hand image in Figure 18 shows the Fornax dwarf galaxy's R-z orbit, this would be similar to the R-z orbit of ID 1 (shown in Figure 6), but the Fornax dwarf galaxy completed fewer orbits than ID 1 did in 10 Gyr. However given enough time the Fornax dwarf galaxy's R-z orbital plot would appear similar to that of ID 1's R-z orbit. The right hand plot is that of the Sagittarius dwarf galaxy's x-z orbit (a Rosetta orbit), if the Sagittarius dwarf galaxy was also given a long enough time then its x-z orbit would eventually have a similar but not exact appearance to that of ID 1's x-y orbital plot (shown in Figure 7), i.e. the appearance of a tyre. Both plots in Figure 18 are very typical for the orbit of a point mass within the potential that I used for the Milky Way.

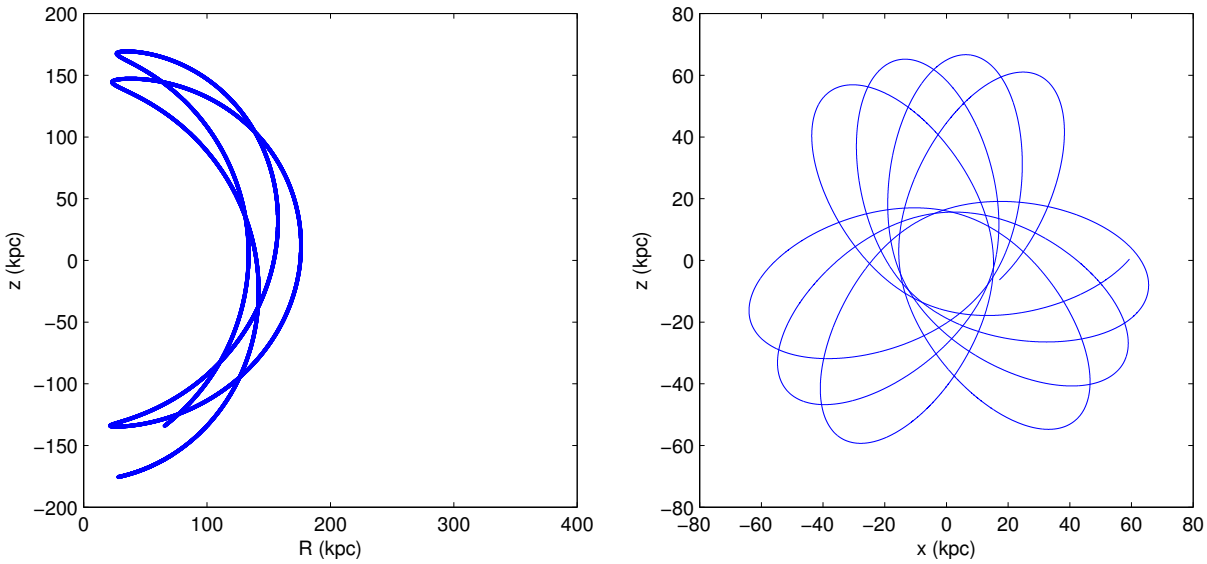

Figure 18: *Left*: R-z orbit of the Fornax dwarf galaxy, this would have had a similar appearance to that of ID 1's R-z orbit shown in Figure 6, however the Fornax dwarf galaxy did not complete as many orbits as ID 1 did. *Right*: x-z orbit of the Sagittarius dwarf galaxy, this shows a typical Rosetta orbit, given enough time it would have a similar appearance as that of ID 1's x-y orbit in Figure 7. Both of these simulations were run for 10 Gyr into the future.

Upon investigation of the j_z values (an indication of the orbital direction of an object) of the satellite galaxies and the globular clusters, I found that 22 globular clusters ($\sim 35\%$ of the globular cluster sample) and 8 satellite galaxies ($\sim 73\%$ of the classical satellite galaxy sample) were retrograde. That is they had negative j_z, which means that they were orbiting in the opposite direction to that of the Milky Way's rotation. The satellite galaxies which were prograde (positive j_z values) were the Sagittarius dwarf galaxy, Draco and the Fornax dwarf galaxy, this could indicate that these have been strongly affected by either the Milky Way and / or other satellite galaxies in order to enable them to orbit in the same direction as the rotation of the Milky Way, since it is believed that accreted objects have retrograde orbits. This is due to the majority of the classical satellite galaxies having retrograde orbits and the majority of the globular clusters having prograde orbits.

5.3 Satellite galaxy - Globular cluster relations

As explained in Section 3, there is evidence that some of the Milky Way's globular clusters may have originated from satellite galaxies that had been tidally disrupted by the Milky Way. One example of this is Pal 12, which has been torn from the Sagittarius dwarf galaxy, the evidence for this was initially from an analysis of its orbit and the orbit of the Sagittarius dwarf galaxy. Other evidence which was found later was that the chemical abundance patterns of Pal 12 matched those of the Sagittarius dwarf galaxy, and Pal 12 is in the Sagittarius dwarf galaxy's tidal debris (Dinescu et al., 2007, and references therein).

Figure 19 shows a plot of the metallicity vs eccentricity for 9 of the 11 classical satellite galaxies (red circles) and the 63 Casetti-Dinescu globular clusters (blue circles). Here I scaled the circles indicating the objects such that their size is equal to $3 \times \log \bar{r}$, where $\bar{r}$ was the time average of the object's distance from the galactic centre throughout the simulation. This meant that the larger the circle then the further from the galactic centre the satellite galaxy or globular cluster spent most of its time. The metallicity, [Fe/H], is the abundance of iron (Fe) divided by the abundance of hydrogen (H) in an object, with respect to the metallicity of the Sun, such that the solar metallicity is 0 on a logarithmic scale. The metallicity is measured using a logarithmic scale, such that a metallicity of 0, -1, or -2, means that the object has the same, a 10^{th}, or a 100^{th} of the Sun's metallicity. I did not include the two Leo dwarf galaxies here, as they had very large distances from the galactic centre. From this plot I found that all the satellite galaxies which contain globular clusters have a metallicity greater than -1.3. It can also be seen that most of the globular clusters have small circles, however some have circles which are almost as large as some of the satellite galaxies'. The globular clusters with the large circles could be an indication that they have been accreted from satellite galaxies and are 'halo' clusters.

One thing that is clear in this plot is that there seems to be a distinction between the eccentricities of the globular clusters and the satellite galaxies, with there being a large amount of globular clusters with eccentricities between ~ 0.7 and 1, whereas there are no satellite galaxies in this range. These globular clusters could have been donated to the Milky Way by satellite galaxies that have now been tidally destroyed and hence do not appear on this plot (see Section 6 for more details). The reasoning behind this is that satellite galaxies which are on very eccentric orbits will feel a stronger tidal force from the Milky Way, as their periapsis is closer to the galactic centre and thus they would be tidally disrupted in 2 - 3 perigalactic passages (4 - 6 Gyr, [Dinescu et al., 2001]). Note however that I did not include the Leo satellite galaxies (due to their large distance from the galactic centre) nor the non-classical satellite galaxies (since I did not have their proper motions).

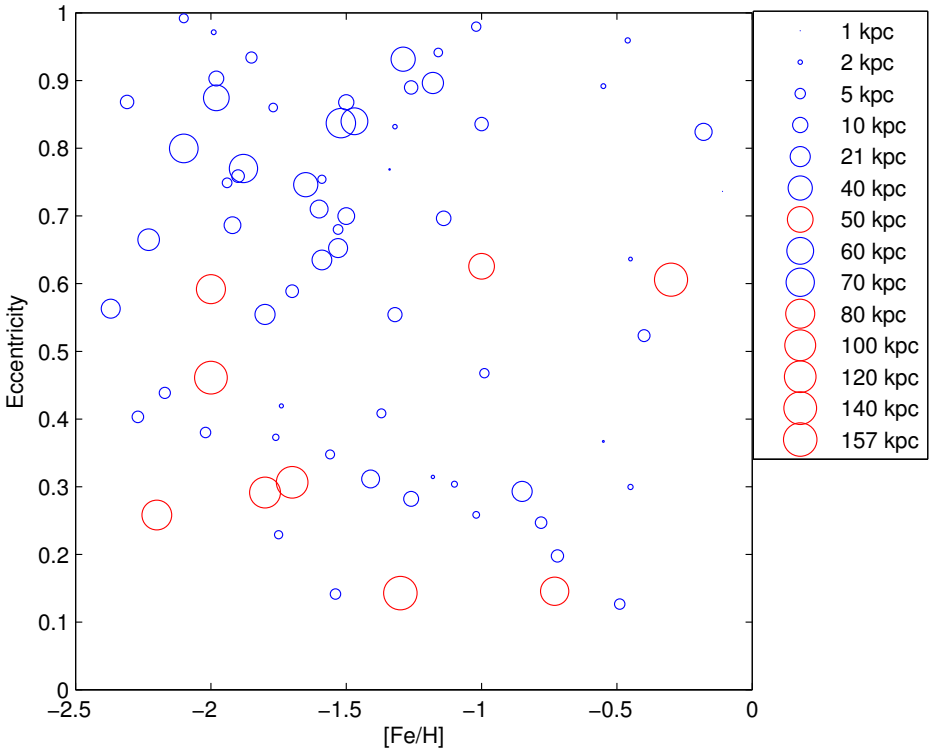

Figure 19: The metallicity against eccentricity for the Casetti-Dinescu globular clusters (blue circles) and the Milky Way's classical satellite galaxies (red circles). The size of the circles is proportional to the mean separation from the galactic centre. As can be seen the satellite galaxies have larger circle sizes (i.e. spend most of their time at larger distances from the galactic centre) than most of the globular clusters, however some of the globular clusters have circles of almost equal size to the satellite galaxies', and thus they may have been accreted to the Milky Way. This simulation was run for 10 Gyr.

The strength of a collision between two globular clusters or a globular cluster and a satellite galaxy (or in the next section a satellite galaxy and the Milky Way) is dependant upon their separation distances. As defined earlier, a collision is an encounter between two objects, where one of these objects comes within the tidal radius of the other. Depending on the extent of the collision, stars or globular clusters may be tidally stripped from the globular cluster or satellite galaxy. However as can be seen in Figure 20, due to the large distances between the globular clusters and the satellite galaxies it is rare for collisions to occur, even on timescales of billions of years. Figure 20 is representative of the distances between the Casetti-Dinsecu globular clusters (blue circles / dots) and the classical satellite galaxies (red circles / dots) used in this simulation. I also used the size of their tidal radii to give the size of their circles shown here, and the objects are located at their current x-y positions, therefore this plot is to scale.

Although the globular clusters appear to be highly concentrated and near each other in this figure, they are also small in comparison to their separations from each other, and hence the likelihood of a collision is small, as was found in Section 4. However it should be noted that I did not include every satellite galaxy (or globular cluster) contained within the Milky Way, only the classical satellite galaxies (and the Casetti-Dinescu globular clusters) were included. This would not drastically affect the likelihood of a collision occurring between the satellite galaxies since there would still be large separations between them, and the satellite galaxies which are not included here are typically less massive and hence smaller than those included here. Similarly for the globular clusters there would still be large separations between them if I had included all 157 globular clusters. Therefore due to their large separations and small sizes collisions between satellite galaxies and globular clusters, or amongst themselves should be uncommon.

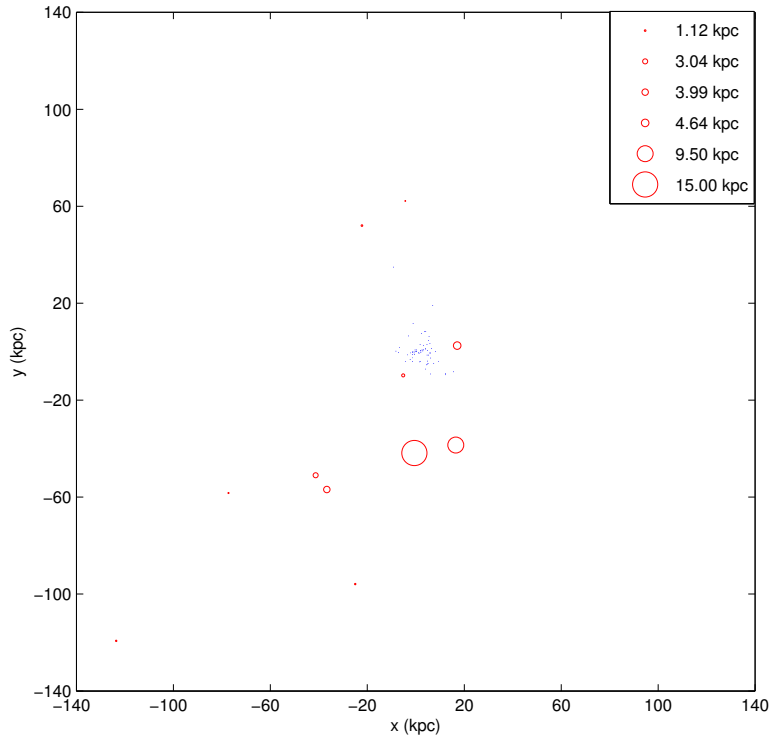

Figure 20: The distance between the circles (satellite galaxies shown in red, and the globular clusters shown in blue) is representative of the true separation between the satellite galaxies and globular clusters. The size of the circles are the size of their tidal radii for the scale of the plot (i.e. this plot is to scale). It can therefore be seen that it is uncommon for globular clusters and satellite galaxies to collide due to their large separations and their small sizes.

5.3.1 Effects of the satellite galaxies' gravitational interactions

Shown in Table 10 (displayed in Appendix 2) are the minimum and maximum distances from the galactic centre (i.e. the pericentre and apocentre values) that the globular clusters (shown in blue) and the satellite galaxies (shown in red) obtained during the 10 Gyr simulation of their orbits, where I included the gravitational interaction between the satellite galaxies and the globular clusters. Figure 21 shows on the left-hand side, the graphical version of Table 10, and the right-hand plot in Figure 21 depicts the pericentres (r_{min}) and apocentres (r_{max}) that the globular clusters and satellite galaxies obtained when I did not include the gravitational interactions. In both plots I did not include the two Leo satellite galaxies, as their orbits did not overlap with any of the globular clusters' orbits, due to the Leo satellite galaxies being very far from the galactic centre. In Table 11 (shown in Appendix 2) I measured the differences that I obtained when I compared the values of the pericentres and apocentres for when I took the gravitational interaction between the satellite galaxies and globular clusters into account and when I did not (i.e. the difference between the left hand plot and the right hand plot in Figure 21). From these values and comparing the plots in Figure 21, it can be seen that there was little difference for most of the objects, however for ID 13 there was a large difference in its apocentre, with its r_{max} changing by -107.19 kpc. This was calculated by subtracting the values from when I did take the gravitational interaction between the satellite galaxies and the globular clusters into account, from the values where I didn't take those interactions into account. Hence if the sign of the difference is negative (or positive), then it implies that the globular cluster had a more (or less) eccentric orbit in the case where gravitational interactions were neglected (or taken into account).

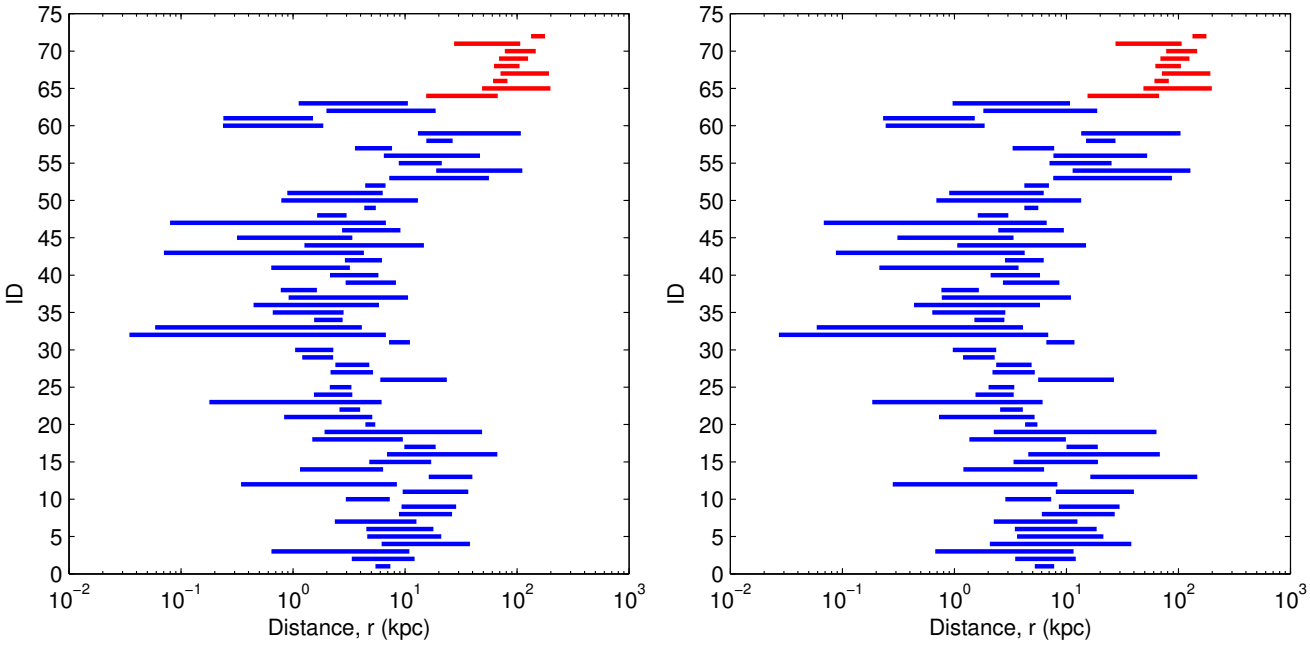

Figure 21: *Left*: The perigalactic and apogalactic distances of the globular clusters (shown in blue) and the satellite galaxies (shown in red). I did not include the two Leo satellite galaxies, as their orbits did not overlap with any of the globular clusters' orbits. *Right*: This is similar to the left-hand plot, however here I neglected the gravitational effects from the satellite galaxies. Both of these simulations were run for 10 Gyr into the future. As can be seen there was not much difference in these plots, with the exception of ID 13's apogalactic value, which changes a lot in the right-hand plot.

Shown in Figure 22 are the effects on the orbit of globular cluster ID 13, for when I took into account only the gravitational interaction between the globular cluster and the Milky Way (shown by the left plots) and when I also included ID 13's gravitational interaction with the 11 classical satellite galaxies (shown on the right side). The two right-hand plots remained the same for when I only used the Sagittarius dwarf galaxy and the LMC instead of all 11 classical satellite galaxies. This was due to the Sagittarius dwarf galaxy and the LMC being the closest satellite galaxies to the galactic centre, and that they are more massive than most of the other satellite galaxies. They also had closer encounters with ID 13 than any of the other classical satellite galaxies, with $r_{sep,min}$ = 9.75 and 9.46 kpc for the Sagittarius dwarf galaxy and the LMC respectively (these were also the only two encounters with ID 13 that occurred within 10 kpc). The $r_{sep,min}$ for the other satellite galaxies ranged from 12.98 kpc to 88.89 kpc (where I ignored the $r_{sep,min}$ of the two Leo satellite galaxies for the reasons mentioned previously). As can be seen in Figure 22, there was a drastic change in ID 13's orbit in the y-z plane due to the two gravitational interactions with the satellite galaxies, which also caused a change in its R-z orbital plot. This is a good example of how a globular cluster's orbit can be changed by gravitational interactions with satellite galaxies, however most of the globular clusters' orbits were not affected this drastically. For example the change in ID 13's apogalactic value was by -107.19 kpc, whereas the next largest change was in ID 53's apogalactic value by -31.40 kpc.

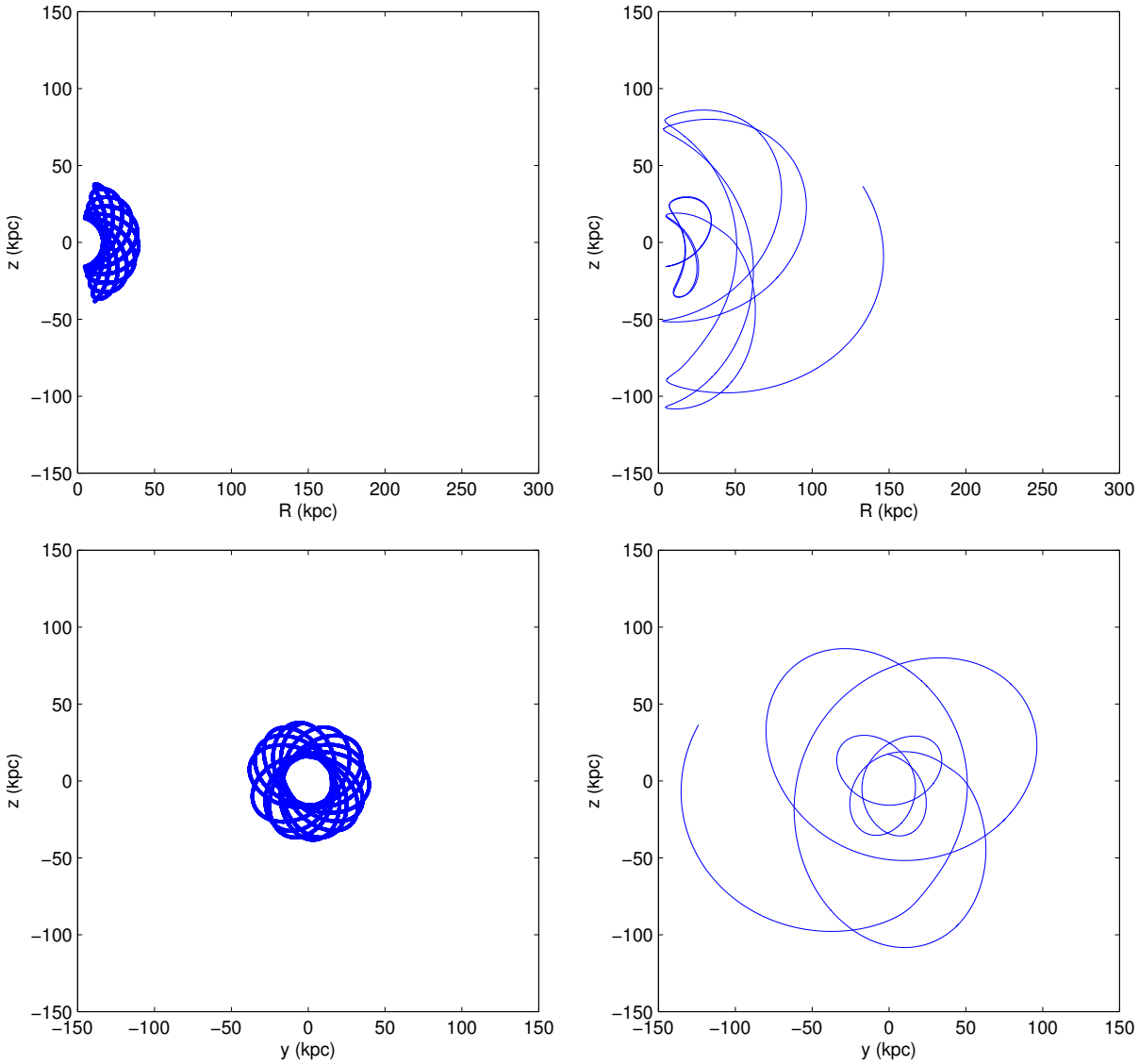

Figure 22: *Left*: R-z (top) and y-z (bottom) plots of ID 13 when I did not include the effects of gravity from the satellite galaxies on the globular cluster. *Right*: R-z (top) and y-z (bottom) plots of ID 13, for when I included the gravitational effects of the 11 classical satellite galaxies on the globular cluster. This plot stays the same if I only include the gravitational interactions of the Sagittarius dwarf galaxy and the LMC, since these 2 satellites had 2 close encounters with ID 13. Despite ID 13's extreme change in its orbit, the majority of the globular clusters' orbits were barely perturbed. These were all simulated for 10 Gyr into the future.

5.4 Satellite galaxies as point masses

From my simulation of the 11 classical satellite galaxies gravitationally interacting with the 63 Casetti-Dinescu globular clusters, I investigated the minimum distance ($r_{sep,min}$) that they came to each other. These results are shown below on the left-hand side of Figure 23, as can be seen there was only one instance where a satellite galaxy (the SMC) and a globular cluster (ID 54) got extremely close to each other (in comparison to the other encounters). This is shown by the lowermost dot, which had a minimum separation of $\sim$230 pc. The other $r_{sep,min}$ were at distances greater than 1 kpc, with the majority between 10 kpc and 100 kpc. The encounter between the SMC and ID 54 occurred at t = 362 Myr, with a relative velocity of $\sim$ 340 kms^{-1}, meaning that they were most likely travelling in opposite directions, since the typical velocity in the Milky Way is around 200 kms^{-1}.

Almost all of the Leo satellite galaxies' $r_{sep,min}$ were greater than 100 kpc, whereas the Sagittarius dwarf galaxy had many small ($<$ 10kpc) $r_{sep,min}$, this was due to their proximities to the galactic centre. In Figure 23, the satellite galaxies are numbered according to their positions in Table 3. The right-hand plot of Figure 23 shows how many globular clusters came within the satellite galaxies' tidal radii (r_t), if a globular cluster came within the tidal radius of a satellite galaxy then its dot is located below the red line. As can be seen there was one interaction (i.e. the one between the SMC and ID 54) which was far inside the tidal radius of the SMC. If this interaction was to occur then it would drastically affect the composition of the globular cluster, i.e. the system may be tidally disrupted. Also there were a few collisions between the Sagittarius dwarf galaxy and other globular clusters, thus suggesting that some of the globular clusters may be tidally disrupted (i.e. the stars are not gravitational bound to each other any more) and contribute their stars to the Milky Way.

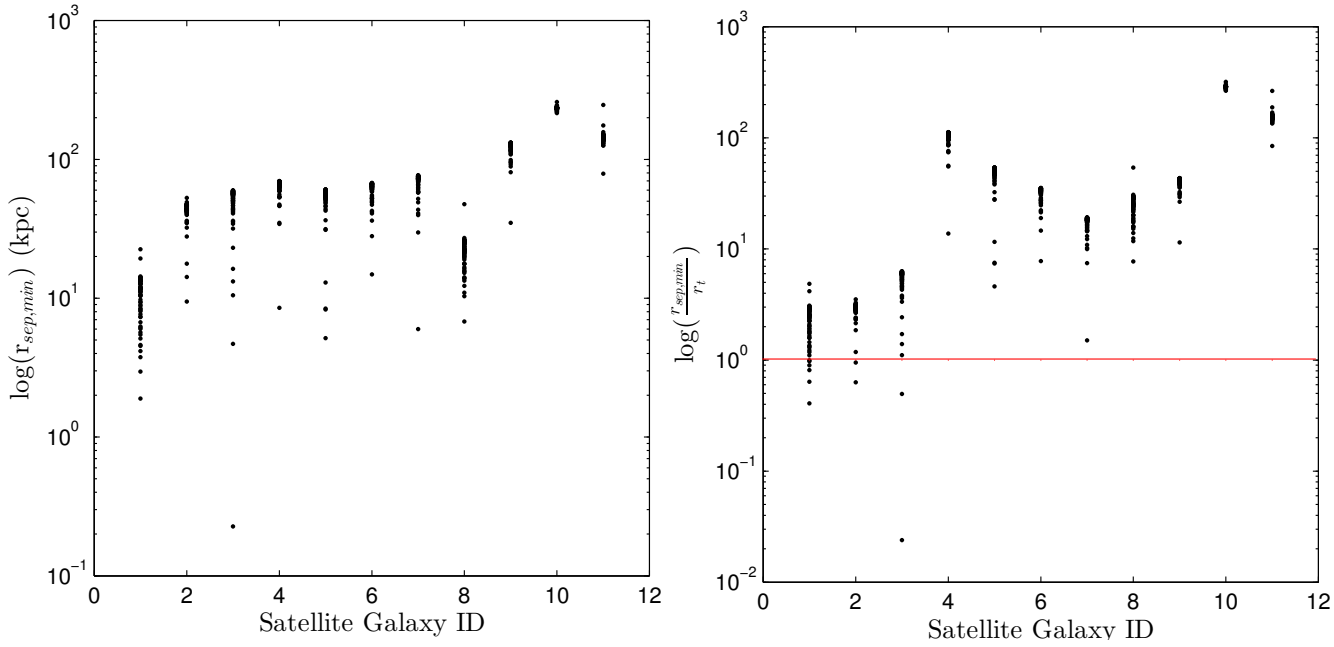

Figure 23: *Left*: The log($r_{sep,min}$) for each satellite galaxy and globular cluster encounter, as can be seen there are not many $r_{sep,min}$ that are less than 10kpc, with only one (SMC - ID 54) being less than 1 kpc. *Right*: The log($\frac{r_{sep,min}}{r_t}$) indicates to what extent the globular clusters came within the satellite galaxies' tidal radii. Any globular clusters below the red line would have had a collision with that satellite galaxy. On the x-axes the satellite galaxies are numbered according to their position in Table 3. This simulation was run for 10 Gyr into the future.

I created a histogram of the number of encounters that occurred within a certain $r_{sep,min}$, and another histogram which showed the number of encounters that occurred within a certain number of tidal radii. This was used to see if there was an $r_{sep,min}$ at which there was a peak in the number of encounters occurring. As can be seen from the left-hand image in Figure 24, there were more ($\sim 30\%$) close encounters around 30 - 60 kpc, and there were very few around 150 - 210 kpc ($\sim 1.4\%$). The right-hand image in Figure 24 shows that, there was a large peak of encounters within 10 tidal radii of the satellite galaxies. Upon inspection of this peak it was found that there was another peak that occurred around 2 - 3 tidal radii. This peak was of equal size to the other peaks shown here (i.e. ~ 70 encounters). The right-hand histogram is a 'zoomed in' version of the original histogram, which went out to 350 tidal radii, however the original histogram did not show any trend that is not well displayed in this image. Similarly to the results found in Section 4.3, there are very few collisions occurring (in this case between globular clusters and satellite galaxies). There was found to be around 1.4% (10 out of 693) of all encounters which ended up in collisions. Therefore collisions of satellite galaxies with globular clusters are more common (percentage wise) than globular clusters colliding amongst themselves. However there are fewer collisions occurring between the satellite galaxies and the globular clusters compared to the number of collisions occurring between the globular clusters. This is mainly due to there being a large number of globular cluster - globular cluster encounters (3906) compared to the number of globular cluster - satellite galaxy encounters (693).

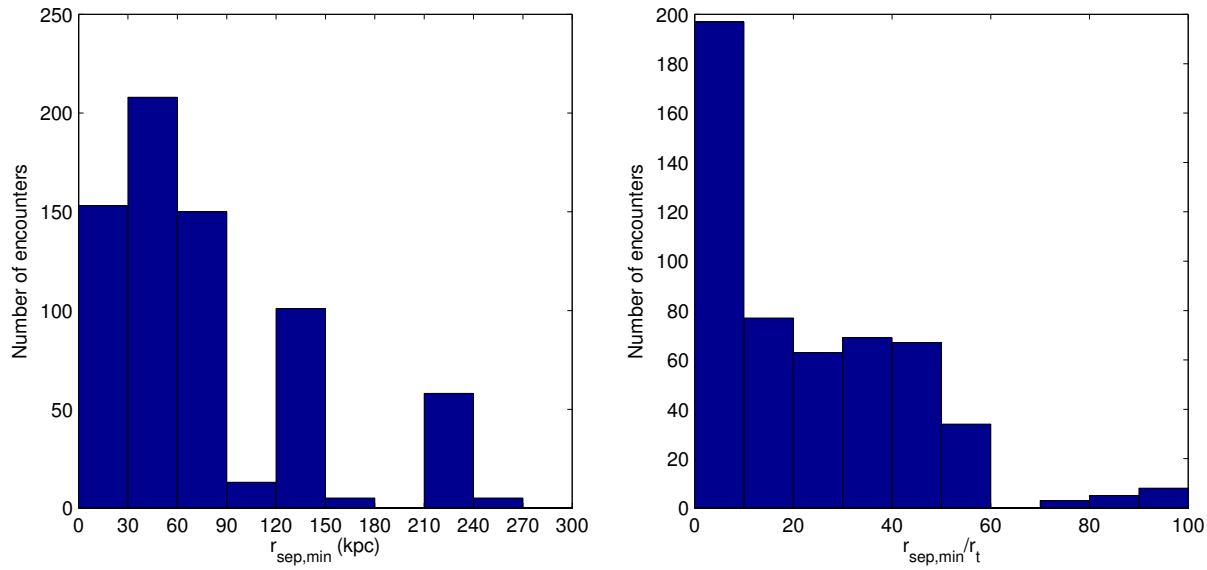

Figure 24: *Left*: Histogram of the number of close encounters as a function of $r_{sep,min}$ between the satellite galaxies and the globular clusters. There were many encounters within 60 kpc ($\sim 52\%$), and few beyond 150 kpc ($\sim 12\%$), due to the Leo satellite galaxies being far from the globular clusters (which were primarily within 30 kpc of the galactic centre). *Right*: Histogram showing the number of encounters that occurred within 100 tidal radii of the satellite galaxies. There were many encounters within 10 tidal radii ($\sim 28\%$), and very few past 60 tidal radii ($\sim 3\%$), for the reason discussed previously. There was found to be roughly 10 (1.4%) collisions occurring in the 10 Gyr simulated.

The closest encounter in the simulations of the satellite galaxies interacting with the globular clusters was between ID 54 and the SMC, where they obtained a $r_{sep,min}$ of 227 pc. The logarithm of their separation distance as a function of time is shown in Figure 25, as can be seen they only get very close once and then they never get within $\sim$ 8 kpc again. Ergo this could just be a 'lucky' encounter, since they spend the majority of their orbits at separations of $\sim$ 80 kpc. This could imply that the close encounter is susceptible to changes in the initial conditions (i.e. the close encounter may not occur if I vary the initial conditions).

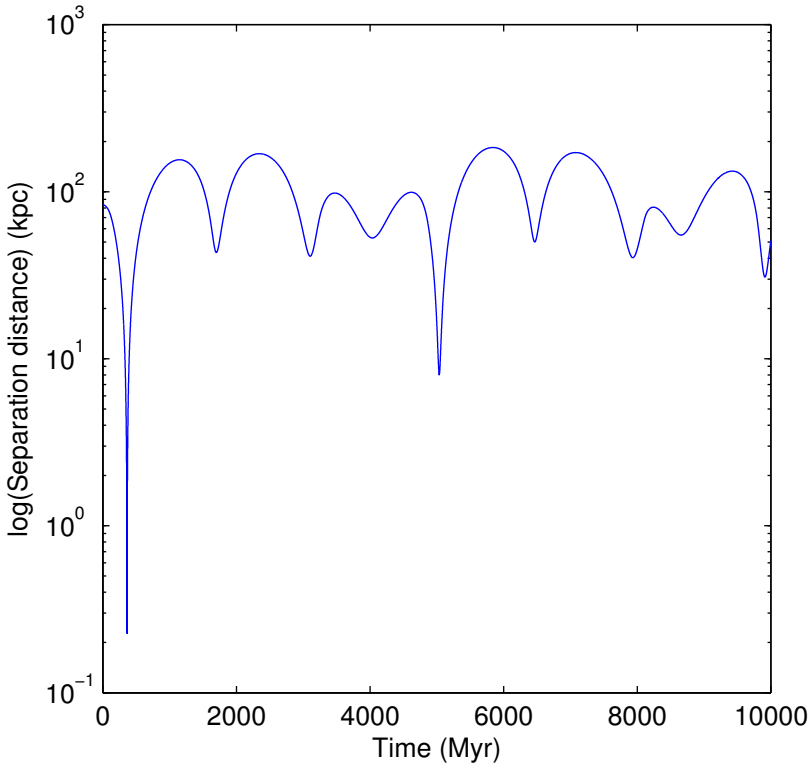

Figure 25: How the logarithm of the separation distance between ID 54 and the SMC varied over the simulated time of 10 Gyr. As can be seen there is only 1 very close encounter throughout the entire simulation and they never get within $\sim$ 8 kpc of each other again. The closest that they get to each other is 227 pc, this is a lot closer than any of the other globular cluster - satellite galaxy encounters, whose next closest encounter is $\sim$ 1 kpc.

5.4.1 Varying the initial positions

Shown in Figure 26 are plots of the orbits of ID 54 in the x-y plane, the blue curve represents its orbit due to the gravitational effects of the Milky Way and the 11 classical satellite galaxies. The black orbit was due to the same gravitational effects, however I changed the initial position of ID 54 by $+1\sigma$, whilst I kept the initial position of the SMC unchanged. Likewise the red orbit was due to the gravitational effects of the Milky Way and the 11 classical satellite galaxies on the orbit of ID 54 (using its original position), but here I changed the initial position of the SMC by $+1\sigma$. The apparent result of adding 1σ to the initial position of either object seems to be that the orbit of the globular cluster will 'expand', likewise if I subtracted 1σ from the initial positions then the globular cluster's orbit would 'shrink'. This further implies that the initial conditions of both the globular clusters and satellite galaxies must be well known in order to predict whether they will collide in the future or not.

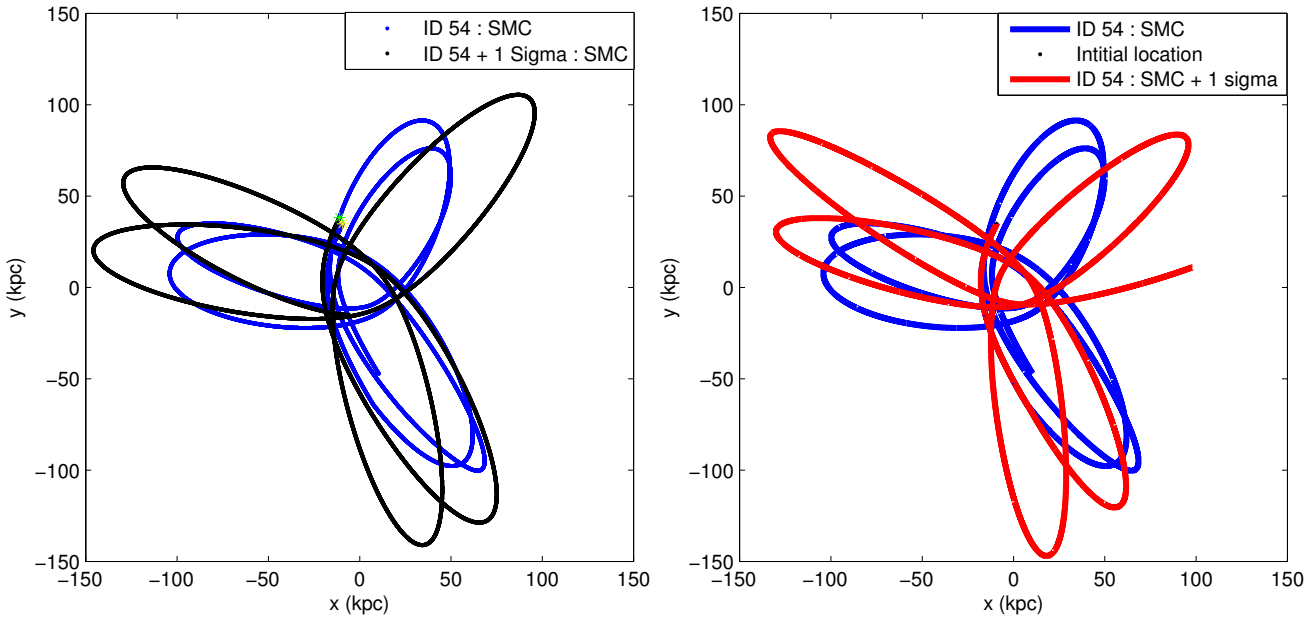

Figure 26: *Left*: x-y plot of the orbit of ID54 (shown in blue), and that of ID54 where I added 1σ to its initial position (shown in black). The initial starting positions are shown by the yellow and green stars respectively. *Right*: x-y plot of the orbit of ID54 (shown in blue), and that of ID54 where I added 1σ to the SMC's initial position (shown in red). The initial starting location of ID 54 is shown by the black circle. Both of these simulations were run for 10 Gyr into the future. The effect of adding (or subtracting) 1σ from the initial position of ID 54 or the SMC was that ID 54's orbit 'expanded' (or 'shrank').

I created a logarithmic plot of the ratio of the separation distances for two encounters vs time, which is shown below in Figure 27. The first encounter for the black (red) curve was between ID 54 + 1σ and the SMC (ID 54 and the SMC + 1σ), and the second encounter was between ID 54 and the SMC. In this plot I have varied the initial positions of both the SMC and ID 54 in order to ascertain how the separation distance would be affected. The black curve is for when I have only altered the initial position of ID 54 by +1σ, and the red curve is for when I have only altered the initial position of the SMC by +1σ. We can see that by changing these initial positions it drastically changes the separation distances, for instance at t $\approx$ 362 Myr, where there is a peak in the red curve (and a smaller peak in the black curve). This was caused since there was an encounter of roughly 25 times the separation distance of the encounter of the unvaried globular cluster pair. i.e. the $r_{sep,min}$ for the red curve was $\sim$ 5.64 kpc instead of $\sim$ 0.227 kpc for the unvaried initial positions' interaction. We can also see that the red and black curves started off very similarly but they diverged over longer periods of time due to their different orbits from their different initial conditions (i.e. small differences added together to produce a large difference).

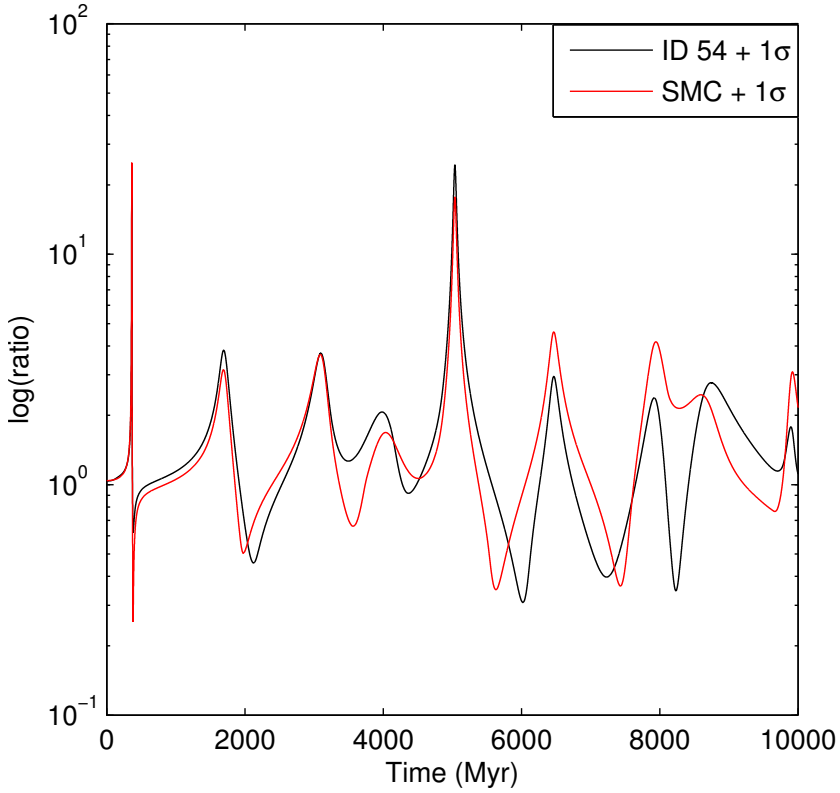

Figure 27: logarithmic plot of the ratio of the separation distances for two encounters vs time. The first encounter for the black (red) curve was between ID 54 + 1σ and the SMC (ID 54 and the SMC + 1σ), and the second encounter was between ID 54 and the SMC.

In Figure 28 is shown how the $r_{sep,min}$ varied depending on how the initial positions were changed. The $r_{sep,min}$ for the unaltered initial positions was 227 pc, however when the initial positions were changed I was able to acquire a $r_{sep,min}$ of 13 pc, although most of the encounters had $r_{sep,min} > 1$ kpc. The scaling for the plot was such that the marker size was set to $4\times\log(20/r_{sep,min})$, this enabled the plot to show the small separations as large circles (and the large separations as small circles), and hence the plot was not over crowded. As can be seen there appears to be a diagonal band across the figure, where the closest encounters occurred. This plot further compounds the ideas brought up previously, where I hypothesised that the close encounters were susceptible to changes in the initial conditions and that until the initial positions of the satellite galaxies and the globular clusters are known well we cannot accurately predict whether they will collide or not.

The recently launched Gaia satellite should increase the accuracy of the positions of the satellite galaxies and globular clusters. According to Windmark et al., (2011) the LMC has a relative uncertainty in its position of currently 5%, however with the results from Gaia this uncertainty could become as small as 0.3%. Also according to Cacciari (2009) 'Gaia will obtain mean distance to all globular clusters up to 30 kpc, and hence their RR Lyraes', to better than 1% (by averaging the individual parallaxes of thousands of cluster members)'. Therefore if this project was repeated, but with the data from Gaia then the results would be a lot more accurate and reliable, and hence we would be able to predict whether satellite galaxies and globular clusters would have collisions with much more conviction.

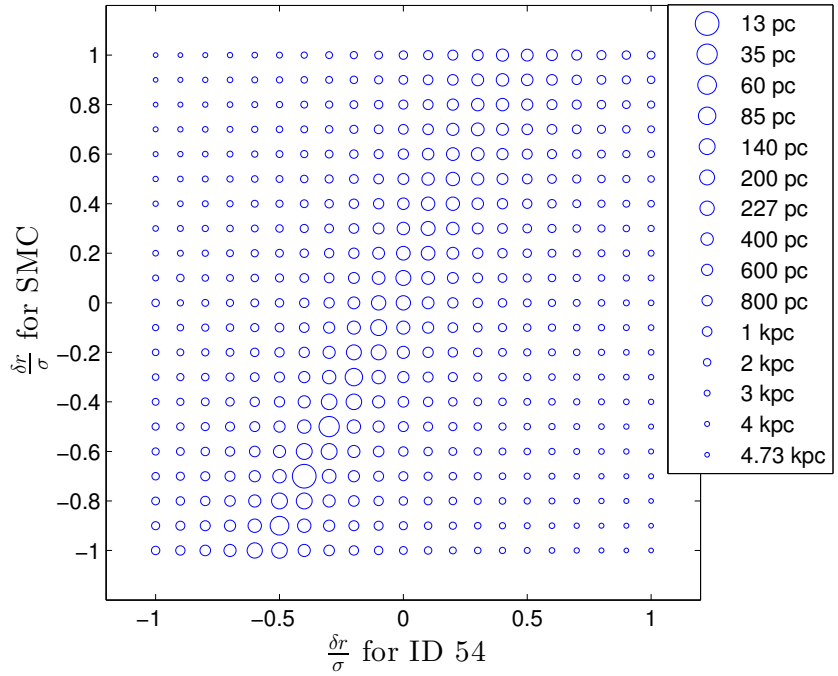

Figure 28: How varying the initial positions of ID 54 and the SMC can change the $r_{sep,min}$. For the unaltered initial positions the $r_{sep,min}$ was 227 pc, but when I altered the initial positions I obtained a closer encounter of 13 pc. However most of the encounters were at larger separations than that obtained from the unaltered initial positions. This simulation was run for 10 Gyr into the future.

I calculated the 2D Gaussian using equation (19) for the interaction of the SMC with ID 54, where I varied the initial positions (as previously discussed) and I measured the $r_{sep,min}$ for each case. I then created a plot of this, which is shown on the left-hand side of Figure 29. This is exactly the same as that which I obtained in Figure 12, since this plot uses the same axis, and hence both i and j are the same for both cases. However the values used to calculate i and j were different, since in Figure 12 I used ID 38 & ID 61, whereas here I used the SMC and ID 54. The right-hand image shows how likely the minimum separations are that were obtained by varying the initial positions. As can be seen there is a cumulative probability of 0.8 for an encounter within 2.6 kpc, and a probability of 0.44 for an encounter within approximately 1.5 kpc (i.e. the SMC's r_h). The mean $r_{sep,min}$ was calculated using equation (20), and was found to be 1.63 kpc, which is in agreement with the fitted curve. As I did for the globular clusters encountering each other I calculated the probability of an encounter within the sum of the tidal radii of the SMC and ID 54, this gave a value of 1 since all of the encounters were within the tidal radius of the SMC. This was due to the SMC having a large tidal radius of 9.5 kpc, and all of the $r_{sep,min}$ values were smaller than 4.73 kpc. However the tidal radius of the SMC shrinks as the SMC's separation from the galactic centre decreases. Despite this, the distance from the galactic centre that this encounter occurred at was 69.46 kpc, consequently the tidal radius of the SMC would have been larger than 9.5 kpc and hence the collision would still occur. This therefore means that assuming that all of the closest encounters occurred at the same distance from the galactic centre, then there should be a collision between ID 54 and the SMC in the future, if their initial positions are correct to within $\pm 1\sigma$.

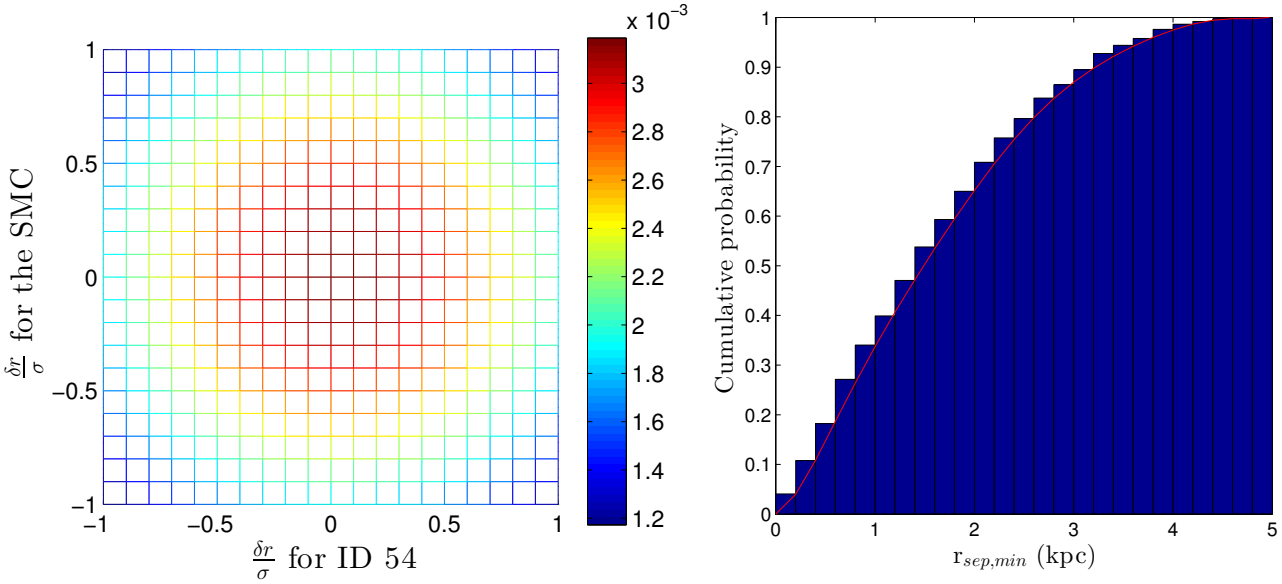

Figure 29: *Left*: Plot showing the 2D Gaussian for the $r_{sep,min}$ where I varied the initial positions for ID 54's interaction with the SMC. This shows how likely it is that I would acquire these $r_{sep,min}$ for a given set of initial conditions. The colourbar is indicative of their probabilities, with the dark red being the most probabilistic. *Right*: How the cumulative probability changes for the minimum separations that were obtained by varying the initial positions for the same interaction, with the most likely $r_{sep,min}$ being within 2.6 kpc (cumulative probability of 0.8).

5.5 Satellite galaxies simulated with potentials

I next wanted to investigate how the minimum separations from the satellite galaxy - globular cluster encounters were affected by modelling the satellite galaxies as distributed masses (i.e. using a Plummer [1911] potential) instead of point masses. The potential that I used is given by equation (21), which is shown in Section 6.1.1, however I used the mass of each of the satellite galaxies instead of the Sagittarius dwarf galaxy, and the reference system was with respect to the satellite galaxy.

The plots shown in Figure 30 are the corresponding plots to those displayed in Figure 23, with the only difference being that the satellite galaxies were modelled as point masses and not distributed masses in Figure 23. By comparing the left-hand plots of Figures 23 and 30, it can be seen that some of the previously close interactions became closer interactions, for example Sextans (satellite galaxy ID 7). However some of the previously close encounters became more distant encounters, such as Ursa minor (satellite galaxy ID 5). Despite this there was still the very close encounter between the SMC and ID 54, albeit the interaction was slightly closer here than in Section 5.4, with a $r_{sep,min} \sim 220$ pc (compared to the previous value of $r_{sep,min} \sim 227$ pc). From comparing the right-hand plots in Figures 23 and 30, we see that the same trend occurs here as it did in the left-hand plots. This therefore suggests that modelling the satellite galaxies as point masses is a good assumption, since not much information was lost and the results were almost the same as if one modelled the satellite galaxies using a potential. Hence the results derived from Section 5.4 are sufficient for the study conducted here.

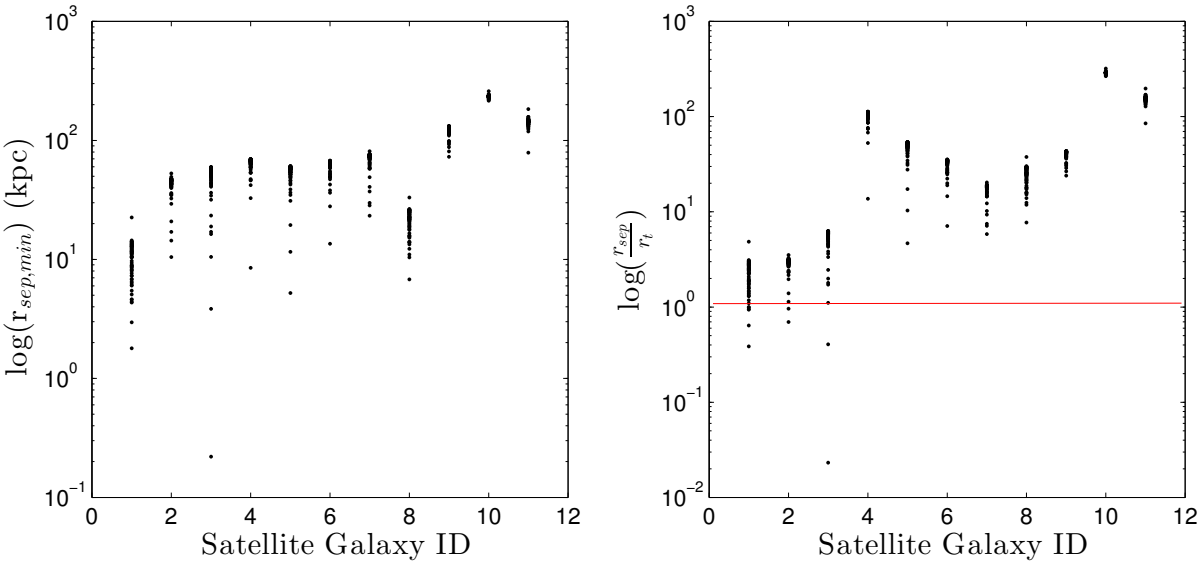

Figure 30: *Left*: The logarithm of the minimum separation for the satellite galaxy - globular cluster encounters vs the satellite galaxies' ID number, for the case where I modelled the satellite galaxies as distributed masses. *Right*: A similar plot to that shown on the left, however here the y-axis is in terms of the satellite galaxies' tidal radii. If there is a black dot (globular cluster encounter) below the red line, then this implies there was a collision within the satellite galaxy's tidal radius. This simulation was run for 10 Gyr into the future.

6 Stripping globular clusters from satellite galaxies

I simulated 10 different Sagittarius-like satellite galaxies, each containing 10 globular clusters, orbiting within the Milky Way. I based these satellite galaxies on the Sagittarius dwarf galaxy since it is believed that there have been similar satellite galaxies in the Milky Way's history. It is believed that via the tidal interactions between the Milky Way and the satellite galaxies, the Milky Way's globular cluster population was increased. The Sagittarius dwarf galaxy has been in the process of being tidally disrupted for at least 3 Gyr, therefore if I used the Sagittarius dwarf galaxy then I would obtain unreliable results since I have not considered tidal effects in my simulations. Ergo I selected the x-y-z position values for the Sagittarius-like satellite galaxies in a process that is described in section 6.2. In order to simply simulate the mass loss of the satellite galaxies, I employed a decreasing mass function which is described in section 6.1.2. I run the simulations for 2 Gyr since this is the length of time that the Sagittarius dwarf galaxy is predicted to have left before it is tidally destroyed (Johnston et al., 1999). I used 10 Sagittarius-like satellite galaxies since Forbes & Bridges (2010) suggested that globular clusters were donated to the Milky Way from 6 - 8 dwarf galaxies, van den Bergh (2000b) suggested that some of the globular clusters came from 3 - 7 Sagittarius-like satellite galaxies, and Mackey & Gilmore (2004) suggested that it was due to approximately 7 dwarf galaxies.

6.1 Satellite model

6.1.1 Satellite potential

I simulated the orbit of the Sagittarius-like satellite galaxies' globular clusters around the satellite galaxies by using a Plummer (1911) model (Law & Majewski, 2010a), which is given by equation (21). I also included the gravitational effects from the Milky Way and the Milky Way's satellite galaxies upon the orbits of these globular clusters. However if the globular clusters ventured outside of the tidal radius of their host satellite galaxy then I considered that satellite galaxy as a point mass. Therefore in this case I used the potential of the Milky Way, along with the gravitational forces from all of the satellite galaxies inside of the Milky Way for simulating the globular cluster orbits.

$$\psi_{\rm Sag} = -\frac{{\rm G}M_{\rm Sag}}{\sqrt{r_{\rm wrts}^2 + r_0^2}} \tag{21}$$

Here $M_{\rm Sag}$ was the mass of the Sagittarius-like satellite galaxy [given by equation (23)], and $r_{\rm wrts}$ was the distance of the globular clusters from their host satellite galaxy. The subscript wrts means that the distance from the host galaxies core was with respect to the Sagittarius-like satellite galaxies' coordinate system, whereas in previous sections r was with respect to the Milky Way's coordinate system. That is the galactic centre is at r = 0 in the Milky Way's coordinate system, however $r_{\rm wrts}$ = 0 is the location of the Sagittarius-like satellite galaxies centre. r_0 was the scale length of the Sagittarius-like satellite galaxies in kpc and was calculated by:

$$r_0 = \left(\frac{M_{\rm Sag}}{10^9 M_\odot}\right)^{\frac{1}{3}} \tag{22}$$

6.1.2 Simplified mass loss

Since the Sagittarius dwarf galaxy is losing mass due to its tidal interaction with the Milky Way, I created a simplified function to simulate this for the Sagittarius-like satellite galaxies. The function used was an exponential decay of the mass, with the final mass of the satellite galaxy being the mass of its core (M 54 / NGC 6715), approximately 1.45×10^6 $M_\odot$ (Gnedin & Ostriker, 1997). The time that I allowed it to decay to its final mass was 2 Gyr [a couple of pericentric passages, (Johnston et al., 1999)], this is roughly the time remaining that the Sagittarius dwarf galaxy is believed to last for. The function took the form:

$$M(t) = M_0 e^{-\gamma t} \tag{23}$$

Using the above constraints, and the current mass [M(0) = M_0 = 1.50×10^8 $M_\odot$] of the Sagittarius dwarf galaxy, I found that I required $\gamma \approx 2.32 \times 10^{-3}$ Myr^{-1}. Since the mass is decaying this therefore causes the tidal radius of the satellite galaxy to shrink. In order to simulate this, I used the equation for a time dependant tidal radius from Zhao (2004), this is basically a rearrangement of what equation (10) would have been if it was modelled as a sphere instead of a potential. Therefore r_t is the spherical radius enclosing the mass, and V_{circ} is the circular velocity of the stars inside of this radius.

$$r_t(t) = \frac{GM(t)}{V_{circ}^2} \tag{24}$$

Here I assumed that the internal circular motion (V_{circ}^2) remained constant throughout the simulation, and using the current Sagittarius dwarf galaxy's parameters, I calculated that, V_{circ} = 12.18 ms^{-1}. This is similar to the typical velocity inside of a satellite galaxy.

The reason that a mass loss function is required is that when a satellite galaxy (or another object) is a distributed mass (not a solid object) and is feeling strong gravitational effects from another object, then stars and / or globular clusters can be stripped from it, and this matter forms streams both in front of and behind the satellite galaxy's orbit. This is known as tidal stripping and via this process the satellite galaxy loses mass, and once this process is complete, then the object is said to have been tidally shredded (or destroyed). For a satellite galaxy the end stage of tidal stripping is hypothesised to be that the core (or the central globular cluster) survives, due to the dynamical friction inside of the satellite galaxy, which can cause globular clusters to migrate to the centre of the satellite galaxies, where the density is the highest and hence it is able to withstand the tidal stripping process longer than the disperse outer regions. There may also be tidal streams (which contain stars, and/or globular clusters) of the satellite galaxy remaining, however for a tidally destroyed globular cluster, the only remnants would be the stars. This tidal stripping process also implies that the satellite galaxy should be on an eccentric orbit since it is believed that the satellite galaxy was accreted, and hence came from a large distance (i.e. large apocentre value), and the satellite galaxy needs to get close to the centre of the Milky Way in order to feel the strong tidal forces, and hence a small distance (i.e. small pericentre value). This large apocentre and small pericentre thus imply an eccentric orbit.

6.2 Generation of the initial conditions

In order to generate the initial conditions of the Sagittarius-like satellite galaxies, I 'tilted' the orbit of the Sagittarius dwarf galaxy, I therefore needed to calculate new Cartesian (x, y, z) coordinates from spherical coordinates (r, θ, φ). I also gave the Sagittarius-like satellite galaxies the same initial velocity values as the Sagittarius dwarf galaxy (i.e. the same u, v, and w). For the r-values, I used the Sagittarius dwarf galaxy's initial r value, and I randomly selected 10θ and 10φ values in order to generate 10 randomly selected Sagittarius-like satellite galaxies. I used φ = 0 to 2π (i.e. a full rotation in φ) in steps of 0.01, and $\theta = \cos^{-1}(1 - 2\alpha)$ [private communication with Krüger, W., Lund University]. In order to obtain the equation for θ I integrated the $\sin(\theta)$ function [i.e. the function used in equations (25) and (26)] between 0 and π to cover half a rotation (since there was a full rotation in φ) of values. This then gave f(θ) = -$\cos(\theta)$ + 1. Since this would give a value of 2 for $\theta = \pi$, and not a value of 1 (where I wanted to choose a random value between 0 and 1), I then needed to divide this function by 2. This then gave f(θ) = $\frac{1}{2}$[-$\cos(\theta)$+1], and a rearrangement using f(θ) = α gave the equation shown previously. I chose α = 0 to 1 in steps of 0.002, in order to have a similar number of values to the number of φ values. This allowed me to be able to randomly select 10 values from a range of around 500 values. Once I had selected the r, θ, and φ values, I then used equations (25) - (27) in order to obtain the Cartesian coordinates.

$$x = r\sin(\theta)\cos(\varphi) \tag{25}$$

$$y = r\sin(\theta)\sin(\varphi) \tag{26}$$

$$z = r\cos(\theta) \tag{27}$$

Once I had created the 10 new randomly selected Sagittarius-like satellite galaxies, I then created 10 randomly chosen globular clusters in a similar method to that described above. The only difference was that I did not use the Sagittarius dwarf galaxy's r-value but instead I had the globular clusters have r = 0.5 to 4.55 kpc in increments of 0.45 kpc. Upon obtaining their x, y, and z value I then calculated their circular velocity (u, v, w) around the Sagittarius-like satellite galaxies, where the only gravitational effect on the globular clusters was from the Sagittarius-like satellite galaxies.

In order to investigate the randomness of the selection of the Sagittarius-like satellite galaxies, I created a plot of their pericentres and apocentres, along with their R-z orbital plots, which are shown in Figure 31. For Figure 31, the Sagittarius-like satellite galaxies were simulated in the Milky Way's potential for 2 Gyrs, and they only felt the gravitational force of the Milky Way. The Sagittarius-like satellite galaxies were also simulated with a constant mass for Figure 31. As can be seen from the left-hand plot most of the Sagittarius-like satellite galaxies look similar (i.e. have similar eccentricity values), however differing slightly (in terms of their pericentre / apocentre values). Nevertheless some of the Sagittarius-like satellite galaxies had pericentre and apocentre values which were vastly different from the others (e.g. ID 3 and ID 5). The right-hand plot of Figure 31, which shows the R-z orbits of the Sagittarius-like satellite galaxies, appears to suggest that there was a bias for the satellite galaxies to have positive z-values. However this was similar to the Sagittarius dwarf galaxy's orbital plot. Some of the Sagittarius-like satellite galaxies had similar R-z plots for example IDs 8 & 10 (shown by the yellow and black curves), whereas some of them had different orbits, such as IDs 4 & 8 (shown by the light-blue and yellow curves). This meant that there was a range of different encounters for each of the Sagittarius-like satellite galaxies with the classical satellite galaxies and the Milky Way's potential field, thereby producing different gravitational effects on the Sagittarius-like satellite galaxies' globular clusters.

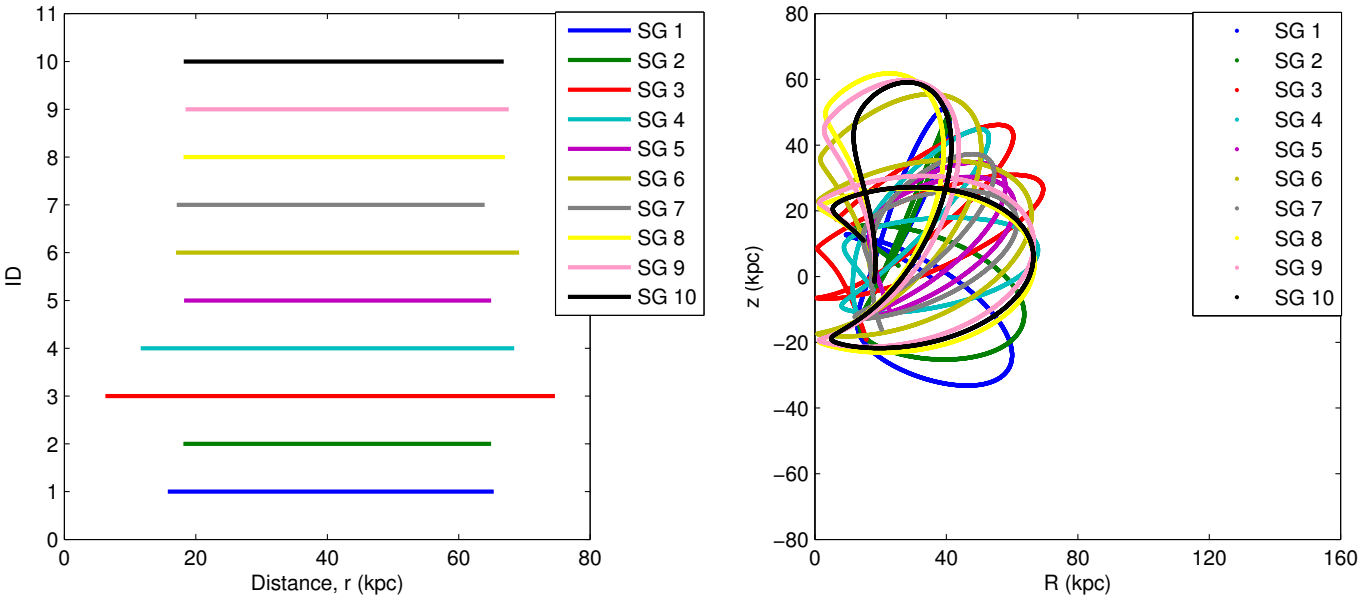

Figure 31: *Left*: The pericentre and apocentre values of the Sagittarius-like satellite galaxies orbiting within the Milky Way's potential. *Right*: R-z plot of the Sagittarius-like satellite galaxies, note the tendency for high positive z-values, which is similar to the Sagittarius dwarf galaxy's R-z orbit. The simulations were run for 2 Gyr.

6.3 Sagittarius-like satellite galaxies

I run 10 simulations (1 for each Sagittarius-like satellite galaxy) with the 10 globular clusters orbiting their host Sagittarius-like satellite galaxy for 2 Gyr and I investigate whether or not the globular clusters remained bound to the satellite galaxy or not. In these simulations, I had one of the Sagittarius-like satellite galaxies orbiting inside the potential of the Milky Way and their globular clusters felt the gravitational forces from their host satellite galaxy, the Milky Way and 10 of the classical satellite galaxies. In the simulations I did not include the Sagittarius dwarf galaxy as this satellite galaxy was replaced by my randomly selected Sagittarius-like satellite galaxies. The first set of these 10 simulations used a constant mass for the Sagittarius-like satellite galaxies, and the left-hand plot in Figure 32 shows how the separation between one of the Sagittarius-like satellite galaxies and its 10 globular clusters changed over time. As can be seen there were only 3 globular clusters that were retained for the whole 2 Gyr of the simulation, this is shown by the curves below the brown line (i.e. the tidal radius of the satellite galaxy). Each colour in the plot refers to a different globular cluster around the satellite galaxy, this is also shown by the GC 4.n identifier given in the legend, where n is indicative of the globular cluster number, starting from the closest globular cluster to the satellite galaxy. This plot is for the $4^{\rm th}$ Sagittarius-like satellite galaxy, the other Sagittarius-like satellite galaxies had similar plots, however they retained 0 (SG: 5), 1 (SG: 1, 2, 9), 2 (SG: 3, 6, 8), or 3 (SG: 4, 7, 10) globular clusters. In all these cases it was not always the same globular clusters that were retained. The reason that GC 4.5 may have been ejected at such a late time in comparison to the other globular clusters which were ejected could be due to the satellite galaxy's pericentric passage (i.e. the tidal stripping was strongest at the closest distance to the galactic centre,due to the small separation between the satellite galaxy and the galactic centre), which occurred around the time of the ejection. It is interesting that in this case the $1^{\rm st}$, $4^{\rm th}$ and $6^{\rm th}$ globular clusters (in terms of separation from the satellite galaxy) are the ones which were retained and not the three innermost globular clusters. This ejection event was seen in most of the simulations of the 10 Sagittarius-like satellite galaxies, however it occurred for different globular clusters, not just the fifth outer globular cluster.

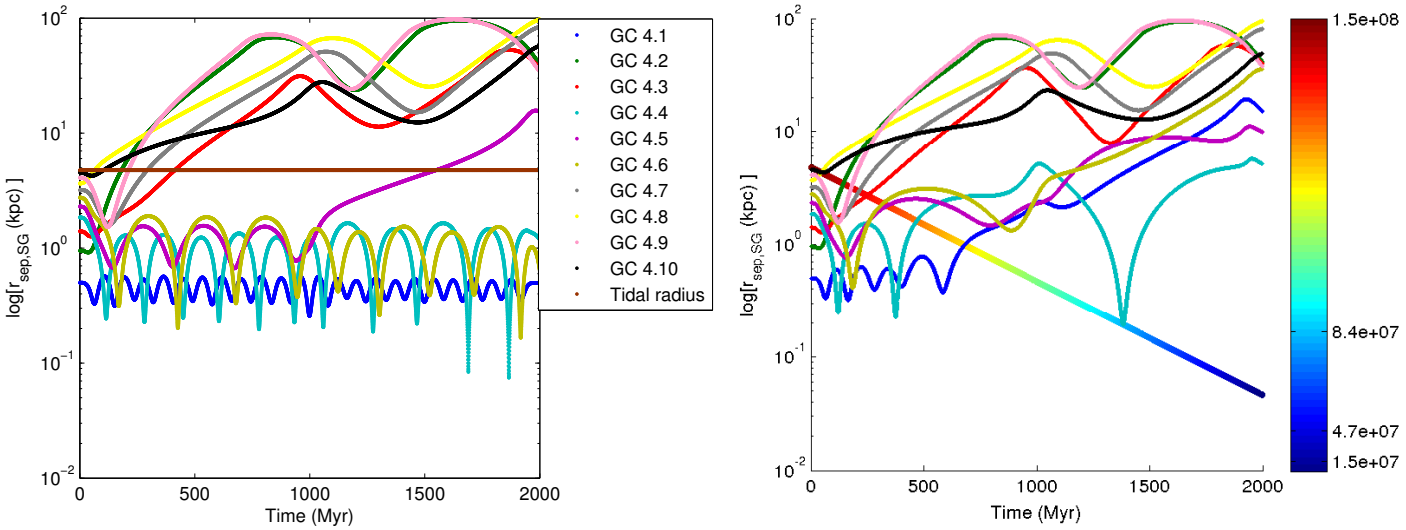

Figure 32: *Left*: The log($r_{\rm sep}$) of the $4^{\rm th}$ randomly selected Sagittarius-like satellite galaxy's globular clusters from the centre of the satellite galaxy. Here I used a constant mass for the satellite galaxy. Most of the globular clusters were ejected early, with the last ejection caused by the pericentric passage. *Right*: The same plot as the left-hand image, however I used equation (23) in order to see how the decreasing mass of the satellite galaxy affects the stripping of its globular clusters. Here all globular clusters were ejected due to the shrinking tidal radius (i.e. mass loss). Both simulations were run for 2 Gyr.

In the second set of simulations, I repeated these 10 simulations, however I used the mass loss function given by equation (23) to model the mass of the Sagittarius-like satellite galaxies. The result of this for the fourth Sagittarius-like satellite galaxy is shown in the right-hand plot of Figure 32, where the rainbow coloured line is that of the satellite galaxy's tidal radius, with the colour bar being representative of the mass of the satellite galaxy. In these simulations all of the globular clusters were donated to the Milky Way after $\sim$ 500 - 800 Myr. This was due to the decreasing tidal radius and decreasing mass of the satellite galaxy, however some of the outermost globular clusters were ejected at the same time in both sets of simulations (i.e their ejections were independent of the constant mass / mass loss of the satellite galaxies).

This means that even if a satellite galaxy is not undergoing strong tidal disruption, such that its mass can be assumed to be constant, then it will still lose globular clusters to the Milky Way. This could be the case for the Fornax dwarf galaxy, since this has similar properties to the Sagittarius dwarf galaxy, such as their metallicity, absolute magnitude, absolute velocity, and their tidal and half-mass radii. However their eccentricities and distances from the galactic centre are very different, this could be the reason why one is undergoing tidal stripping and the other is not. Therefore if we have two Sagittarius-like satellite galaxies orbiting within the Milky Way for 5 Gyr (approximately the lifetime of the Sagittarius dwarf galaxy), and they donate all 9 (the number of globular clusters that the Sagittarius dwarf galaxy is believed to have initially contained) of their globular clusters then the number of globular clusters donated to the Milky Way over its lifetime is approximately 36 - 45 (i.e. $\sim$ 23 - 29% of the Milky Way's globular cluster population). This would mean that 4 - 5 Sagittarius-like satellite galaxies have donated 36 - 45 globular clusters to the Milky Way in approximately the 13 Gyr of the Milky Way's existence. This is a similar value to those proposed by Forbes et al., (2010), who suggested that 27 - 47 globular clusters had been donated from 6 to 8 dwarf galaxies, van den Bergh (2000), who suggested that less than 35 globular clusters were donated from 3 to 7 Sagittarius-like satellite galaxies, and Mackey & Gilmore (2004) who suggested 41 globular clusters from roughly 7 satellite galaxies.

In order to investigate whether we can ascertain if some of the Milky Way's globular clusters share properties with any of the Sagittarius-like satellite galaxies' globular clusters I simulated the orbit of both sets of the globular clusters for 10 and 11 Gyr respectively. These times were used since I wanted both sets to be orbiting inside of the Milky Way for the same length of time, and since the Sagittarius-like satellite galaxies' globular clusters were bound to their host satellite for 1 Gyr, then their simulation needed to be run for an extra Gyr. From these simulations I created an R-z orbital plot for each of the Sagittarius-like satellite galaxies' globular clusters (grouped by their host satellite). The R-z plots for the Sagittarius-like satellite galaxies 4 (SG 4, bottom) and 9 (SG 9, top) are shown on the left hand side of Figure 33. I chose these two satellites since SG 4's globular cluster's R-z plot was similar to those of SG 5 and 7's globular cluster's, likewise SG 9's globular cluster's had similarities with SG 6, 8, and 10's globular cluster's. SG 1, 2 and 3's globular cluster's had R-z plots which were unlike those shown here due to them being a mix of differently perturbed R-z orbits. For comparison to the Milky Way's globular clusters (note this is only the Casetti-Dinescu sample), I randomly selected two sets of 10 globular clusters and created a R-z plot of them, these are shown on the right-hand side of Figure 33.

From a comparison of the Sagittarius-like satellite galaxies' globular clusters' R-z orbits to those of the Milky Way's globular clusters', we can see that the Milky Way's globular clusters tended to be less eccentric (i.e. they didn't have such large positive or negative z-values). Also if we take these 20 randomly selected orbits as being representative of the whole globular cluster population, then the Milky Way's globular clusters had a tendency to orbit closer to the Milky Way (0 kpc - 30 kpc) and rarely go beyond 40 kpc, whereas the Sagittarius-like satellite galaxies' globular clusters tended to orbit between 10 kpc and 80 kpc. One thing that was noticeable was that the globular clusters from the same host galaxy had very similar R-z orbits to each other, whereas the Milky Way's globular clusters appeared to have many different R-z orbits. This could suggest that the Milky Way's globular clusters came from many different satellite galaxies or they were formed in the Milky Way.

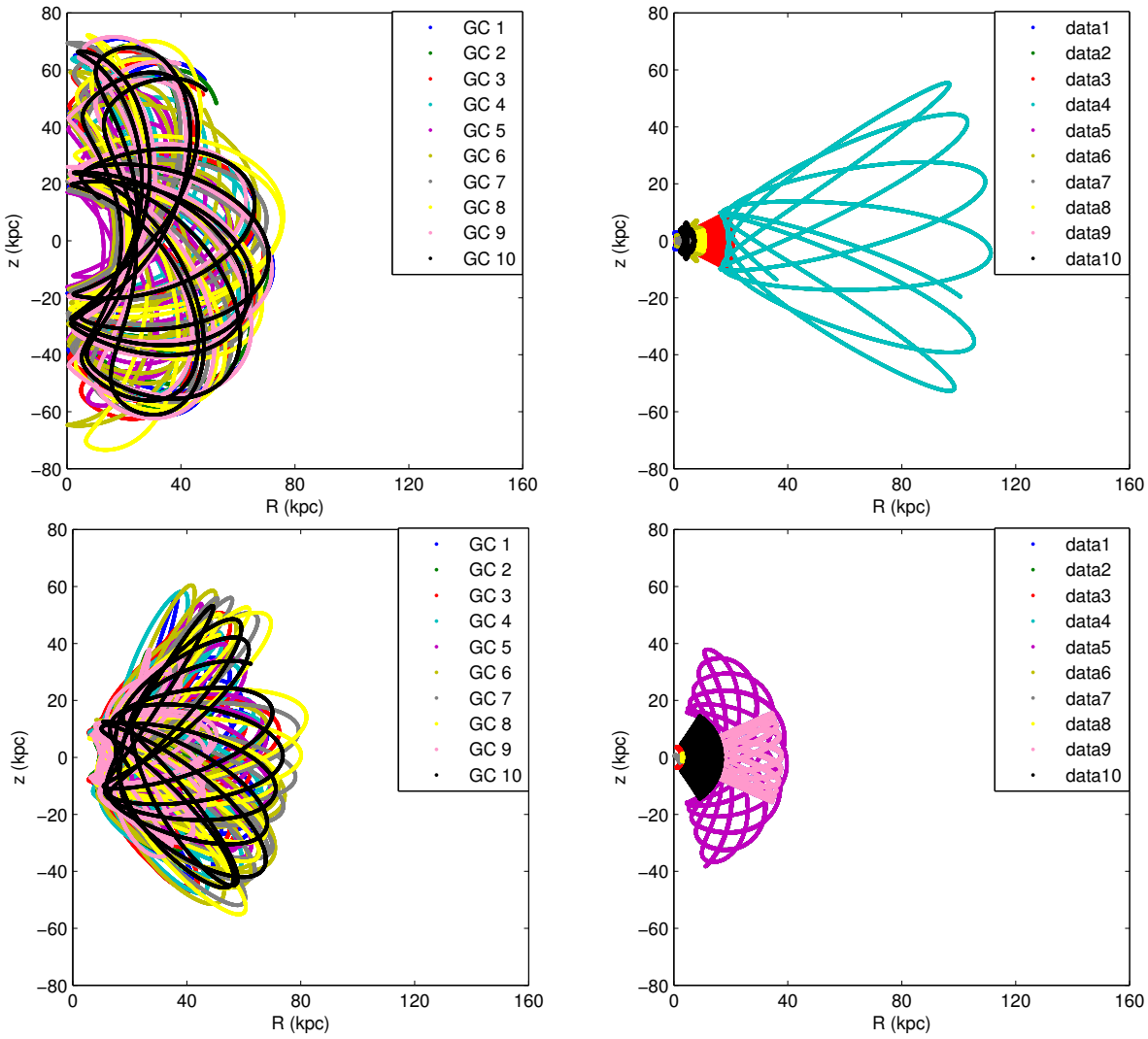

Figure 33: *Top left*: R-z plot of the Sagittarius-like satellite galaxy 9's globular clusters. There were similar plots for the globular clusters of the Sagittarius-like satellite galaxies 6, 8 and 10. *Bottom left*: R-z plot of the Sagittarius-like satellite galaxy 4's globular clusters. There were similar plots for the globular clusters of the Sagittarius-like satellite galaxies 5 and 7. *Right*: Two R-z plots of 10 randomly selected Casetti-Dinescu globular clusters. These simulations were run for 11 Gyr, for those on the left, and 10 Gyr, for those on the right.

I also investigated the eccentricities and j_z of both sets of globular clusters, these are shown as the upper and lower plots in Figure 34 respectively, with the Sagittarius-like satellite galaxies' globular clusters on the left side and the Milky Way's globular clusters on the right side. The left-hand plots are from the simulations detailed previously, and the right-hand plots are from a simulation of all of the Casetti-Dinescu globular clusters in a manner similar to the process outlined in Section 5. Thus both sets of globular clusters orbited in the Milky Way's potential for 10 Gyr.

From a comparison of the eccentricities (i.e. the top 2 plots) it can be seen that the Sagittarius-like satellite galaxies' globular clusters tended to be highly eccentric, with values ranging from $\sim$ 0.5 - 1, whereas the Milky Way's globular clusters had a large distribution of eccentricities from $\sim$ 0.1 - 1. This could imply that the Milky Way's globular clusters which had high eccentricities may have been donated by satellite galaxies, and those with low eccentricities may have been formed in the Milky Way. The high eccentricities of the Sagittarius-like satellite galaxies' globular clusters is due to the Sagittarius-like satellite galaxies having high eccentricities themselves (which is required for strong tidal stripping).

From comparing the j_z plots (the 2 lowermost plots) we can see that most of the Casetti-Dinescu globular clusters had values between $j_z = \pm$ 2 kpc^{2}Myr^{-1}, whereas most of the Sagittarius-like satellite galaxies' globular clusters fit within a wide spread of $j_z = \pm$ 7 kpc^{2}Myr^{-1}. However if we split the left-hand plot into three sections, where the middle section is from j_z = -2 kpc^{2}Myr^{-1} to j_z = +2 kpc^{2}Myr^{-1}, then the satellite galaxies had a very similar split to how they were split from comparing the R-z plots (i.e Figure 33). The split was such that those within $j_z = \pm$ 2 kpc^{2}Myr^{-1} were globular clusters from SGs 3, 6, 8, 9, and 10 (corresponding to the globular clusters with R-z plots similar to the upper-left plot in Figure 33), and the globular clusters outside were SGs 1, 2, and 5, with negative values, and SGs 4 and 7, with positive values (corresponding to the globular clusters with R-z plots similar to the lower-left plot in Figure 33). The Casetti-Dinescu globular clusters had 5 outliers in their j_z plot when I implemented the $j_z = \pm$ 2 kpc^{2}Myr^{-1} cut, this could suggest that those below this cut (ID 8, NGC 3201; ID 59, Pal 13) came from one satellite galaxy and those above the cut (ID 4, NGC 1851; ID 11, NGC 4590; ID 54, NGC 7006) came from another, while those inside of the $j_z = \pm$ 2 kpc^{2}Myr^{-1} region may have came from other satellite galaxies or they were created in the Milky Way.

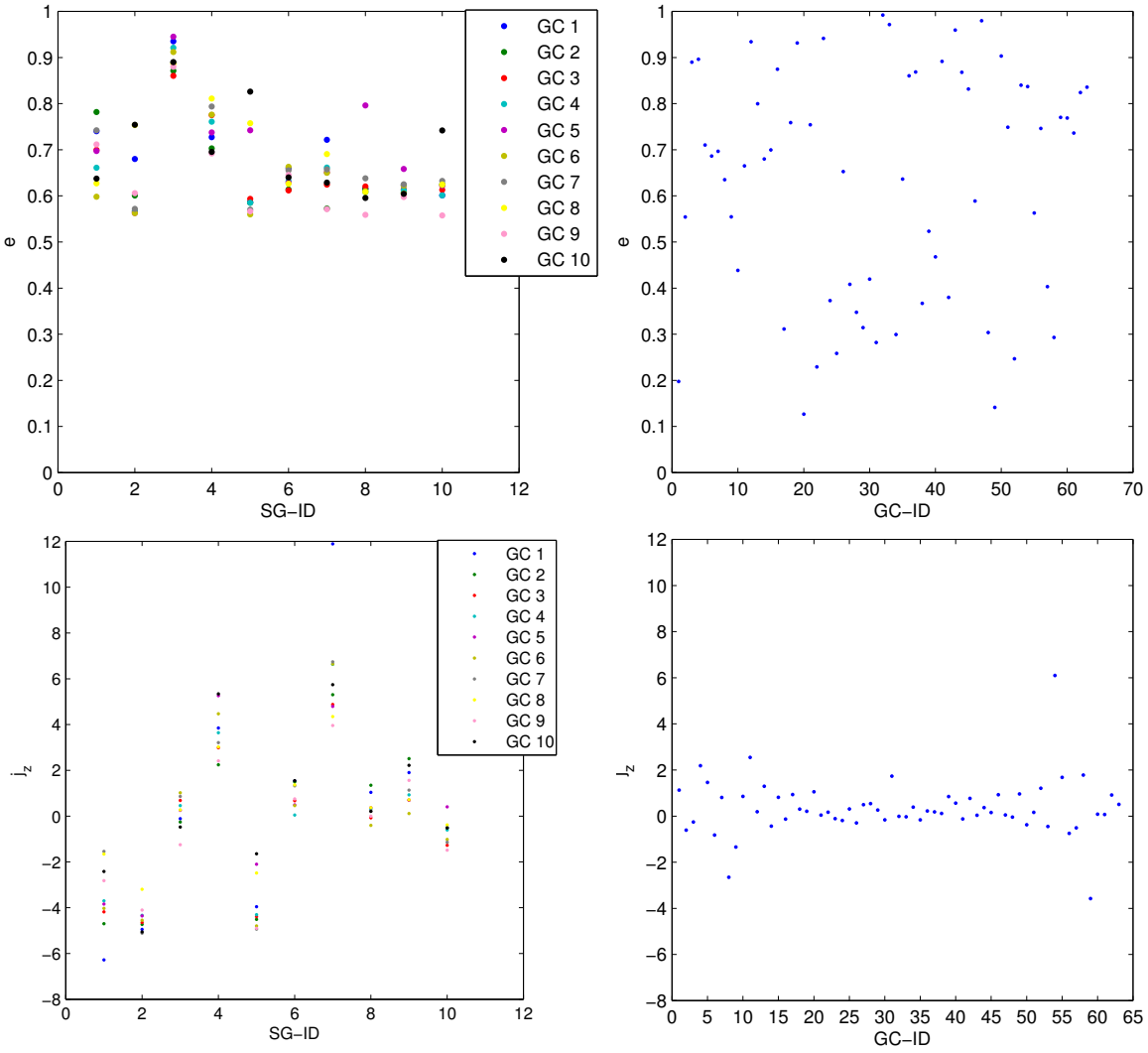

Figure 34: *Top left*: The eccentricity of the Sagittarius-like satellite galaxies' globular cluster orbits vs their host ID. *Top right*: The eccentricity of the Casetti-Dinescu globular clusters vs their ID number. *Bottom left*: The j_z of the Sagittarius-like satellite galaxies' globular cluster orbits vs their host ID. *Bottom right*: The j_z of the Casetti-Dinescu globular clusters vs their ID number. The outliers in the j_z plot are GC-IDs 4, 8, 11, 54, and 59.

Next I analysed the pericentric and apocentric values (obtained from the same simulation as the j_z and eccentricity values) of both the Sagittarius-like satellite galaxies' globular cluster and the Casetti-Dinescu globular clusters (and the classical satellite galaxies). These are shown by the left and right plots of Figure 35 respectively. It is obvious from looking at these plots that there is a large difference in the pericentric values of the Sagittarius-like satellite galaxies' globular cluster and the Milky Way's globular clusters. However when I compared the plots between r $\sim$ 1 kpc and r $\sim$ 10 kpc, which covered the range of values of most of the Sagittarius-like satellite galaxies' globular cluster (with the exception of GC 3), then I was able to see which of the Milky Way's globular clusters were within this range, and thus they could have been accreted in a similar manner. There were 9 Casetti-Dinescu globular clusters that were within this range, they are IDs 8 (NGC 3201), 9 (NGC 4147), 11 (NGC 4590), 13 (NGC 5024), 17 (Pal 5), 54 (NGC 7006), 55 (NGC 7078), 58 (Pal 12), and 59 (Pal 13).

This was an interesting result, since IDs 8, 11, 54, and 59 also shared similar j_z values as the accreted Sagittarius-like satellite galaxies' globular clusters. They also had eccentricities of 0.64, 0.67, 0.84, and 0.77 respectively, which was within the range of the Sagittarius-like satellite galaxies' globular clusters' values. Also when I included the average values the of GC 3's pericentre-apocentre distances and used them as the new limits then ID 4 also fell within this range (along with approximately 10 other globular clusters). ID 4 also had values of j_z, and eccentricity (e = 0.90) within the ranges of the Sagittarius-like satellite galaxies' globular clusters. This could therefore suggest that IDs 4, 8, 11, 54 and 59 had been accreted from a Sagittarius-like satellite galaxy. Another interesting fact was that IDs 9 and 58 were associated with being accreted from the Sagittarius dwarf galaxy (as mentioned earlier), and thus this supports my claim that the other globulars mentioned here came from Sagittarius-like satellite galaxies.

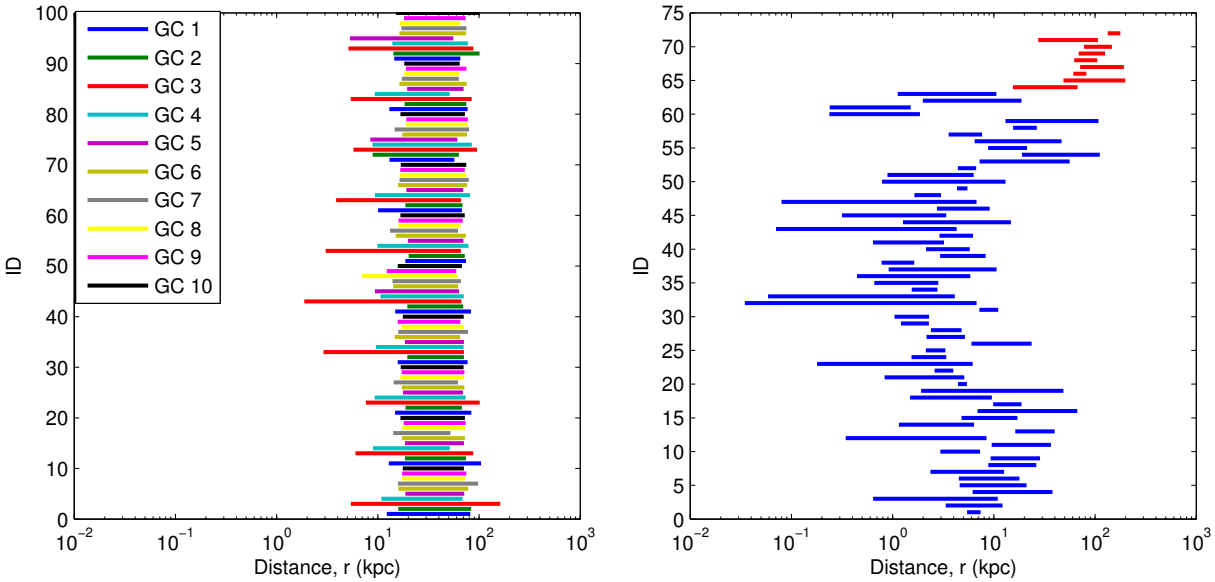

Figure 35: *Left*: The pericentre and apocentre values for the Sagittarius-like satellite galaxies' globular clusters. Most globular clusters had values within r $\sim$ 10 kpc - 100 kpc. *Right*: The pericentre and apocentre values for the Casetti-Dinescu globular clusters (blue) and the classical satellite galaxies(red), not including the Leo satellite galaxies. There were only 8 globular clusters within the same range of r-values, 4 of which also shared j_z and eccentricity values with the Sagittarius-like satellite galaxies' globular clusters. The simulations were run for 11 Gyr and 10 Gyr respectively.

In figure 36 is shown the final orbital energy[18] of the globular clusters, with those belonging to the Sagittarius-like satellite galaxies shown on the left and those belonging to the Milky Way (shown on the right). Most of the Sagittarius-like satellite galaxies' globular clusters had energies between -0.05 kpc^2Myr^{-2} and -0.1 kpc^2Myr^{-2}, whereas the Milky Way's globular clusters had a wide dispersion between energies of $\sim$ -0.045 kpc^2Myr^{-2} to $\sim$ -0.25 kpc^2Myr^{-2}. The reason behind this is that the agittarius-like satellite galaxies' globular clusters all came from similar satellite galaxies, whereas the globular clusters in the Milky Way have most likely came from different satellite galaxies and some may have been created in the Milky Way. Upon investigation of which of the Milky Way's globular clusters had energies within the range of the Sagittarius-like satellite galaxies' globular clusters, it was found that there were 7 globular clusters. They were IDs 11 (NGC 4590), 16 (NGC 5466), 19 (NGC 5904), 53 (NGC 6934), 54 (NGC 7006), 56 (NGC 7089), and 59 (Pal 13). Of these globular clusters, IDs 11, 54, and 59 also shared similar j_z, pericentre-apocentre, and eccentricity values as the Sagittarius-like satellite galaxies' globular clusters. This was further evidence that they may have been accreted to the Milky Way from a Sagittarius-like satellite galaxy. However I earlier predicted that IDs 4 and 8 could have been accreted from Sagittarius-like satellite galaxies, but their energy values were slightly outside of the range (with energies of $\sim$ -0.12 kpc^2Myr^{-2} of the Sagittarius-like satellite galaxies' globular clusters that were found here. In fact all the globular clusters which shared similar pericentre-apocentre values with the Sagittarius-like satellite galaxies' globular clusters had energies within $\pm$ 0.025 kpc^2Myr^{-2} of the energy values of the Sagittarius-like satellite galaxies' globular clusters. Although IDs 4 and 8 lay outside of the range of energies that the Sagittarius-like satellite galaxies' globular clusters had in these simulations, so did the globular cluster IDs 9 and 58 (with values of $\sim$ -0.11 kpc^2Myr^{-2}) which are associated with the Sagittarius dwarf galaxy. This could therefore suggest that IDs 4 and 8 were accreted from a different type of dwarf galaxy to the ones that IDs 11, 54, and 59 were accreted from, or that they were accreted at an earlier / later time and have been effected by the Milky Way's gravitational torques.

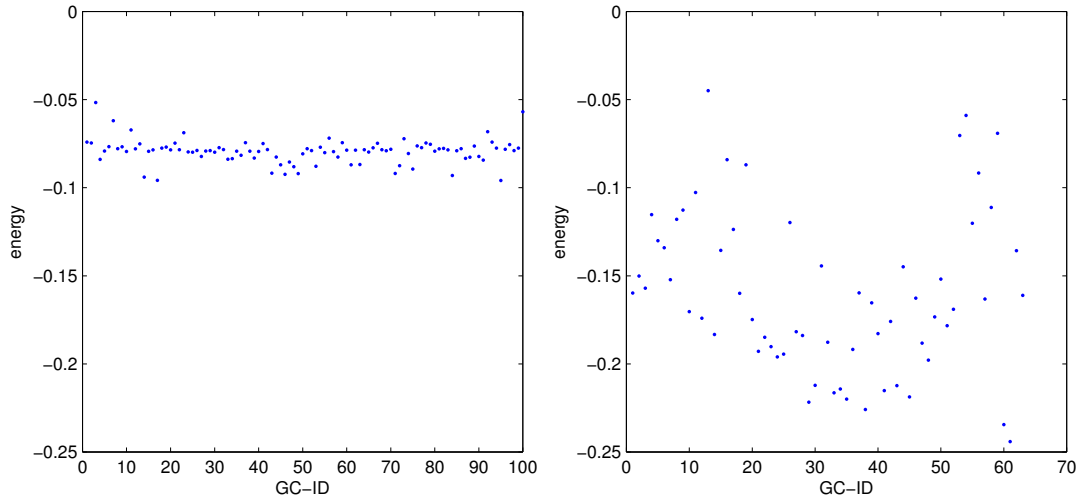

Figure 36: *Left*: The final energies of the Sagittarius-like satellite galaxies' globular clusters, all of which were interior to E = -0.05 kpc^2Myr^{-2} to E = -0.1 kpc^2Myr^{-2}. *Right*: The final energies of the Casetti-Dinescu globular clusters. Of the globular clusters which shared j_z, eccentricity, and pericentre-apocentre values, only IDs 11, 54 and 59 were within the range of the Sagittarius-like satellite galaxies' globular clusters' energies. This could suggest that IDs 4 and 8 were accreted from a different Sagittarius-like satellite galaxy, or they were accreted at a different period of time. The simulations were run for 11 Gyr and 10 Gyr respectively.

[18]The energy is per unit mass and has units of kpc^2Myr^{-2}.

I investigated the metallicities and R-values of the globular clusters associated with the Sagittarius dwarf galaxy (shown by the red stars), and in Figure 36 I have plotted them alongside all of the Milky Way's globular clusters which were in the Harris database[19]. The globular clusters associated with the Sagittarius dwarf galaxy are (from the top of the plot to the bottom) Terzan 7, Pal 12 (ID 58), NGC 4147 (ID 9), NGC 6715 (M54), Arp 2, and Terzan 8. The blue dots are the other globular clusters in the Milky Way from the Harris database. The green diamonds / triangles are the globular clusters that I found evidence to suggest that they were accreted to the Milky Way from Sagittarius-like satellite galaxies (i.e. ID 4, ID 8, ID 11, ID 54, and ID 59). As can be seen from this plot there was a wide spread in the metallicities of the Sagittarius dwarf galaxy's globular clusters, however it appears that they were grouped into three different pairs. This wide spread in metallicity can also be seen in the Milky Way's globular clusters, however there appears to be globular clusters beyond 30 kpc only if they had metallicities below -1.2. Note that this is the exact opposite to the value found in Figure 19, where out of the classical satellite galaxies, only those with [Fe/H] $>$ -1.3 contained globular clusters. This could therefore suggest that the globular clusters beyond 30 kpc were accreted from satellite galaxies which have now been tidally destroyed. However this would then imply a bias in Metallicity for the destruction of satellite galaxies containing globular clusters. Yet metallicity is often used as a proxy for age, and the lower the metallicity (the more negative), then the older the object is assumed to be. Therefore these (now destroyed) satellite galaxies could have been orbiting and destroyed many Gyr ago.

We can also see that the globular clusters shown in green match roughly matched the distribution of the Sagittarius dwarf galaxy's globular clusters in their R values, with the exception of ID 54. ID 54 is the only Casetti-Dinescu globular cluster which had an R $>$ 30 kpc, therefore in this paper I could not investigate whether any of the other globular clusters beyond R = 30 kpc have been accreted. This would have been interesting as they stand out from the rest of the globular clusters in this plot due to their large R-value and hence they are possibly accreted globular clusters (albeit unprovable here). This would however explain the lack of satellite galaxies containing globular clusters with low metallicities, as they have all been tidally destroyed.

I decided that since I found these five globular clusters (IDs 4, 8, 11, 54 and 59) which may have been accreted from Sagittarius-like satellite galaxies, that it may be beneficial to search the literature in order to see if anyone else came to similar conclusions regarding any of these. I found that there was a paper written by Dinescu et al. (2001) that discussed the orbits of globular clusters in the outer galaxy, specifically ID 54 (NGC 7006). In this paper they state ID 54 formed in a system which more closely resembled the Fornax dwarf galaxy than the Sagittarius dwarf galaxy, since ID 54's mass and concentration closely resembled the Fornax dwarf galaxy's globular clusters. They also say that it is more plausible that clusters similar to ID 54 formed in Sagittarius / Fornax - like satellite galaxies, which were tidally destroyed rather early. I also found that in a paper by Martin et al., (2004) that NGC 1851 (ID 4) was once known as a dwarf galaxy called Canis Major, however it is now believed to be a globular cluster which came from the now tidally destroyed Canis Major. NGC 1851 along with some other globular clusters [NGCs 1904 (ID 5), 2298 (ID 6), 2808 (ID 7)] are found in the Monoceros 'ring' structure, which is debris of the tidal stripping of the Canis Major dwarf galaxy. There is a large debate as to whether Pal 13 (ID 59) has been accreted from the Sagittarius dwarf galaxy, with Bellazzini et al., (2003) stating that it has been but Palma et al., (2002) and Law & Majewski (2010b) stating that it has not been, but Siegel et al., (2001) claim that Pal 13 is an accreted young halo object from an unknown dwarf galaxy. This further supports the results found here and suggest that all five of the clusters (IDs 4, 8, 11, 54 and 59) formed in Sagittarius dwarf galaxy/Fornax-like satellite galaxies.

[19]Note that there were no metallicity values for Ko2, Ko1, FSR 1735, 2MS-GC01, GLIMPSE01.

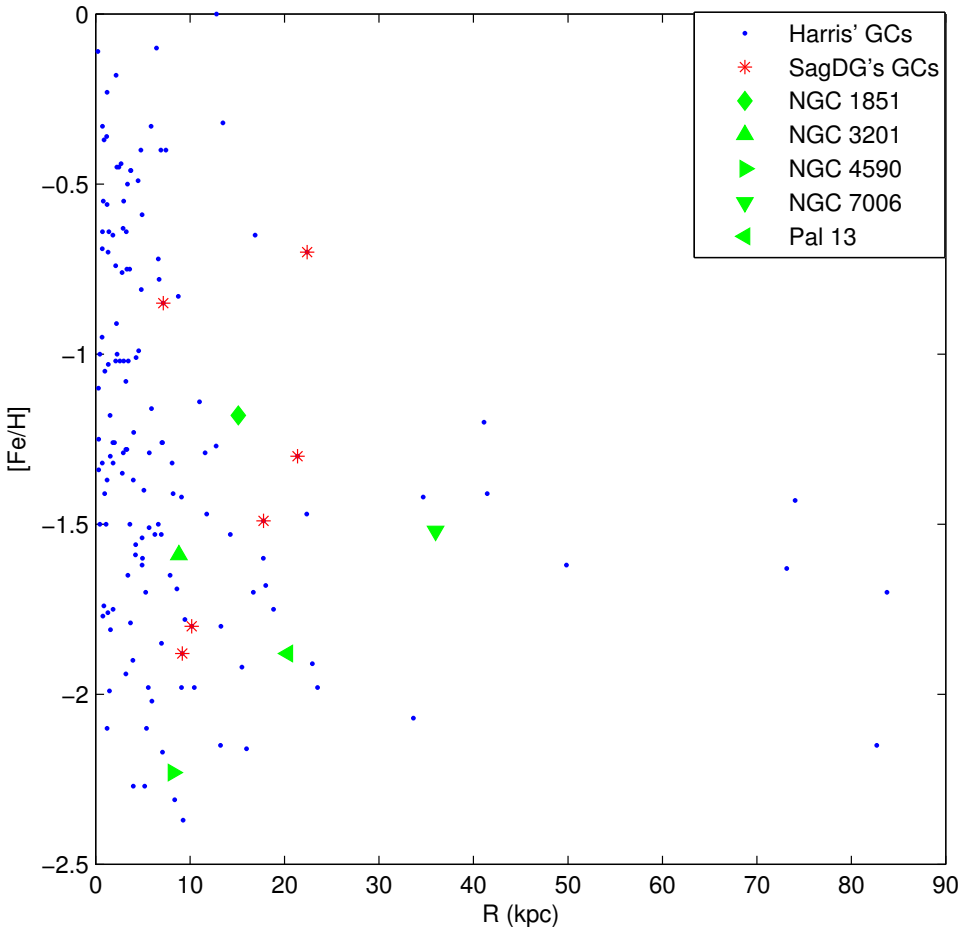

Figure 37: The metallicity and distance from the galactic centre (R) for the globular clusters in the Milky Way. The red stars are indicative of those globular clusters which belong to the Sagittarius dwarf galaxy, and the blue dots are those from the Harris catalogue. The green diamond / triangles are the globular clusters which I found that share properties with the accreted globular clusters from the Sagittarius-like satellite galaxies'. Interestingly only globular clusters with [Fe/H] $<$ -1.2 had R $>$ 30 kpc.

7 Conclusion

Firstly I simulated the interaction between the Casetti-Dinescu globular clusters inside the potential of the Milky Way, and I investigated their orbits and how likely they were to collide within the 10 Gyr into the future. I run the simulations for 10 Gyr, with one simulation including the self interactions between the globular clusters, and the other neglecting them. I also varied the initial positions of the globular cluster pair which had the closest encounter for the latter simulation by $\pm 1\sigma$ (in steps of 0.1σ). I found that 22 (35%) of the Casetti-Dinescu globular clusters had retrograde orbits (possible signature of accretion to the Milky Way, based upon the classical satellite galaxies retrogradeness), and that there was only one encounter with a separation of around 10 pc, with the rest of the encounters occurring at separations between 0.1 kpc and 10 kpc. This therefore means that it is rare for globular clusters to have close encounters with other globular clusters. There was only 0.64% of encounters where collisions occurred (i.e. 24 - 25 collisions), however some of the globular clusters had collisions with different clusters (for example ID 14, which had 7 collisions), but most globular clusters had no collisions. Upon varying the initial positions of IDs 38 and 61, I obtained an encounter of 3 pc, however the majority of the encounters occurred at separations which were larger than that obtained for the unvaried initial positions (i.e. 10 pc). I also found that by adding (or subtracting) 1σ to (or from) the initial positions, then the orbit of the globular cluster would widen (or shrink). This therefore meant that globular cluster - globular cluster collisions are rare and that they depend on the initial conditions of the globular clusters. I further investigated this case and found that the probability of a collision between ID 38 and ID 61 was 0.0024, thus it is very unlikely that they will collide in the future despite being the globular cluster pair with the closest encounter in the simulation.

After this I included the 11 classical satellite galaxies in the simulation of the globular clusters in the Milky Way, and I investigated how the interaction of the satellite galaxies affected the orbits of the globular clusters. For this I simulated the satellite galaxies as point masses in the first simulation and then as a distributed mass later (through the use of a Plummer model potential). I found that 8 (73%) of the classical satellites had retrograde orbits, and that all of the satellite galaxies which contained globular clusters had a metallicity which was greater than -1.3. I found that the globular clusters with R $>$ 30 kpc in the Harris database all had [Fe/H] $<$ -1.2, and that the only satellite galaxies which contain globular clusters all have [Fe/H] $<$ -1.3 (see Figures 19 and 37). This could therefore suggest that these globular clusters were accreted from satellite galaxies that have since been tidally destroyed. These tidally destroyed satellite galaxies most likely had large eccentricities, since there were no satellite galaxies with eccentricities greater than 0.7 in Figure 19. These large eccentricities would have caused the satellite galaxies to be tidally destroyed in 2 - 3 pericentre passages, and it would leave the accreted globular clusters on eccentric orbits (for example ID 54 whose e = 0.71, and r ¿ 30 kpc). I also found that the gravitational interactions between the satellite galaxies and the globular clusters does not effect the globular clusters' orbit very much, with the exception of ID 13's orbit. ID 13's orbit was drastically changed by two close encounters ($r_{\mathrm{sep,min}}$ = 9.75 kpc and 9.46 kpc) with the Sagittarius dwarf galaxy and the LMC. From the first simulation I found that most of the encounters between the satellite galaxies and the globular clusters occurred with separations of less than tens of kpc but greater than 1 kpc, with the exception of the SMC's encounter with ID 54. This encounter had a minimum separation of 227 pc, and occurred at 362 Myr after the start of the simulation (i.e. 362 Myr from now). For the encounters between the classical satellite galaxies and the globular clusters, there was only $\sim 1.4\%$ (i.e. 10 collisions) which occurred in collisions, and the only satellite galaxies which were involved in these collisions were the Sagittarius dwarf galaxy, the LMC, and the SMC (i.e. the three closest satellites). This therefore implied that collisions between satellite galaxies and globular clusters are rare, however when I varied the initial positions of the SMC and ID 54 and simulated their encounter I found that they always had a collision (i.e. their minimum separation was always within the tidal radius of the SMC). This therefore meant that ID 54 will collide with the SMC in the future, unless the positional values of

the SMC / ID 54 are not correct within $\pm 1\sigma$. I also found that when I modelled the satellite galaxies using a potential that the results were very similar to those found from modelling the satellite galaxies as point masses. This therefore meant that one could model the satellite galaxies as point masses and not lose too much information, and for the purposes of this project it was a good assumption, since the closest encounter, i.e. between the SMC and ID 54, had a $r_{sep,min}$ = 227 pc for the point mass case and a $r_{sep,min} \sim 220$ pc for the distributed mass case.

Lastly I simulated the interaction of 10 randomly selected Sagittarius-like satellite galaxies, which each contained 10 globular clusters, orbiting within the potential of the Milky Way, and I investigated the gravitational interaction between these satellite galaxies (one at a time) and the classical satellite galaxies (excluding Sagittarius dwarf galaxy). I also included a function which simulated the mass loss of the Sagittarius-like satellite galaxies, and I modelled the Sagittarius-like satellite galaxies using a potential in order for their globular clusters to orbit inside of their tidal radius. However if the globular clusters were stripped from the satellite galaxy then they felt the gravitational force from its host galaxy as that of a point mass. From this simulation I investigated the orbits of the globular clusters which were accreted from the Sagittarius-like satellite galaxies and compared them to the Casetti-Dinescu globular clusters. I found that all of the globular clusters were stripped from their host satellite galaxy after 500 - 800 Myr. I also found that none of the accreted globular clusters from the Sagittarius-like satellite galaxies were ejected from the Milky Way, and that they all had large eccentricity values distributed between 0.5 and 1, whereas the Casetti-Dinescu globular clusters had a wide distribution of eccentricity values between 0.1 and 1. I also found that the majority of the Casetti-Dinescu globular clusters occupied a region within j_z = $\pm$ 2 kpc^2Myr^{-1}, with only 5 globular clusters (IDs 4, 8, 11, 54, and 59) outside of this range, and all five of these had eccentricity values within 0.5 and 1 (i.e. within the Sagittarius-like satellite galaxies' globular clusters' range of eccentricities).

I then investigated the pericentre and apocentre distances of the two groups of globular clusters and found that the majority of the Sagittarius-like satellite galaxies' globular clusters had orbits within 1 kpc - 10 kpc, with the exception of GC 3 which generally had closer pericentre and more distant apocentre passages. Four of the five globular clusters (IDs 8, 11, 54, and 59) had their respective values within the range of the majority of the Sagittarius-like satellite galaxies' globular clusters' range. Whereas ID 4 had pericentre-apocentre values which were within the range of the Sagittarius-like satellite galaxies' globular clusters when I had included GC 3. I further investigated the orbital energies of the Casetti-Dinescu globular clusters and the Sagittarius-like satellite galaxies' globular clusters, and I found that there were only three of the five globular clusters (IDs 11, 54, and 59) within the region covered by the Sagittarius-like satellite galaxies' globular clusters' values. IDs 4 and 8 had values slightly outside of this range. Since these five globular clusters (IDs 4, 8, 11, 54, and 59) shared properties (j_z, pericentre-apocentre, eccentricity, and energy) with the globular clusters which were accreted from the simulated Sagittarius-like satellite galaxies then this could mean that IDs 4, 8, 11, 54, and 59 may have been accreted from Sagittarius-like satellite galaxies. If we have two Sagittarius-like satellite galaxies orbiting within the Milky Way for 5 Gyr (approximately the lifetime of the Sagittarius dwarf galaxy), and they donate all 9 (the number of globular clusters that the Sagittarius dwarf galaxy is believed to have initially contained) of their globular clusters then the number of globular clusters donated to the Milky Way over its lifetime is approximately 36 - 45 (i.e. $\sim$ 23 - 29$\%$ of the Milky Way's globular cluster population). This would mean that 4 - 5 Sagittarius-like satellite galaxies have donated 36 - 45 globular clusters to the Milky Way in approximately the 13 Gyr of the Milky Way's existence. This is a similar value to those proposed by Forbes et al., (2010), who suggested that 27 - 47 globular clusters had been donated from 6 to 8 dwarf galaxies, van den Bergh (2000), who suggested that less than 35 globular clusters were donated from 3 to 7 Sagittarius-like satellite galaxies, and Mackey & Gilmore (2004) who suggested 41 globular clusters from roughly 7 satellite galaxies. The five globular clusters mentioned previously [IDs 4 (NGC 1851), 8 (NGC 3201), 11 (NGC 4590), 54 (NGC 7006), and 59 (Pal 13)] could be 5 of the 36 - 45 globular clusters that have been accreted to the Milky Way in the Milky Way's lifetime.

Appendix 1: Globular clusters' initial conditions

ID	Name	x (kpc)	y (kpc)	z (kpc)	u (kms^{-1})	v (kms^{-1})	w (kms^{-1})
1	104av	6.10	-2.60	-3.20	83.20 ± 10.60	-74.80 ± 7.20	48.10 ± 5.30
2	288av	8.10	0.00	-8.90	24.80 ± 13.60	-293.80 ± 22.90	51.40 ± 0.30
3	362av	4.90	-5.10	-6.20	23.90 ± 25.10	-295.70 ± 23.50	-68.40 ± 24.90
4	1851*	12.30	-8.90	-6.90	237.90 ± 37.50	-218.10 ± 27.70	-101.70 ± 32.80
5	1904*	15.60	-8.30	-6.30	120.40 ± 31.60	-192.40 ± 30.10	13.10 ± 35.80
6	2298*	12.30	-9.50	-3.00	-79.60 ± 48.00	-224.00 ± 24.60	118.70 ± 51.50
7	2808cc	6.00	-9.20	-1.90	15.10 ± 20.90	-111.80 ± 6.00	68.30 ± 22.00
8	3201cc	7.40	-4.80	0.70	-185.10 ± 13.70	-450.50 ± 1.60	130.70 ± 9.00
9	4147av	9.30	-4.10	18.80	-23.30 ± 48.20	-350.40 ± 53.50	117.20 ± 12.70
10	4372cc	5.10	-4.90	-1.00	105.80 ± 17.70	-157.80 ± 10.00	77.00 ± 12.10
11	4590*	3.90	-7.20	6.10	212.70 ± 34.50	25.00 ± 25.70	13.50 ± 25.20
12	4833cc	4.40	-5.40	-0.90	92.90 ± 24.50	-291.20 ± 16.50	-42.40 ± 10.80
13	5024Od	5.20	-1.40	17.60	-40.40 ± 83.90	34.90 ± 84.70	-59.50 ± 15.10
14	5139*	4.80	-3.90	1.30	-58.00 ± 11.40	-261.70 ± 9.00	0.20 ± 10.40
15	5272av	6.50	1.30	10.00	-66.30 ± 26.10	-111.10 ± 25.60	-134.90 ± 5.80
16	5466Od	4.60	3.00	15.30	228.30 ± 78.70	-98.50 ± 78.50	196.80 ± 23.00
17	5KC	-8.20	0.20	16.60	76.40 ± 14.20	-333.30 ± 38.80	15.30 ± 13.90
18	5897*	-2.30	-3.20	6.30	31.40 ± 31.30	-304.70 ± 58.60	118.90 ± 43.80
19	5904av	2.90	0.30	5.50	-331.40 ± 40.40	-184.10 ± 49.30	-207.50 ± 36.80
20	5927cc	1.60	-4.20	0.70	205.60 ± 15.50	-115.80 ± 23.20	37.00 ± 15.00
21	5986cc	-1.30	-4.00	2.40	3.30 ± 13.30	-240.90 ± 28.60	31.80 ± 19.40
22	6093*	-1.40	-1.20	3.30	-11.00 ± 10.60	-348.40 ± 45.90	-98.20 ± 29.90
23	6121av	5.90	-0.30	0.60	-51.30 ± 2.60	-235.50 ± 21.50	-10.20 ± 4.40
24	6144*	-0.50	-1.20	2.40	-173.70 ± 9.00	-260.20 ± 37.70	14.70 ± 27.80
25	6171CH	2.10	0.30	2.50	-0.60 ± 11.40	-76.20 ± 30.40	-43.10 ± 26.40
26	6205av	5.20	4.60	4.60	225.00 ± 28.70	-77.10 ± 22.50	-137.00 ± 20.30
27	6218av	3.90	1.20	2.10	-61.30 ± 23.00	-115.10 ± 41.60	-114.20 ± 39.80
28	6254av	4.10	1.10	1.70	-97.60 ± 10.80	-117.10 ± 29.00	82.40 ± 19.80
29	6266cc	1.30	-0.80	0.90	77.30 ± 3.20	-67.70 ± 15.00	71.40 ± 14.00
30	6273cc	-0.70	-0.50	1.40	-125.60 ± 5.70	-80.40 ± 22.80	112.60 ± 22.20

Table 6: Globular cluster values part 1. The initial position (x-y-z) and velocity (u-v-w) values for the Casetti-Dinescu globular clusters. Where x is positive outwards from the galactic centre, y is positive towards the galactic rotation, z is positive towards the north galactic pole, with u, v, w being their corresponding velocities. The ID number refers to the number that I used to refer to the globular clusters in the simulations. In the name column are the globular cluster's NGC numbers [with the exceptions of HP1 (1Or), Pal5 (5KC), Pal 12 (12Di), and Pal 13 (13Si)], along with the reference initials associated with the Casetti-Dinescu database.

ID	Name	x (kpc)	y (kpc)	z (kpc)	u (kms^{-1})	v (kms^{-1})	w (kms^{-1})
31	6284cc	-7.10	-0.40	2.60	-27.40 ± 9.30	-460.60 ± 72.40	-4.50 ± 50.90
32	6287cc	-1.20	0.00	1.80	279.50 ± 7.80	-212.30 ± 40.10	-8.00 ± 36.10
33	6293cc	-1.40	-0.40	1.30	121.40 ± 5.60	-163.50 ± 39.10	-155.90 ± 39.00
34	6304*	2.10	-0.40	0.60	104.20 ± 3.80	-57.10 ± 11.30	30.80 ± 8.80
35	6316*	-2.30	-0.50	1.00	-71.10 ± 9.50	-166.40 ± 33.30	37.10 ± 29.90
36	6333cc	0.30	0.70	1.50	-258.30 ± 8.40	-91.60 ± 23.40	-8.00 ± 21.10
37	6341av	5.50	6.30	4.70	18.20 ± 23.30	-166.50 ± 21.30	51.30 ± 30.70
38	6342cc	-0.30	0.70	1.40	-152.90 ± 6.20	-234.30 ± 38.30	-9.50 ± 27.80
39	6356cc	-6.80	1.70	2.70	-69.30 ± 10.80	-324.80 ± 53.10	57.50 ± 45.30
40	6362*	2.00	-4.10	-2.30	90.00 ± 14.00	-129.90 ± 20.20	41.40 ± 16.10
41	6388cc	-1.50	-2.50	-1.20	-36.10 ± 8.20	-200.40 ± 29.80	-21.50 ± 21.90
42	6397cc	5.90	-0.80	-0.50	38.90 ± 6.00	-97.60 ± 10.90	-109.90 ± 10.30
43	6441cc	-3.50	-1.30	-1.00	-3.40 ± 5.70	-231.70 ± 45.40	44.90 ± 30.20
44	6584*	-4.30	-4.00	-3.80	-72.60 ± 26.30	-370.90 ± 53.90	-184.00 ± 41.00
45	6626cc	2.60	0.70	-0.50	-42.20 ± 3.40	-173.60 ± 26.60	-109.80 ± 21.50
46	6656cc	4.90	0.50	-0.40	147.50 ± 2.10	-19.50 ± 6.50	-99.20 ± 13.90
47	6712CH	1.80	2.90	-0.50	97.70 ± 5.80	-35.40 ± 11.90	-136.30 ± 20.20
48	6723cc	-0.30	0.00	-2.60	86.70 ± 6.60	-73.40 ± 22.20	10.70 ± 18.20
49	6752*	4.70	-1.40	-1.70	31.90 ± 5.10	-29.60 ± 9.40	21.60 ± 7.20
50	6779Od	3.70	8.30	1.40	106.40 ± 40.10	-80.60 ± 21.50	3.40 ± 44.10
51	6809av	3.10	0.80	-2.10	-210.00 ± 10.40	-222.30 ± 32.70	-61.20 ± 21.50
52	6838CH	5.80	3.30	-0.30	-86.30 ± 15.40	-65.40 ± 10.10	-2.70 ± 15.20
53	6934Od	-1.10	11.60	-5.10	67.60 ± 62.40	-532.70 ± 50.20	-120.00 ± 74.90
54	7006Di	-9.20	34.9	-13.70	-113.80 ± 72.70	-436.90 ± 41.50	148.40 ± 68.00
55	7078av	4.10	8.40	-4.80	-229.90 ± 69.20	-291.00 ± 39.20	-112.90 ± 56.00
56	7089av	2.40	7.50	-6.70	98.70 ± 42.00	-215.30 ± 39.20	-328.10 ± 51.60
57	7099*	3.10	2.50	-5.90	63.10 ± 20.90	-329.90 ± 30.90	51.30 ± 20.10
58	12Di	-3.00	6.5	-14.00	-220.60 ± 29.10	-321.70 ± 41.70	-20.40 ± 18.20
59	13Si	7.00	19.1	-17.60	249.30 ± 41.10	-39.80 ± 23.30	-100.40 ± 24.60
60	6522Tr	0.30	0.10	-0.50	26.30 ± 3.80	58.60 ± 9.00	-224.00 ± 24.60
61	6528HS	0.10	0.20	-0.60	-218.30 ± 1.60	9.60 ± 9.50	1.40 ± 9.00
62	6553HS	2.00	0.50	-0.30	6.80 ± 2.10	227.70 ± 16.80	13.00 ± 2.20
63	1Or	1.20	-0.30	0.30	-66.30 ± 1.40	211.10 ± 22.10	-40.50 ± 13.30

Table 7: Globular cluster values part 2. The initial position (x-y-z) and velocity (u-v-w) values for the Casetti-Dinescu globular clusters. Where x is positive outwards from the galactic centre, y is positive towards the galactic rotation, z is positive towards the north galactic pole, with u, v, w being their corresponding velocities. The ID number refers to the number that I used to refer to the globular clusters in the simulations. In the name column are the globular cluster's NGC numbers [with the exceptions of HP1 (1Or), Pal5 (5KC), Pal 12 (12Di), and Pal 13 (13Si)], along with the reference initials associated with the Casetti-Dinescu database.

ID	Name	M (10^5 $M_\odot$)	[Fe/H]	r_h (pc)	r_t (pc)	e	j_z (kpc^2 Myr^{-1})	r_{helio} (kpc)
1	104av	14.50	-0.72	6.01	92.26	0.20	1.13	4.50 ± 0.45
2	288av	1.11	-1.32	7.75	45.17	0.55	-0.61	8.90 ± 0.89
3	362av	3.78	-1.26	2.21	44.05	0.89	-0.25	8.60 ± 0.86
4	1851*	5.61	-1.18	2.53	38.54	0.90	2.19	12.10 ± 1.21
5	1904*	3.57	-1.60	4.37	56.84	0.71	1.46	12.90 ± 1.29
6	2298*	0.72	-1.92	3.56	45.61	0.69	-0.82	10.80 ± 1.08
7	2808cc	13.20	-1.14	2.45	29.59	0.70	0.81	9.60 ± 0.96
8	3201cc	1.95	-1.59	6.94	50.21	0.64	-2.65	4.90 ± 0.49
9	4147av	0.67	-1.80	2.66	73.66	0.55	-1.34	19.30 ± 1.93
10	4372cc	3.20	-2.17	8.05	39.09	0.44	0.85	5.80 ± 0.58
11	4590*	3.06	-2.23	4.55	71.92	0.67	2.54	10.30 ± 1.03
12	4833cc	0.95	-1.85	4.91	89.14	0.93	0.19	6.60 ± 0.66
13	5024Od	7.33	-2.10	5.91	36.35	0.80	1.30	17.90 ± 1.79
14	5139*	26.40	-1.53	7.78	115.78	0.68	-0.44	5.20 ± 0.52
15	5272av	7.82	-1.50	3.97	106.18	0.70	0.81	10.20 ± 1.02
16	5466Od	1.33	-1.98	10.60	135.54	0.87	-0.13	16.00 ± 1.60
17	5KC	0.28	-1.41	16.02	161.36	0.31	0.93	23.20 ± 2.32
18	5897*	2.00	-1.90	4.48	88.08	0.76	0.30	12.50 ± 1.25
19	5904av	8.34	-1.29	3.81	25.63	0.93	0.21	7.50 ± 0.75
20	5927cc	3.71	-0.49	1.51	51.22	0.13	1.05	7.70 ± 0.77
21	5986cc	4.98	-1.59	1.47	21.83	0.75	0.04	10.40 ± 1.04
22	6093*	3.67	-1.75	0.72	14.69	0.23	0.17	10.00 ± 1.00
23	6121av	2.25	-1.16	6.26	14.68	0.94	-0.11	2.20 ± 0.22
24	6144*	1.52	-1.76	1.23	55.76	0.37	-0.19	8.90 ± 0.89
25	6171CH	2.04	-1.02	2.59	25.15	0.26	0.31	6.40 ± 0.64
26	6205av	6.27	-1.53	3.77	16.74	0.65	-0.30	7.10 ± 0.71
27	6218av	4.93	-1.37	2.83	63.72	0.41	0.49	4.80 ± 0.48
28	6254av	2.25	-1.56	2.42	23.04	0.35	0.54	4.40 ± 0.44
29	6266cc	8.98	-1.18	0.61	28.74	0.31	0.27	6.80 ± 0.68
30	6273cc	15.60	-1.74	0.58	4.44	0.42	-0.16	8.80 ± 0.88

Table 8: Globular cluster values part 3. The mass (M), metallicity ([Fe/H]), half-mass radius (r_h), tidal radius (r_t), eccentricity (e), and the z-component of the initial angular momentum (j_z) for the Casetti-Dinescu globular clusters. I have also included the heliocentric separation (r_{helio}), along with their respective errors.

ID	Name	M (10^5 $M_\odot$)	[Fe/H]	r_h (pc)	r_t (pc)	e	j_z (kpc^2 Myr^{-1})	r_{helio} (kpc)
31	6284cc	2.17	-1.26	1.72	6.75	0.28	1.74	15.30 ± 1.53
32	6287cc	1.03	-2.10	0.46	51.02	0.99	-0.01	9.40 ± 0.94
33	6293cc	2.34	-1.99	0.37	6.42	0.97	-0.03	9.50 ± 0.95
34	6304*	1.93	-0.45	0.90	5.80	0.30	0.39	5.90 ± 0.59
35	6316*	10.20	-0.45	0.66	8.48	0.64	-0.16	10.40 ± 1.04
36	6333cc	2.89	-1.77	0.47	5.52	0.86	0.22	7.90 ± 0.79
37	6341av	3.64	-2.31	3.04	42.36	0.87	0.18	8.30 ± 0.83
38	6342cc	1.95	-0.55	0.44	7.35	0.37	0.11	8.50 ± 0.85
39	6356cc	8.19	-0.40	1.64	17.62	0.52	0.85	15.10 ± 1.51
40	6362*	1.17	-0.99	3.23	24.73	0.47	0.56	7.60 ± 0.76
41	6388cc	15.00	-0.55	0.62	5.78	0.89	-0.12	9.90 ± 0.99
42	6397cc	1.59	-2.02	4.07	27.59	0.38	0.77	2.30 ± 0.23
43	6441cc	13.00	-0.46	0.73	9.08	0.96	0.04	11.60 ± 1.16
44	6584*	2.19	-1.50	1.63	19.08	0.87	0.37	13.50 ± 1.35
45	6626cc	4.42	-1.32	1.23	8.85	0.83	0.15	5.50 ± 0.55
46	6656cc	5.36	-1.70	4.65	7.57	0.59	0.93	3.20 ± 0.32
47	6712CH	2.45	-1.02	1.39	7.95	0.98	0.05	6.90 ± 0.69
48	6723cc	3.74	-1.10	1.22	83.72	0.30	-0.04	8.70 ± 0.87
49	6752*	3.64	-1.54	3.54	24.15	0.14	0.96	4.00 ± 0.40
50	6779Od	1.89	-1.98	3.27	5.73	0.90	-0.38	9.40 ± 0.94
51	6809av	2.41	-1.94	3.28	18.47	0.75	0.16	5.40 ± 0.54
52	6838CH	0.37	-0.78	3.22	17.46	0.25	1.21	4.00 ± 0.40
53	6934Od	2.15	-1.47	2.23	31.16	0.84	-0.45	15.60 ± 1.56
54	7006Di	2.52	-1.52	4.29	71.56	0.84	6.10	41.20 ± 4.12
55	7078av	9.84	-2.37	3.21	65.04	0.56	1.68	10.40 ± 1.04
56	7089av	8.81	-1.65	2.81	64.89	0.75	-0.75	11.50 ± 1.15
57	7099*	2.74	-2.27	2.38	37.88	0.40	-0.51	8.10 ± 0.81
58	12Di	0.20	-0.85	5.92	80.57	0.29	1.78	19.00 ± 1.90
59	13Si	0.05	-1.88	3.57	24.15	0.77	-3.58	26.00 ± 2.60
60	6522Tr	0.59	-1.34	0.18	2.87	0.77	-0.19	7.70 ± 0.77
61	6528HS	0.93	-0.11	0.08	2.89	0.74	0.08	7.90 ± 0.79
62	6553HS	2.61	-0.18	0.99	5.22	0.82	0.07	6.00 ± 0.60
63	1Or	0.96	-1.00	5.50	14.59	0.84	0.91	6.80 ± 0.68

Table 9: Globular cluster values part 4. The mass (M), metallicity ([Fe/H]), half-mass radius (r_h), tidal radius (r_t), eccentricity (e), and the z-component of the initial angular momentum (j_z) for the Casetti-Dinescu globular clusters. I have also included the heliocentric separation (r_{helio}), along with their respective errors.

Appendix 2: Effects of the satellite galaxies' gravitational interactions

ID	Name	r_{min} (kpc)	r_{max} (kpc)	ID	Name	r_{min} (kpc)	r_{max} (kpc)
1	104av	5.44	7.39	38	6342cc	0.78	1.63
2	288av	3.34	12.14	39	6356cc	2.94	8.28
3	362av	0.64	10.92	40	6362*	2.14	5.78
4	1851*	6.16	37.95	41	6388cc	0.64	3.22
5	1904*	4.59	21.00	42	6397cc	2.90	6.22
6	2298*	4.51	17.93	43	6441cc	0.07	4.28
7	2808cc	2.36	12.64	44	6584*	1.26	14.72
8	3201cc	8.82	26.24	45	6626cc	0.32	3.39
9	4147av	9.28	28.61	46	6656cc	2.74	9.09
10	4372cc	2.96	7.32	47	6712CH	0.08	6.74
11	4590*	9.53	36.67	48	6723cc	1.64	3.01
12	4833cc	0.34	8.44	49	6752*	4.32	5.48
13	5024Od	16.29	39.88	50	6779Od	0.79	13.03
14	5139*	1.15	6.36	51	6809av	0.89	6.31
15	5272av	4.80	17.11	52	6838CH	4.40	6.68
16	5466Od	6.91	66.61	53	6934Od	7.21	56.06
17	5KC	9.86	18.77	54	7006Di	18.95	111.36
18	5897*	1.48	9.55	55	7078av	8.79	21.25
19	5904av	1.91	48.72	56	7089av	6.46	46.66
20	5927cc	4.42	5.42	57	7099*	3.57	7.65
21	5986cc	0.83	5.10	58	12Di	15.45	26.59
22	6093*	2.60	3.97	59	13Si	13.05	107.94
23	6121av	0.18	6.17	60	6522Tr	0.24	1.88
24	6144*	1.54	3.38	61	6528HS	0.24	1.51
25	6171CH	2.13	3.31	62	6553HS	1.98	18.76
26	6205av	6.00	23.58	63	1Or	1.12	10.61
27	6218av	2.16	5.17	64	Sagittarius	15.44	67.06
28	6254av	2.39	4.78	65	LMC	48.75	198.63
29	6266cc	1.21	2.28	66	SMC	61.12	81.92
30	6273cc	1.04	2.2915	67	Draco	71.08	192.80
31	6284cc	7.20	11.04	68	Ursa Minor	62.11	105.30
32	6287cc	0.04	6.75	69	Sculptor	68.91	125.55
33	6293cc	0.06	4.11	70	Sextans	77.75	146.44
34	6304*	1.54	2.77	71	Carina	27.40	106.85
35	6316*	0.66	2.82	72	Fornax	133.40	177.79
36	6333cc	0.44	5.84	73	LeoII	235.98	1643.06
37	6341av	0.91	10.62	74	LeoI	144.39	572.35

Table 10: The pericentre (r_{min}) and apocentre (r_{max}) values from the galactic centre for the orbits of the satellite galaxies and the globular clusters. Here I have included the effects of the gravitational interactions between the satellite galaxies and the globular clusters, as well as those from the Milky Way on the satellite galaxies and the globular clusters. The simulation was run for 10 Gyr.

ID	Name	Δ r_{min} (kpc)	Δ r_{max} (kpc)	ID	Name	Δ r_{min} (kpc)	Δ r_{max} (kpc)
1	104av	0.23	-0.38	32	6287cc	0.01	-0.12
2	288av	-0.14	0.00	33	6293cc	0.00	0.02
3	362av	-0.03	-0.67	34	6304*	0.03	-0.03
4	1851*	4.09	0.05	35	6316*	0.03	-0.03
5	1904*	0.97	-0.37	36	6333cc	0.01	0.03
6	2298*	1.05	-0.69	37	6341av	0.14	-0.33
7	2808cc	0.15	0.11	38	6342cc	0.01	-0.02
8	3201cc	2.79	-0.77	39	6356cc	0.24	-0.36
9	4147av	0.75	-1.16	40	6362*	0.03	-0.02
10	4372cc	0.12	0.02	41	6388cc	0.43	-0.52
11	4590*	1.48	-3.34	42	6397cc	0.08	-0.05
12	4833cc	0.06	0.15	43	6441cc	-0.02	0.04
13	5024Od	-0.06	-107.19	44	6584*	0.20	-0.25
14	5139*	-0.05	0.04	45	6626cc	0.01	0.01
15	5272av	1.43	-1.99	46	6656cc	0.28	-0.41
16	5466Od	2.35	-1.59	47	6712CH	0.01	0.08
17	5KC	-0.13	-0.23	48	6723cc	0.02	-0.02
18	5897*	0.13	-0.35	49	6752*	0.11	-0.12
19	5904av	-0.34	-14.91	50	6779Od	0.10	-0.53
20	5927cc	0.16	-0.08	51	6809av	-0.01	0.05
21	5986cc	0.10	-0.11	52	6838CH	0.19	-0.29
22	6093*	0.04	-0.11	53	6934Od	-0.40	-31.40
23	6121av	-0.01	0.04	54	7006Di	7.60	-16.67
24	6144*	-0.01	0.00	55	7078av	1.73	-3.98
25	6171CH	0.11	-0.11	56	7089av	-1.18	-5.95
26	6205av	0.41	-3.01	57	7099*	0.26	-0.13
27	6218av	-0.03	-0.04	58	12Di	0.48	-0.79
28	6254av	0.03	-0.10	59	13Si	-0.50	3.62
29	6266cc	0.01	-0.01	60	6522Tr	-0.01	-0.01
30	6273cc	0.08	-0.07	61	6528HS	0.01	-0.01
31	6284cc	0.59	-0.76	62	6553HS	0.17	-0.04
				63	1Or	0.16	-0.16

Table 11: Δ r_{min} and Δ r_{max} show the difference between the pericentre and apocentre values, for when I included the effects of gravity from the satellite galaxies on the globular clusters and when I did not.

Appendix 3: Ammendment to the mass of the SMC

The value for the mass of the SMC used here is $4\times10^8 M_\odot$, however I later found that most papers use a value within 2 - 7 $\times10^9 M_\odot$ (Stanimirović et al., 2004; Bekki & Stanimirović, 2009), some papers simply state that the mass of the SMC is 10% of the mass of the LMC. I therefore re-ran the simulations using this mass and investigated how the results differed from those found here. I found that the results shown in Section 5 were very similar whether I used $4\times10^8 M_\odot$ or $4\times10^9 M_\odot$ as the mass of the SMC. Therefore I have not included the new plots showing these results.

For the re-run of the simulations in Section 6, I included the self interactions of the globular clusters, the self interactions of the satellite galaxies, and I simulated the satellite galaxies using a potential function instead of a point mass. I also used randomly selected values for the velocities of the Sagittarius-like satellite galaxies, using the same method as that which was used to generate their randomly selected positions. These new simulations of Section 6 would give a more realistic view of the results from Section 6, since in Section 6 I wanted to minimise the computational time and memory usage. However from the results from the new simulations, I found that my original results (shown in Section 6) partially agree with the new more realistic results. The corresponding plots to those shown in Section 6 are shown hereafter.

In Figure 38 are the plots of the final energies of the Sagittarius-like satellite galaxies' globular clusters (left) and the Milky Way's globular clusters (right). As can be seen there are most of the Sagittarius-like satellite galaxies' globular clusters within the same energy region (i.e. between -0.1 $\text{kpc}^2\text{Myr}^{-2}$ and -0.05 $\text{kpc}^2\text{Myr}^{-2}$) as was found in Section 6, however there are some which are more energetic and hence they are outside of the energy region. We can also see that there is a large spread in the energies of the Milky Way's globular clusters, similar to that shown in Figure 36. I found that there are 17 of the Milky Way's globular clusters which have energies between -0.1 $\text{kpc}^2\text{Myr}^{-2}$ and -0.05 $\text{kpc}^2\text{Myr}^{-2}$, and are thus similar in energy to the accreted globular clusters. However there are some which have high energies (IDs 54, 59, 62) and resemble the more energetic accreted globular clusters, therefore taking the total of the Milky Way's globular clusters which have similar energies to the accreted globular clusters to 20. The five globular clusters (IDs 4, 8, 11, 54, 59) which were found in Section 6 to share properties with the accreted globular clusters also share similar energies to the accreted globular clusters here.

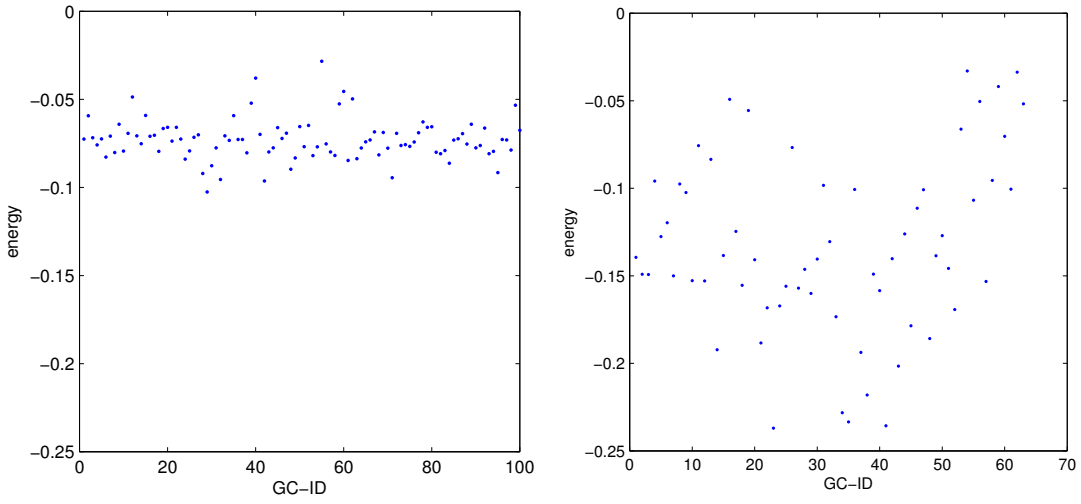

Figure 38: *Left*: The final energy of the Sagittarius-like satellite galaxies' globular clusters, all of which had energies between -0.1 $\text{kpc}^2\text{Myr}^{-2}$ and -0.05 $\text{kpc}^2\text{Myr}^{-2}$. *Right*: The final energies of the Casetti-Dinescu globular clusters. The simulations were run for 11 Gyr and 10 Gyr respectively.

Shown below in Figure 40 are the pericentre (r_{min}) and apocentre (r_{max}) distances of the Sagittarius-like satellite galaxies' globular clusters (left), where each colour represents a different globular cluster and the colours repeat from the bottom of the figure to the top due to there being 10 different Sagittarius-like satellite galaxies which contained these 10 globular clusters (only 1 Sagittarius-like satellite galaxy was simulated at a time). On the right are the pericentre and apocentre values for the Milky Way's globular clusters (blue) and 9 of the 11 classical satellite galaxies (red), I did not include the Leo satellite galaxies for the reasons previously mentioned.

I investigated which of the Milky Way's globular clusters had $r_{min} \geq 40$ kpc and $r_{max} \leq 200$ kpc, since this was the range that most of the Sagittarius-like satellite galaxies' globular clusters had for their pericentre and apocentre values. I found that there were 18 of the Milky Way's globular clusters within this range, of these 22 only 7 had energy values within the range of energies that the Sagittarius-like satellite galaxies' globular clusters had. These were IDs 4, 9, 11, 13, 26, 31 and 58. Notice that unlike in Section 6 IDs 8, 54 and 59 do not have values within this range, this was due to ID 8 having a closer pericentre in this set of simulations, ID 54 was ejected from the system ($r_{max,54} \sim 263$ kpc), and ID 59 had a larger apocentre value than in Section 6. ID 54 was ejected from the Milky Way possibly due to its collision with the SMC ($r_{sep,min} \sim 238$ pc).

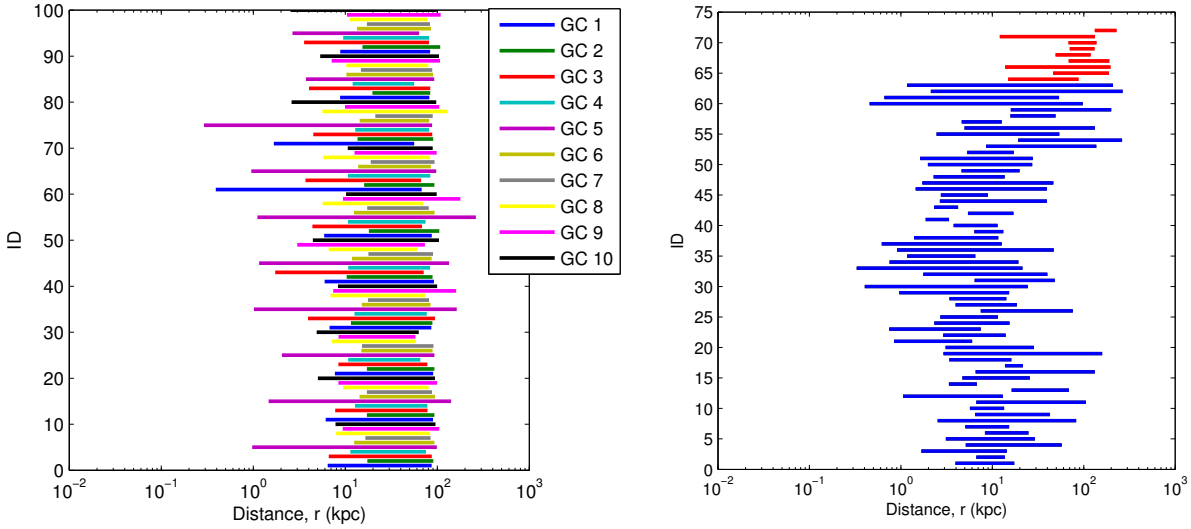

Figure 39: *Left*: The pericentre and apocentre values for the Sagittarius-like satellite galaxies' globular clusters. Most globular clusters had values within r $\sim$ 40 kpc - 100 kpc. *Right*: The pericentre and apocentre values for the Casetti-Dinescu globular clusters (blue) and the classical satellite galaxies(red), not including the Leo satellite galaxies. There were only 7 globular clusters within the same range of energy values as the Sagittarius-like satellite galaxies' globular clusters. The simulations were run for 11 Gyr and 10 Gyr respectively.

In Figure 40 are the final eccentricities and initial j_z values of the Sagittarius-like satellite galaxies' globular clusters (left) and the Milky Way's globular clusters (right). Note that the initial j_z for the Milky Way's globular clusters are the same as shown in Figure 34, however the Sagittarius-like satellite galaxies' globular clusters have different values. This was due to the Sagittarius-like satellite galaxies having different initial conditions here compared to those in Section 6 as I used randomly selected velocity values for the Sagittarius-like satellite galaxies here. Nevertheless this does not change the results from the j_z values. Likewise the eccentricity values here and in Section 6 are fairly similar, however the eccentricities of the Sagittarius-like satellite galaxies' globular clusters tend to be a little higher here, with most of them having eccentricities higher than 0.6.

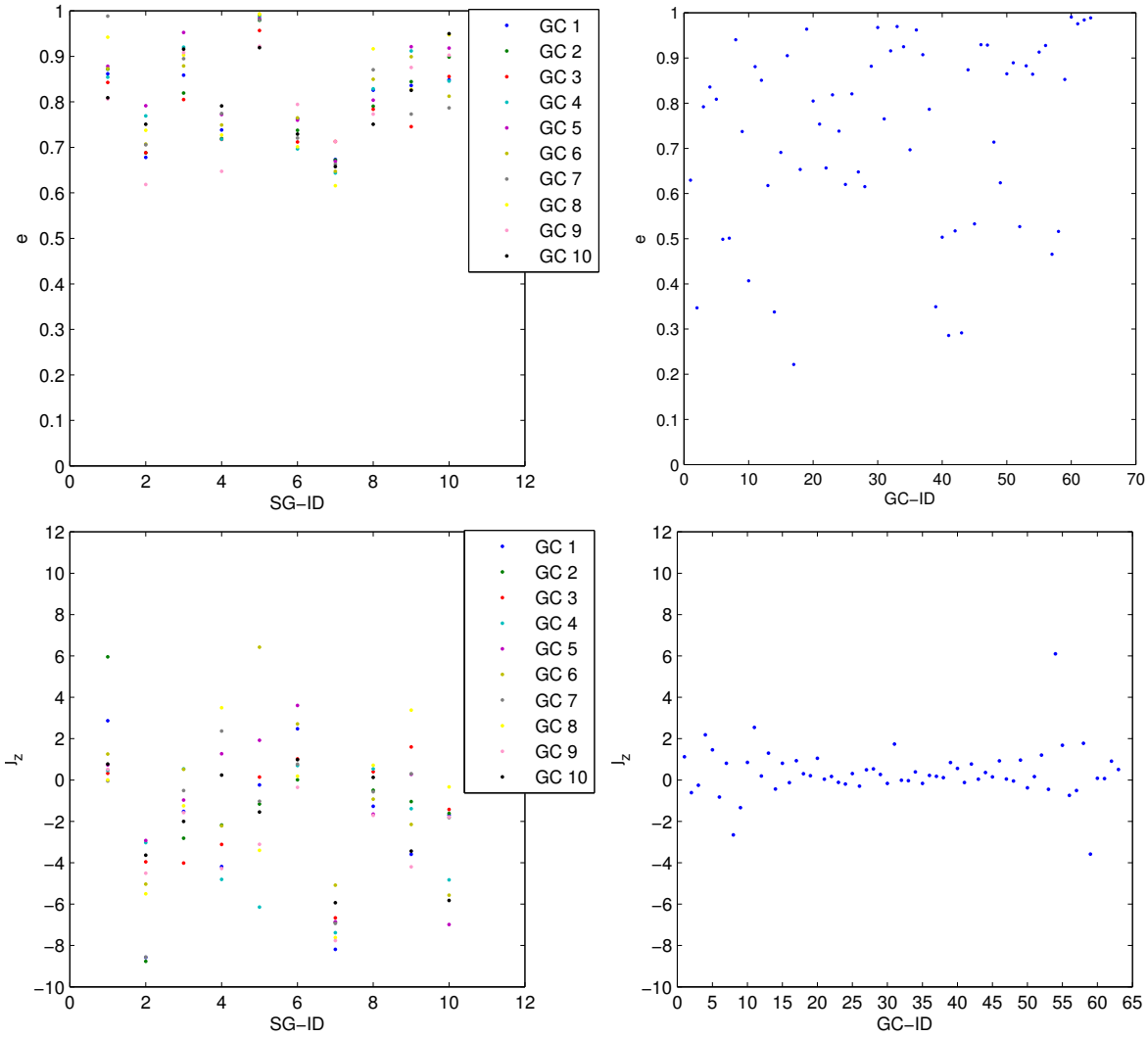

Figure 40: *Top left*: The eccentricity of the Sagittarius-like satellite galaxies' globular cluster orbits vs their host ID. *Top right*: The eccentricity of the Casetti-Dinescu globular clusters vs their ID number. *Bottom left*: The j_z of the Sagittarius-like satellite galaxies' globular cluster orbits vs their host ID. *Bottom right*: The j_z of the Casetti-Dinescu globular clusters vs their ID number. The outliers in the j_z plot are GC-IDs 4, 8, 11, 54, and 59.

To summarise these results, there were 2 of the 63 Casetti-Dinescu globular clusters which had similar eccentricity, energy, j_z, pericentre and apocentre values to those found from the Sagittarius-like satellite galaxies' globular clusters. These were IDs 4 and 11, note that in Section 6 IDs 8, 54, and 59 were also included in this list. However in this simulation ID 8 had too small of a pericentre value, ID 59 had too large of an apocentre value, and ID 54 was ejected from the Milky Way, and hence it's apocentre was greater than 100kpc.

If I had ignored the selection criteria that they must be outliers in the j_z plot then there were would have been 6 globular clusters that share similar properties to the accreted globular clusters. These were IDs 4 (NGC 1851), 9 (NGC 4147), 11 (NGC 4590), 13 (NGC 5024), 26 (NGC 6205) and 31 (NGC 6284). NGC 4147 is believed to have been accreted from the Sagittarius dwarf galaxy, and thus this add strength to my hypothesis that these 5 globular clusters have been accreted from Sagittarius-like satellite galaxies. These results do not necessarily mean that the results from Section 6 are incorrect, since IDs 54 and 59 may have been accreted from a more energetic satellite galaxy or have been accreted more recently. ID 8's pericentre values were similar to some of the pericentre values for that Sagittarius-like satellite galaxies' GC 5, however if I had included these values then the number of possibly accreted globular clusters in the Casetti-Dinescu database would have drastically risen.

References

Aaronson, M., Mould, J., 1982, ApJ, 48, 161
Barber, C., Starkenburg, E., Navarro, J. F., McConnachie, A. W., Fattahi, A., 2014, MNRAS, 437, 959
Beaulieu, S. F., Elson, R., Gilmore, G., Johnson, R. A., Tanvir, N., Santiago, B., 1999, IAUS, 190, 460
Bekki, K., Freeman, K. C., 2003, MNRAS, 346, 11
Bekki, K., Stanimirović, S., 2009, MNRAS, 395, 342
Bellazzini, M., Ferraro, F. R., Ibata, R., 2003, AJ, 125, 188
Bennett, J. O., Donahue, M., Schneider, N., Voit, M., 2009, "The Cosmic Perspective" , Addison-Wesley
Binney J., Tremaine S., 2008, "Galactic Dynamics", Princeton University Press, Princeton
Bodenheimer P., Laughlin G. P., Różyczka M., Yorke H. W., 2006, "Numerical Methods in Astrophysics: An Introduction", Taylor & Francis
Boylan-Kolchin, M., Bullock, J. S., Sohn, S. T., Besla, G., van der Marel, R. P., 2013, AJ, 768, 140
Cacciari, C., 2009, Mem. S.A.It, 80, 97
Casetti-Dinescu, D. I., Girard, T. M., Herrera, D., van Altena, W. F., López, C. E., Castillo, D. J., 2007, AJ, 134, 195
Casetti-Dinescu, D. I., Girard, T. M., Korchagin, V. I., van Altena, W. F., López, C. E., 2010, AJ, 140, 1282
Casetti-Dinescu, D. I., Girard, T. M., Jílková, L., van Altena, W. F., Podestá, F., López, C. E., 2013, AJ, 146, 33
Chiba, M., Mizutani, A., 2004, Publ. Astron. Soc. Aust., 21, 237
Chrysovergis, M., Kontizas, M., Kontizas, E., 1989, A&AS, 77, 357
Dinescu, D. I., Girard, T. M., van Altena, W. F., 1999, AJ, 117, 1792
Dinescu, D. I., Majewski, S. R., Girard, T. M., Cudworth, K. M., 2001, AJ, 122, 1916
Dinescu, D. I., Girard, T. M., van Altena, W. F., López, C. E., 2003, AJ, 125, 1373
Dormand, J. R., Prince, P. J., 1978, CeMec, 18, 223
Elson, R. A. W., Fall, S. M., Freeman, K. C., 1987, ApJ, 323, 54
Forbes, D. A., Bridges, T., 2010, MNRAS, 404, 1203
Freeman K. C., 1993, in Smith G., Brodie J., eds, ASP Conf. Ser. Vol. 48, The Globular Clustersgalaxy Connection. Astron. Soc. Pac., San Francisco, p. 608
Gnedin, O. Y., Ostriker, J. P., 1997, ApJ, 474, 223
Harris, W.E. 1996, AJ, 112, 1487
Helmi, A., White, S. D. M., 2001, MNRAS, 323, 529
Ideta, M., Makino, J., 2004, ApJ, 616, 107
Irrgang, A., Wilcox, B., Tucker, E., Schiefelbein, L., 2013, A&A, 549, 137
Jiang, I.-G., Binney, J., 2000, MNRAS , 314, 468
Johnson, J. A., Bolte, M., Bond, H. E., et al., 1999, IAUS, 190, 450
Johnston, K. V., Majewski, S. R., Siegel, M. H., Reid, I. N., Kunkel, W. E., 1999, AJ, 118, 1719
Johnston, K. V., Spergel, D. N., Hernquist, L., 1995, ApJ, 451, 598
Karl, S. J., Naab, T., Johansson, P. H., et al., 2010, ApJ, 715, 88
Kirby, E. N., Boylan-Kolchin, M., Cohen, J. G., Geha, M., Bullock, J. S., Kaplinghat, M., 2013, ApJ, 770, 16
Klessen, R. S., Zhao, H. S., 2002, ApJ, 566, 838
Kontizas, M., Chrysovergis, M., Kontizas, E., et. al., 1987, A&AS, 68, 147
Kutta, W., 1901, Zeitschrift, für Mathematische Physik, 46, 435
Law, D. R., Johnston, K. V., Majewski, S. R., 2005, ApJ, 619, 807
Law, D. R., Majewski, S. R., 2010a, ApJ, 714, 229
Law, D. R., Majewski, S. R., 2010b, ApJ, 718, 1128
Lindegren, L., 2010, "Dynamical Astrophysics" compendium from ASTM13 course

Lloyd Evans, T., 1980, MNRAS, 193, 87
Lyubenova, M., Kuntschner, H., Rejkuba, M., et al., 2012, A&A, 543, 75
Mackey, A. D., Gilmore G. F., 2003, MNRAS, 338, 85
Mackey, A. D., Gilmore G. F., 2004, MNRAS, 355, 504
Martin, N. F., Ibata, R. A., Bellazzini, M., Irwin, M. J., Lewis, G. F., Dehnen, W., 2004, MNRAS, 348, 12
Martínez-Delgado, D., Gómez-Flechoso, M. A., Aparicio, A., Carrera, R., 2004, ApJ, 601, 242
Mateo, M., 1998, ARA&A, 36, 435 [M98]
McConnachie, A. W., 2012, AJ, 144, 4
Miyamoto, M., Nagai, R., 1975, PASJ, 27, 533
Mo, H., van den Bosch, F., White, S., 2010, "Galaxy formation and evolution", Cambridge University Press, Cambridge
Mould, J., Aaronson, M., 1982, ApJ, 263, 629
Mould, J. R., Da Costa, G. S., Crawford, M. D., 1984, ApJ, 280, 595
Noyola, E., Gebhardt, K., 2007, AJ, 134, 912
Paczyński, B., 1990, ApJ, 348, 485
Palma, C., Majewski, S. R., Johnston, K. V., 2002, ApJ, 564, 736
Pawlowski, M. S., Pflamm-Altenburg, J., Kroupa, P., MNRAS, 423, 1109
Pawlowski, M. S., Kroupa, P., 2013, MNRAS, 435, 2116
Piffl, T., Scannapieco, C., Binney, J., Steinmetz, M., Scholz, R. D., Williams, M. E. K., et al., 2014, A&A, 562, 91
Plummer, H. C., 1911, MNRAS, 71, 460
Schneider, P., 2006, "Extragalactic astronomy and cosmology", Springer
Siegel, M. H., Majewski, S. R., Cudworth, K. M., Takamiya, M., 2001, AJ, 121, 935
Sohn, S. T., Besla, G., van der Marel, R. P., Boylan-Kolchin, M., Majewski, S. R., Bullock, J. S., 2013, AJ, 768, 139
Stanimirović, S., Staveley-Smith, L., Jones, P. A., 2004, ApJ, 604, 176
Subramanian, S., Subramaniam, A, 2012, ApJ, 744, 128
Toomre A., 1977, in Tinsley B. M., Larson R. B., eds, The Evolution of Galaxies and Stellar Populations. Yale Univ. Obser., New Haven, p. 401
van den Bergh, S., 2000a, "The galaxies of the local group", Cambridge University Press, Cambridge
van den Bergh, S., 2000b, PASP, 112, 932
van der Marel R. P., 2006, in Livio M., Brown T. M., eds, STSI Symp. Ser. Vol. 17, "The Local Group as an Astrophysical Laboratory", Cambridge University Press, Cambridge
Wadepuhl, M., Springel, V., 2011, MNRAS, 410, 1975
Whitmore, B. C., Chandar, R., Schweizer, F., et al., 2010, AJ, 140, 75
Windmark, F., Lindegren, L., Hobbs, D., 2011, A&A, 530, 76
Wolf, J., Martinez, G. D., Bullock, J. S., et al., 2010, MNRAS, 406, 1220
Zhao, H. S., 2004, MNRAS, 351, 891